A picture shows me at a glance what it takes dozens of pages of a book to expound

Ivan Turgenev, Russian writer, 1862

DEVELOPMENT OF THE CAUDAL VENA CAVA IN THE PIG EMBRYO

A THREE-DIMENSIONAL ANGIOGENIC MODEL

Pieter Cornillie

Thesis submitted in fulfilment of the requirements for the degree of Doctor in Veterinary Medical Sciences (Ph.D.)

Promoter: Prof. dr. Paul Simoens

Promoter: Prof. dr. Wim Van den Broeck

Department of Morphology, Faculty of Veterinary Medicine, Ghent University,
Salisburylaan 133, 9820 Merelbeke, Belgium

2008

The printing of this work was sponsored by:

Development of the caudal vena cava in the pig embryo: a three-dimensional angiogenic model

Pieter Cornillie, 2008, Ghent University

ISBN 978-90-5864-138-0

CONTENTS

GENERAL INTRODUCTION 1

CHAPTER 1: INTRODUCTION 5

1.1. Vasculogenesis and angiogenesis: an update 5
1.1.1. Definitions 5
1.1.2. Concepts of vasculogenesis 6
1.1.2.1. Extraembryonic vasculogenesis 6
1.1.2.2. Intraembryonic vasculogenesis 7
1.1.2.3. Blood vessels derived from vasculogenesis 8
1.1.3. Mechanisms of angiogenesis 9
1.1.3.1. VEGFs as the promoters of endothelial proliferation 10
1.1.3.2. Angiopoietins and vessel stabilisation 11
1.1.3.3. Ephrins and the specification of arteries and veins 13
1.1.3.4. CCN family proteins as supervisors of angiogenesis 13
1.2. The development of the caudal vena cava in the pig as a model for angiogenesis .. 15
1.2.1. Introduction 15
1.2.2. Selection of a suitable physiological study object 16
1.2.3. Original theory on the morphological development of the caudal vena cava in the pig embryo 19
1.2.3.1. The caudal cardinal veins 20
1.2.3.2. The subcardinal veins 20
1.2.3.3. The supracardinal veins 22
1.2.3.4. The final construction of the caudal vena cava 24
1.3. Literature 26

CHAPTER 2: PROBLEMS AND SCIENTIFIC AIMS 35

2.1. Questioning the existing supracardinal model 35
2.1.1. Introduction 35
2.1.2. Alternative theories on the development of the caudal vena cava 36
2.1.2.1. The supracardinal model 36
2.1.2.2. The caudal cardinal model 37
2.1.2.3. The sacrocardinal model 40
2.1.2.4. The lateral sympathetic model 41
2.1.2.5. The subcardinal model 41
2.1.2.6. Discussion 43
2.1.3. Anatomical variations of the venous system 48
2.1.3.1. Case descriptions 48
2.1.3.2. Discussion 51
2.2. Scientific aims 57
2.3. Literature 58

CHAPTER 3: MATERIALS AND METHODS 69

3.1. Introduction 69
3.2. Computer assisted three-dimensional reconstruction 70
3.2.1. Embryo collection 70
3.2.2. Fixation and tissue processing 70

3.2.3. Selection of the embryos for reconstruction 71
3.2.4. Acquisition of the digital images 71
3.2.5. Three-dimensional reconstruction 72
3.2.5.1. Data input 72
3.2.5.2. Image alignment 72
3.2.5.3. Casting 74
3.2.5.4. Image segmentation 75
3.2.5.5. Resampling 77
3.2.5.6. Surface generation 77
3.2.6. Evaluation 78
3.3. Microvascular corrosion casting 79
3.4. Discussion 81
3.4.1. Artefacts and final image quality 81
3.4.2. Elimination of non-invasive three-dimensional techniques 84
3.5. Literature 88

CHAPTER 4: RESULTS 93
4.1. Vascular development in the 3.7-18.0 mm pig embryo 93
4.1.1. General remarks 93
4.1.2. Vascular configuration in the 3.7 mm embryo 93
4.1.3. Vascular configurations in the 4.6 and 4.7 mm embryos 94
4.1.4. Vascular configurations in the 10.0 and 12.0 mm embryos 97
4.1.5. Vascular configuration in the 18.0 mm embryo 99
4.1.6. Discussion 102
4.2. Development of the infrarenal part of the porcine caudal vena cava in the late embryonic and early foetal period 105
4.2.1. General remarks 105
4.2.2. Venous pattern in the lumbar region of the 20.0 mm embryo 105
4.2.3. Venous pattern in the 22.5 mm embryo 106
4.2.4. Venous pattern in the lumbar region of the 27.6 mm embryo 109
4.2.5. Venous pattern in the lumbar region of the 36.7 mm foetus 112
4.2.6. Corrosion casting of the 9 cm foetus 114
4.2.7. Discussion 117
4.3. Literature 121

GENERAL DISCUSSION 127
SUMMARY 146
SAMENVATTING 152
DANKWOORD 157
CURRICULUM VITAE 161
BIBLIOGRAPHY 163

GENERAL INTRODUCTION

Whilst the final chapters of this thesis were written, the scientific world lost one of its greatest pioneers in angiogenesis research. On January 14th, 2008, professor Judah Folkman died in Denver, Colorado at the age of 74. In 1971, he published a seminal paper in which he for the first time postulated that all tumour growth is angiogenesis-dependent and that cancer can be treated by interfering with the new blood vessel formation induced by the tumour. Although initially largely ignored by other scientists, his ideas gradually gained support and opened a field of investigation now pursued by researchers in many fields worldwide. In the past decades, a wide range of signalling molecules, receptors and molecular pathways involved in blood vessel formation and vascular regression has been characterised and new therapeutic strategies in the treatment of cancer and many other diseases are currently being developed based on these insights.

The present Ph.D. thesis is also inspired by this particular field of research. In this specific work, the embryonic development of the caudal vena cava in the pig embryo is proposed as a possible model to study the molecular mechanisms controlling vascular development in an equilibrated physiological environment.

In the first chapter, an overview is given of the most relevant endogenous molecular mechanisms controlling blood vessel formation and vascular regression according to the most recent insights. Subsequently, the need for a new vascular model to study these delicate molecular interactions in a more physiological environment will be discussed. As this thesis presents the development of the caudal vena cava in the pig embryo as such a model, a short overview of the morphological characteristics of its developmental pattern based on data from literature will be given.

In the second chapter, our current knowledge on the morphological developmental pattern of the caudal vena cava in mammals is seriously questioned. By means of two different approaches, one based on an in-depth review of the current literature and the second focussing on practical experiences in the dissection room, it will be demonstrated that certain unravelled aspects regarding this developmental pattern still impede the practical application of this model in further angiogenesis research. The formulated scientific aims of

the present study therefore express the author's intentions to demystify these specific morphological and topographical aspects.

The third chapter is focussing on the materials and methods used in this research. Not only a detailed description of the applied methodology - from the collection of the embryos to the final three-dimensional reconstruction of their vascular architecture - is given, also the specific reasons why these particular techniques have been chosen to investigate the development of the caudal vena cava will be discussed.

Next, the results of these investigations are presented in chapter four. In the first section, the general vascular architecture in five specific embryonic stages is described. In the next section involving five late embryonic and early foetal stages, special attention is given to the development and topographical relationships of the most caudal segment of the caudal vena cava specifically. All findings are subsequently critically compared with earlier reports in literature.

In the final general discussion, the most important steps in the development of the caudal vena cava in the pig as observed in this study are summarized in a comprehensive model. After focussing on the main resemblances and differences with previously described models, some particular aspects of this developmental pattern that can be of interest in angiogenesis research are highlighted.

CHAPTER 1: INTRODUCTION

1.1. Vasculogenesis and angiogenesis: an update

1.2. The development of the caudal vena cava in the pig as a model for angiogenesis

1.3. Literature

Elaborate version of the principles described in:

Cornillie P., W. Van den Broeck and P. Simoens (2008). Three-dimensional reconstruction of the remodelling of the systemic vasculature in early pig embryos. *Microscopy Research and Technique* 71, 105-111 *(Sections 1.1. till 1.2.2.)*

Cornillie, P. and P. Simoens (2005). Prenatal development of the caudal vena cava in mammals: review of the different theories with special reference to the dog. *Anatomia, Histologia, Embryologia* 34, 364-372. *(Section 1.2.3.)*

CHAPTER 1: INTRODUCTION

1.1. Vasculogenesis and angiogenesis: an update

1.1.1. Definitions

A functional vascular system is essential for the development and survival of the tissues and organs in the body by supplying crucial molecules such as oxygen and nutrients as well as removing unwanted metabolites and waste products. In 1628, William Harvey discovered that the *heart* pumps the blood through the *arteries* to the various organs, and that the returning blood is collected by the *veins*. A few decades later, the *capillaries* have been identified as a link between both systems, not only closing the circulatory loop but also serving as a site of exchange of molecules and metabolites between the circulatory system and the various tissues (Carmeliet, 2005).

The formation of blood vessels is of utmost importance during embryonic development. The vascular system is in fact one of the first functional systems to be established in the early prenatal period (Coultas et al., 2005). It is generally accepted that blood vessels develop via two consecutive processes, viz. vasculogenesis and angiogenesis (Demir et al., 2007).

During *vasculogenesis*, the earliest primitive capillaries are formed *de novo* out of local mesodermal cell condensations that differentiate into clusters of (hem)angioblasts in a previously avascular tissue (Ferguson et al., 2005). The angioblasts or endothelial progenitor cells subsequently coalesce to form a primitive tubular network lined by a simple endothelium (Yancopoulos et al., 2000).

In the subsequent process called *angiogenesis*, the development of new blood vessels towards previously avascular tissue is accomplished by sprouting, branching, bridging or intussusceptive growth from already existing vessels (Milkiewicz et al., 2006). Furthermore, during angiogenesis, the initial vascular network is remodelled through both pruning and vascular enlargement. The vessel walls mature and their endothelial cells integrate tightly with the surrounding supporting cells such as smooth muscle cells or pericytes to form a stable and mature vessel (Yancopoulos et al., 2000).

Whilst angiogenesis has great relevance in embryonic development, it is downregulated in the adult organism and is only involved in the development of very distinct structures such as the corpus luteum, the placenta, the mammary glands and hair follicles (Bahramsoltani and Plendl, 2007). However, in many pathological conditions, angiogenesis can be reactivated. This *neovascularisation* is an essential factor in wound healing, fracture repair and the replenishment of ischemic tissue (Milkiewicz et al., 2006; Velazquez, 2007). Conversely, it is an unwanted and complicating element in tumour growth and dispersion as well as several degenerative vascular overgrowth diseases such as retinopathies (Folkman, 2002; Milkiewicz et al., 2006).

Although the degradation and pruning of existing vessels is an intrinsic part of angiogenesis, the controlled regression of stabilised blood vessels is often referred to as *anti-angiogenesis, inverse angiogenesis or reverse angiogenesis* (Bahramsoltani and Plendl, 2007), which must be differentiated from angiogenic inhibition, *i.e.* the prevention of new capillary outgrowth.

The induction of new capillaries involves more than a simple upregulation of angiogenic activity. It is thought to be the net result of a delicate balance of positive and negative regulators (Ribatti et al., 2007). The change from a vascular quiescent state to an angiogenic phenotype through a change in equilibrium between the inhibitors and stimuli is commonly called the *angiogenic switch*. Whereas an exaggerated angiogenic switch forms a central element in the progression and expansion of malignant tumours (Naumov et al., 2006), it remains regretfully insufficient in other diseases such as myocardial ischemia (Carmeliet, 2005).

It is predicted however that the development of new therapeutic strategies based on recent insights in angiogenesis and anti-angiogenesis will be beneficial to more than 500 million people worldwide in the coming decades (Carmeliet, 2005).

1.1.2. Concepts of vasculogenesis

1.1.2.1. Extraembryonic vasculogenesis

In nearly all mammalian embryos, the first site of vasculogenesis is the mesodermal layer of the extra-embryonic yolk sac (Dyer et al., 2001). The development of the initial blood vessels in the yolk sac is strongly correlated with the formation of the first blood cells as both are believed to share a common precursor: the hemangioblast (Bautch et al., 2000; Baron,

2003). During late gastrulation, differentiating hemangioblasts of the yolk sac mesoderm condense in morphologically identifiable cells clusters indicated as blood islands (Dyer et al., 2001). The inner cells of these blood islands become the hematopoietic stem cells, the precursors of all the blood cells, whilst the outer cells become angioblasts, the precursors of the blood vessels (Gilbert, 2000). The angioblasts subsequently differentiate into vascular endothelial cells which coalesce with the endothelial cells of neighbouring blood islands to form vascular channels constructing the primitive network of discrete vitelline blood vessels (Dyer et al., 2001). In mouse embryos, this process is initiated at the end of the first week of gestation, whilst in man and most domestic animals, it is a typical feature of the third week p.c. (Sadler, 1985; Rüsse, 1991a; Shalaby et al., 1995).

1.1.2.2. Intraembryonic vasculogenesis

Following the construction of primitive blood vessels in the yolk sac, an early intraembryonic vasculature which eventually will connect with the vitelline vessels is also established. Remarkably, intraembryonic vasculogenesis is quite different from the developmental pattern described in the yolk sac as it is only rarely associated with simultaneous blood cell formation (Levenberg, 2005). The first morphological sign of differentiation is the condensation of mesodermal cells forming solid masses of angioblasts or endothelial progenitor cells. In a later stage, hollowing of these clusters can be observed after regression of the central angioblasts, resulting in lumen formation of the vessel. The outer cells subsequently differentiate into the endothelial lining of the blood vessel wall (Bailey and Fleming, 2003).

Only the blood vessel components derived from the splanchnopleural mesoderm, such as the hepatic vasculature or the ventral walls of the dorsal aortae, are associated with hematopoiesis, in contrast to the endothelial lineages derived from the paraxial mesoderm which have no hematopoietic potentials (Pardanaud et al., 1996; Furata et al., 2006). Furthermore, hematopoiesis is only seen in the arterial vascular beds (Urness et al., 2000). Contrary to the formation of blood islands in the yolk sac, the hematopoietic cells inside the developing intraembryonic vessels remain anchored to the vascular wall inside so-called blood-island-like structures (Bailey and Fleming, 2003; Ratajska and Czarnowska, 2006). It has been proven that these hematopoietic stem cells do not originate from colonizing cells derived from the yolk sac but from locally differentiating mesodermal cells (Pardanaud et al., 1996). However, it is still unclear whether both the vascular wall and the hematopoietic cells

differentiate simultaneously from a common precursor (the hemangioblast) or whether first the endothelium is formed directly out of angioblasts and only in a later stage the hematopoietic cells differentiate from this hemogenic endothelium (Bailey and Fleming, 2003).

1.1.2.3. Blood vessels derived from vasculogenesis

The number of blood vessels that arise through vasculogenesis is limited: apart from the extraembryonic early vitelline circulation, the only identifiable vessels directly differentiating *in situ* out of differentiating angioblasts are the endocardial tubes, the dorsal aortae and the cardinal veins (Ferguson et al., 2005). A honeycomb-like capillary plexus connects these major arteries and veins to allow the proper circulation and distribution of blood as soon as the primitive heart starts to pump (Yancopoulos et al., 2000). The initial vascularisation of developing organs such as the liver, kidneys and lungs is also established through vasculogenesis (LaRue et al., 2003). *De novo* extraembryonic vasculogenesis can furthermore be found in the allantois, an extraembryonic sac responsible for the induction of placental tissue and the formation of the umbilical vessels (Ferguson et al., 2005). An overview of the major embryonic vessels that are initially built through vasculogenesis is given in figure 1.

Vasculogenesis has long been thought to occur only in the early phases of embryonic vascular development. However, recent data support the existence of circulating endothelial progenitor cells (angioblasts) derived from the bone marrow in the adult (Döme et al., 2007). These endothelial progenitor cells are able to differentiate when needed into vascular endothelium through a mechanism recapitulating embryonic vasculogenesis (Ribatti, 2007). This type of "remote vasculogenesis", a term used to indicate that the endothelial progenitor cells differentiate into vascular tissue at a location different from their site of origin, has been observed in malignant cancers (Döme et al., 2007) or during wound-healing in adult tissues (Velazquez, 2007). Because this type of adult neovascularisation is relying on circulating progenitor cells instead of residential angioblasts *in situ*, some authors claim that it is inappropriate to indicate this process as a form of vasculogenesis, which should be strictly reserved to indicate the embryologic process characterised by locally proliferating cells differentiating into vascular tissue (Ferguson et al., 2005). However, also during embryonic development, it has been described that circulating and migrating endothelial progenitor cells are used to vascularise remote locations (LaRue et al., 2003; Serini et al., 2003). This

process is considered to be an integral part of embryonic vasculogenesis and is more specifically indicated as “type II vasculogenesis” (Coffin and Poole, 1991; Serini et al., 2003).

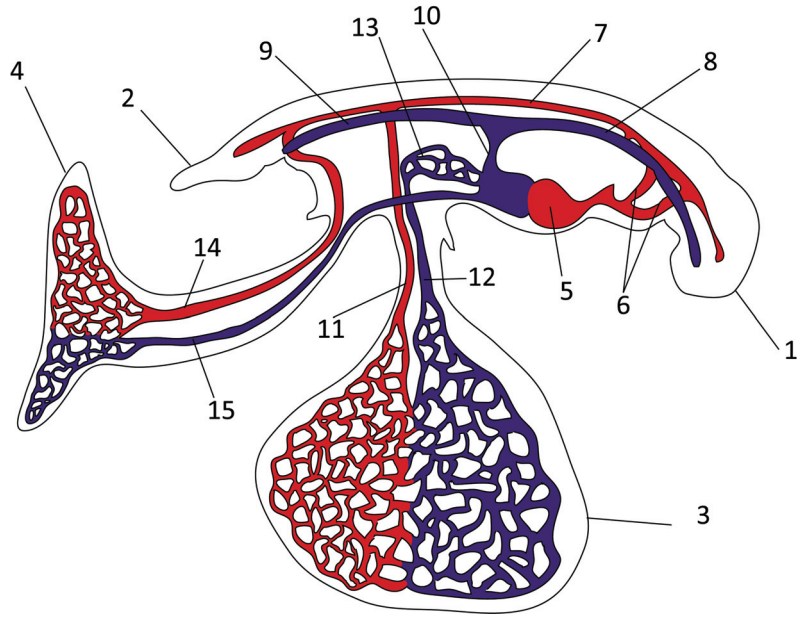

Fig. 1: Right lateral view on the early embryonic vasculature that is built through vasculogenesis. At this stage, all blood vessels are paired. The single heart is bilateral symmetric. Only the right-sided counterpart of the vasculature is drawn. *Orientation points:* 1: head process, 2: tail, 3: vitelline sac, 4: allantois. *Intra-embryonic circulation:* 5: ventricle of the heart, 6: first two pairs of branchial arch arteries, 7: dorsal aorta, 8: cranial cardinal vein, 9: caudal cardinal vein, 10: common cardinal vein. *Extra-embryonic circulation*: 11: vitelline artery, 12: vitelline vein, 13: intrahepatic plexus of the vitelline veins (intraembryonic), 14: umbilical artery, 15: umbilical vein. After Patten (1948).

1.1.3. Mechanisms of angiogenesis

During subsequent angiogenesis, the primitive capillary network formed after the initial phase of vasculogenesis not only needs to be further elaborated in order to supply newly developing tissues and organs, it also requires substantial remodelling, involving the regression of vessels that have become obsolete and the maturation and stabilisation of vital circulatory channels (Ribatti, 2006). Furthermore, during angiogenesis, the fate of the blood vessels is determined and veins and arteries are made (Gilbert, 2000). In normal circumstances, angiogenesis is a highly ordered process under tight regulation of numerous molecular mechanisms involving signalling molecules, cell-cell interactions and cell-matrix

interactions (Papetti and Herman, 2002; Ribatti, 2006). Many of the molecules involved in angiogenesis are not vascular-specific and include amongst others fibroblast growth factors (FGF), transforming growth factor β (TGF-β), tumour necrosis factor α (TNF-α), hepatocyte growth factor (HGF), epidermal growth factor (EGF), platelet derived growth factor (PDGF),... (Papetti and Herman, 2001; Milkiewicz et al., 2006). On the other hand, three vascular-specific groups of molecules and their receptors are considered as the key regulators of angiogenesis, namely vascular endothelial growth factors (VEGF), the angiopoietins and the ephrins (Yancopoulos et al., 2000). The entire process of angiogenesis is furthermore promoted and modulated through a unique mechanism involving CCN family proteins (Kubota and Takigawa, 2007). The principles described in the next two sections are summarized in figure 2.

1.1.3.1. VEGFs as the promoters of endothelial proliferation

The vascular endothelial growth factors are the most documented group of angiogenic factors. They are produced in high levels in tissues where angiogenesis is required (Papetti and Herman, 2002). Especially VEGF-A and its receptors VEGFR-1 and VEGFR-2 have a vital role in both angiogenesis and vasculogenesis (Yancopoulos et al., 2000). Studies in knock-out mice have revealed that VEGFR-2 is essential for hemangioblast differentiation and the proliferation and migration of endothelial cells, whilst VEGFR-1 is required for tube formation and cell-cell interactions within the endothelium (Hanahan, 1997).

VEGF transcription by mesenchymal or stromal cells is greatly stimulated by hypoxia, but can also be induced by inflammatory mediators as well as by mechanical forces such as cell stretch (Milkiewicz et al., 2006). VEGF exerts several effects on vascular endothelial cells. It enhances vascular permeability by loosening the adherens junctions between the endothelial cells, and induces endothelial cell proliferation as well as the growth of capillary sprouts from pre-existing blood vessels. The VEGF-mediated release of proteolytic enzymes by the endothelial cells into the perivascular extracellular matrix clears the path for the proliferating capillaries. VEGF also inhibits endothelial cell apoptosis and thus acts as a survival factor (Papetti and Herman, 2002).

VEGF is such a potent and critical vascular regulator that its dosage must be exquisitely regulated in spatial, temporal and quantitative matter to avoid vascular disaster. However, despite its critical role in the initiation of vascularisation in both the embryo as the

adult, it is only able to promote by itself the formation of leaky, immature and unstable vessels (Yancopoulos et al., 2000).

1.1.3.2. Angiopoietins and vessel stabilisation

The angiopoietins form a group of recently discovered proteins (Davis et al., 1996) of which Angiopoietin-1 (Ang1) and its natural antagonist Angiopoietin-2 (Ang2) are the most important members. Both molecules bind primarily to the tyrosinase kinase receptor Tie2[*] which is, like the orphan receptor Tie1, selectively expressed on the vascular endothelium (Yancopoulos et al., 2000). Although no ligand capable of binding and activating Tie1 has been identified so far, it is known that this orphan receptor is also involved in modulating the endothelial cell response to these angiogenic signals through physical interaction with the Tie2 receptor as both receptors exist in hetero-oligomeric complexes at the cell surface (Marron et al., 2007).

Angiopoietins do not play a role in the formation of the primary capillary plexus and exert no mitogenic effect. However, they are of vital importance in the remodelling and maturation of blood vessels (Ward and Dumont, 2002; Morisada et al., 2006).

Ang1 is secreted by cells directly surrounding the vascular endothelium, the so-called pericytes or mural cells, such as precursors of smooth muscle cells (Maisonpierre et al., 1997; Kim et al., 2000; Moyon et al., 2001) and acts as an agonist by inducing autophosphorylation of the Tie2 receptor on the vascular endothelial cells (Davis et al., 1996). Ang1 stimulates the formation of tight associations between adjacent endothelial cells and between endothelial cells and perivascular mural cells, hereby not only ensuring the impermeability of the previously leaky vessel, but also creating a proper muscular wall around the simple endothelial tube which was formerly only lined with a basement membrane (Morisada et al., 2006). It further acts as a strong anti-apoptotic factor and also allows blood vessels to expand (Kim et al., 2000; Yancopoulos et al., 2000; Morisada et al., 2006). Ang1 deficient mice embryos are unable to remodel the initial vascular network created by vasculogenesis and die at embryonic day 12.5 (Suri et al., 1996).

[*] Tie is the acronym of *T*yrosine kinase containing *I*mmunoglobulin-like loops and *E*pidermal growth factor similar domains (Yuan et al., 2000)

Ang2 antagonises the effects of Ang1 by binding and occupying the Tie2 receptor without activating it (Maisonpierre et al., 1997). However, in some specific *in vitro* conditions, Ang2 was able to induce autophosphorylation of the Tie2 receptor as well (Ward and Dumont, 2002). In embryonic tissue, Ang2 is secreted by the vascular pericytes and acts as a paracrine factor (Maisonpierre et al., 1997; Moyon et al., 2001) whilst in adult and tumoral tissues, Ang2 is almost exclusively expressed and secreted by endothelial cells, acting as an autocrine factor (Fiedler et al., 2004). Ang2 causes destabilisation of blood vessels by reversing the effects induced by Ang1 (Yancopoulos et al., 2000).

Ang1 and Ang2 can both act as pro-angiogenic and anti-angiogenic factors, depending on the presence of VEGF and other mediators of angiogenesis in the nearby environment (Fig. 2). In absence of VEGF, vessel destabilisation caused by Ang2 will eventually result in vascular degradation, apoptosis of the endothelial cells and disappearance of the blood vessel (Yancopoulos et al., 2000). On the other hand, vessel destabilisation is to a certain

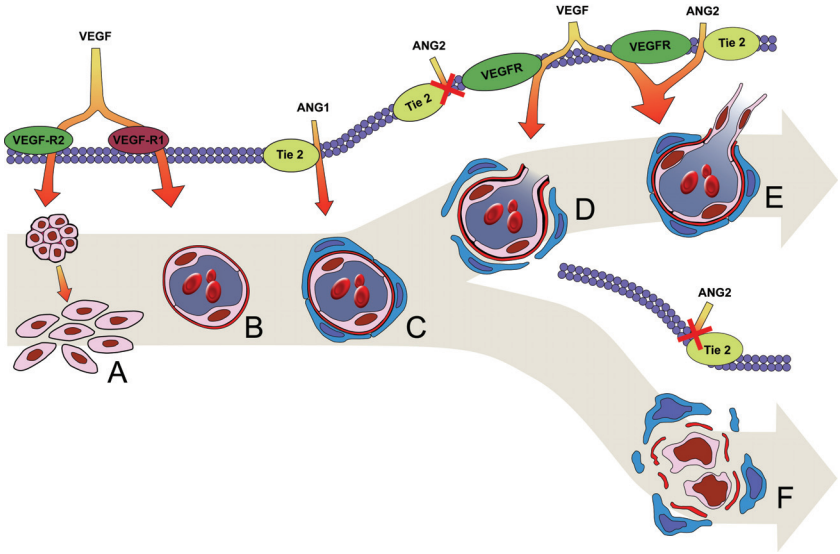

Fig. 2: Actions of angiopoietins and VEGF during vasculogenesis and angiogenesis. A: Migration and proliferation of endothelial cells mediated by VEGF activation of the VEGF receptor-2, B: tube formation and endothelial cell-cell interaction through activation of the VEGF receptor-1, C: recruitment of and interaction with pericytes, maintenance of vessel integrity and quiescence under influence of Ang1 activation of the Tie2 receptor, D: Ang2, by blocking the Tie2 receptor, induces in the presence of VEGF loosening of the supportive cells and allows access of angiogenic inducers to the endothelium, E: in certain in vitro conditions, Ang2 can activate the Tie2 receptor, which will in the presence of VEGF lead to the formation of capillary sprouts and new blood vessels, F: in absence of VEGF, the inhibiting action of Ang2 on the Tie2 receptor leads to vessel regression and apoptosis. (Modified from Fam et al., 2003).

extent essential to allow endothelial sprouting induced by VEGF. In fact, to permit vascular branches to be formed, mural cells must first be removed and the endothelial basement membrane must be degraded (Yancopoulos et al., 2000; Papetti and Herman, 2002). Therefore, high levels of the Ang1, even in the presence of VEGF, act anti-angiogenic by stabilising the endothelium and vascular wall, preventing endothelial sprouts and branches to be formed (Papetti and Herman, 2002; Thurston, 2002). On the other hand, Ang1 allows blood vessels to survive, grow and expand, hereby ensuring sufficient blood flow to developing tissues and organs. Under influence of Ang1, the primitive capillary network is also transformed in a mature and stable network with larger and smaller vessels (Papetti and Herman, 2002). Furthermore, under certain *in vitro* conditions, Ang1 can induce endothelial migration, tubule formation and sprouting (Metheny-Barlow and Li, 2003).

1.1.3.3. Ephrins and the specification of arteries and veins

The differentiated identity of arterial blood vessels has long been thought to depend largely on the influence of hemodynamic forces (Lawson et al., 2001). However, recent data suggest that molecular differences between arteries and veins are already apparent well before the onset of circulation (Wang et al., 1998; Urness et al., 2000; Herzog et al., 2001; Rossant and Hirashima, 2003). Especially the receptor EphB4, which is just like the VEGF and Tie receptors belonging to the family of receptor tyrosine kinases, and its ligand ephrin-B2 display remarkable distinct distribution patterns, with ephrin-B2 marking the endothelium of primordial arterial vessels, whilst EphB4 marks the endothelium of future veins (Rossant and Hirashima, 2003). Although the exact action of this receptor and its ligand on arteriovenous differentiation is unknown, it has been shown that in mouse embryos lacking activin receptor kinase-1, an upstream regulator of the arterial expression of ephrin-B2, the closely adjacent dorsal aortae and cardinal veins formed after vasculogenesis cannot be prevented from fusing with each other during subsequent angiogenesis (Urness et al., 2000). On the other hand, mouse embryos lacking ephrin-B2 and EphB4 suffer during early angiogenic remodelling from fatal defects that are somewhat reminiscent of those seen in mice lacking Ang1 or Tie2 (Yancopoulos et al., 2000), complicating the study towards the exact function of these molecules in arteriovenous differentiation during further angiogenesis.

1.1.3.4. CCN family proteins as supervisors of angiogenesis

During the process of angiogenesis, a vast amount of molecules exert their power on the vascular endothelial cells and other types of cells in the same microenvironment. As a

response to these signals, many of these cells will in turn release different extracellular matrix components such as adhesion molecules, proteinases,... It is not the scope of the present thesis to give a full overview of all the molecular pathways and cell interactions. However, to illustrate the complexity of the mechanisms involved in angiogenesis, the recently discovered role of the CCN family proteins in this particular field is displayed in this paragraph.

It was almost unimaginable how blood vessels manage to become properly organized in the massive jungle of molecules until very recently the concept of molecular guidance by CCN family proteins during angiogenesis was introduced (Kubota and Takigawa, 2007). The CCN (cyr61, ctgf, nov) family of proteins contains six different members each composed of up to four modules capable of interacting with a large amount of signalling and regulatory proteins as well as adhesion molecules, cellular receptors and extracellular matrix components (Perbal, 2004). Due to this capacity, it is suggested that the CCN proteins serve as integrators and modulators of extracellular information and that their effect on angiogenesis is based on the outcome of the negotiations with pro- and antiangiogenic molecules. Furthermore, as the CCN proteins can interact with extracellular matrix proteins as well as cellular adhesion molecules, it is suggested that the CCN proteins guide the sprouting endothelial cells and assist in the correct placement of all tissue components contributing in the formation of a new blood vessel (Kubota and Takigawa, 2007).

1.2. The development of the caudal vena cava in the pig as a model for angiogenesis

1.2.1. Introduction

As the growth of new blood vessels is a crucial step in the progression of cancer, allowing tumour growth and metastasis, angiogenesis has become the main focus in clinical oncology and the development of new therapeutic approaches in the fight against cancer (Folkman, 2002). Because of the predominant role of VEGF in angiogenesis, most of the currently developed strategies to inhibit tumour vascularisation target VEGF and its receptors (Carmeliet, 2005, Döme et al., 2007). On the other hand, the enhancement of the activity of VEGF became a major focus in the area of research dealing with ischemic disease conditions in which the induction of angiogenesis might be beneficial (Griffioen and Molema, 2000).

In both the fields of therapeutic angiogenesis and angiosuppressive therapy targeting VEGF, some promising successes have been scored in pre-clinical experiments on laboratory animals with experimentally induced disorders (Griffioen and Molema, 2000). Conversely and despite the fact that some antiangiogenic agents have already effectively been applied in the treatment of very specific types of cancer (Döme et al., 2007), test results of many of these potential drugs during clinical trial phases and subsequent follow-up in human patients are rather disappointing (Griffioen and Molema, 2000; Carmeliet, 2005). Clinical setups involving VEGF administration or enhancement of its activity in the treatment of ischemic diseases have been aborted prematurely due to the absence of any significant positive effect (Griffioen and Molema, 2000). Also the effects of antiangiogenic agents interfering with VEGF activity in tumour development are less promising than expected as they only tend to prevent neovascularisation in remote micrometastases, whilst the primary tumour is left almost unaffected (Folkman, 2002). As a matter of fact, emerging evidence indicates that the inhibition of a single target (*in casu* VEGF) leads to upregulation of additional angiogenic factors countering the desired antiangiogenic effect (Carmeliet, 2005).

It has become clear that the interaction and delicate balance between several angiogenic factors must be taken into account to enable the design of more effective strategies in which the core element will be the combination of (anti)angiogenic agents with complementary action mechanisms (Carmeliet, 2005). Based on these insights, the angiopoietins, amongst many other molecules, have attracted the special attention of several

research groups working on angiosuppressive therapies in oncology, due to their role in vessel stabilisation, survival and quiescence as well as vascular proliferation or degradation following destabilisation (Metheny-Barlow and Li, 2003). Moreover, as it is generally known that tumour vessels remain leaky and unorganised and also fail to mature and create a proper vascular wall, a dominant role for angiopoietin 2 in tumour angiogenesis in particular has been suggested (Yancopoulos et al., 2000).

As already mentioned, angiopoietin 1 and its natural antagonist angiopoietin 2 can both act as proangiogenic or angiosuppressive mediators, depending on the environmental circumstances and the presence of other angiogenic molecules. However, this assumption is mainly based on findings from experimental setups in which the delicate balance between these angiogenic mediators has deliberately been disrupted e.g. through gene knock-out or gene overexpression assays (Yancopoulos et al., 2000). Furthermore, translating the data from highly controlled *in vitro* models, in which the effect of only a single or a limited number of angiogenic factors on endothelial cells are studied, towards the situation *in vivo* has also proven to be extremely difficult as the cell-cell interactions and cell-matrix interactions that are critical *in vivo* are very limited in many of the *in vitro* models used (Norrby, 2006; Ucuzian and Greisler, 2007).

Therefore, the role of the angiopoietins and their receptor(s) in the regulation of angiogenesis certainly needs to be further investigated in more natural conditions before a successful, safe and reliable therapeutic strategy based on their mechanisms of (inter)action can be designed. Close monitoring of the expression of these molecules during well-described physiological phases of vessel stabilisation or degradation can be a first step towards new insight in this complex matter.

1.2.2. Selection of a suitable physiological study object

Whereas vessel stabilisation, remodelling and degradation is an ubiquitous feature in embryonic development, angiogenesis under defined physiological stimuli in adult tissues is a rare event, mostly confined to the female reproductive system (Charnock-Jones et al., 2004). Furthermore, adult angiogenesis is significantly less ordered than the highly choreographed manner of vascular development and regression in the embryo (Dor et al., 2003). Therefore, focussing on the developing embryonic vasculature as physiological study object for angiogenesis is the most evident option.

Two specific components of embryonic vascular development that can be of particular interest in this context are the remodelling of the branchial arch arteries into the aortic arch and its major branches on the one hand, and the segmented construction of the caudal vena cava out of several early embryonic veins on the other hand. Both these developmental patterns are characterised by the substantial remodelling of an initial primitive embryonic vascular architecture composed of a certain number of well-characterised and identifiable blood vessels. Furthermore, only a few of these blood vessels are maintained as large, stable arteries or veins in the adult organism, whilst most other vessels of these primitive embryonic networks are progressively degraded and finally lost (McGeady et al., 2006). The spatio-temporal characteristics of these developing vascular components in the embryo are well-described in different animal species including man, making it possible in an experimental setup to select a specific region in an embryo of a certain age to find a blood vessel of interest either appearing and being stabilized or being degraded and disappearing.

The construction of the caudal vena cava is of particular interest, because of its typical left-right asymmetrical developmental pattern. In fact, the early embryonic somatic veins originate as bilateral symmetric pairs of vessels. Whilst the left-sided embryonic veins are to disappear, some segments of the right-sided veins further develop and fuse with each other to eventually form the caudal vena cava (Huntington and McClure, 1920). This offers great perspectives for the research towards the mechanisms regulating vessel stabilisation or degradation as at the same transversal level in the same embryo, two formerly identical vessels, each submitted to a different fate, can be observed. Whilst the one on the left-hand side is degraded and bound to regress into an undefined capillary network, its right-sided counterpart is stabilised and allowed to further mature as a single solid vessel.

Interestingly, the involvement of the angiogenic mediators angiopoietin-1 (Ang1) and the Tie1-receptor in the establishment of this specific left-right asymmetrical developmental pattern has clearly been demonstrated by Loughna and Sato (2001). A major but unexpected finding in their experiments with double knock-out mouse embryos lacking both Ang1 and Tie1 was the fact that these embryos exhibited a specific absence of a right-sided venous structure whilst the left-hand side venous network, including the cardinal veins in particular, was normal. These findings furthermore strongly suggested that the development of the venous architecture is at least partially genetically determined. In fact, it has long been

assumed that the selection of the definitive venous channel out of a plexus of small venules was the result of purely hemodynamic forces and that the blood flow is increased along whichever pathway offers the least resistance (Noden and de Lahunta, 1985).

As, due to embryonic lethality, only mouse embryos of 9.5 dpc and younger could be studied in this knock-out experiment by Loughna and Sato (2001), no further information on the involvement of these mediators in the subsequent venous remodelling resulting in the construction of the caudal vena cava was obtained. Remarkably, since their initial report, no further studies on the possible mechanisms of this asymmetric regulation of venous system development referring to this original work have been published to date.

Additionally, from comparative point of view, mouse embryos might not be the most suitable specimens to study the factors regulating the further development of the caudal vena cava. Contrary to the situation in man (McClure and Butler, 1925) and domestic animals such as the cat (Huntington and McClure, 1920), sheep or pig (Butler, 1927), the caudal vena cava in rodent species is believed to develop much more directly out of the cardinal veins, requiring less remodelling and fewer contributions from different other early embryonic veins (Butler, 1927). More information on this species-specific developmental pattern in rodents will be given in chapter 2.

A non-rodent species of particular interest in research on angiogenesis is the pig. Especially in the field of cardiovascular medicine, pigs have increasingly been used in studies of chronic myocardial ischemia (Hughes et al., 2003) in which more recently also special attention is given to the role of angiopoietins and their receptors in the development of therapeutic strategies (Cheng et al., 2006; Ye et al., 2007). The special interest in this species has further led to the characterisation and publication of the entire mRNA sequences of porcine Ang1 (NCBI GenBank NM_213959) and Ang2 (NM_213808) and partial sequences of Tie1 (AJ867846) and Tie2 (AF251494), enabling the application of PCR and *in situ* hybridization detection techniques on porcine tissues. Furthermore, several antibodies against these porcine angiogenic mediators are now commercially available for applications such as western blotting, immunofluorescence and immunohistochemistry. These factors, together with the availability of a clear morphological description of the development of the caudal vena cava in the pig embryo (Butler, 1927) form a solid base for the research on the mechanisms involved in the typical left-right asymmetrical patterning in venous development during embryogenesis.

1.2.3. Original theory on the morphological development of the caudal vena cava in the pig embryo

The morphological aspects of the development of the caudal vena cava in the pig are extensively illustrated in the available literature. Initially described by Butler (1927), this morphological developmental pattern became widely known and recognised mainly as a result of its incorporation in the work of Patten (1948), whose books became standard works in the field of embryology. All currently available books on veterinary embryology use this developmental pattern in the pig as a general model to explain the development of the caudal vena cava in domestic mammals (Noden and de Lahunta, 1985; Rüsse and Sinowatz, 1991; McGeady et al., 2006). In the following text and figures, a concise description of this developmental model will be given. To provide an overview of the topographical relationships of all vessels involved in the construction of the caudal vena cava to each other and the surrounding tissues, the introductory figure 3 is presented first.

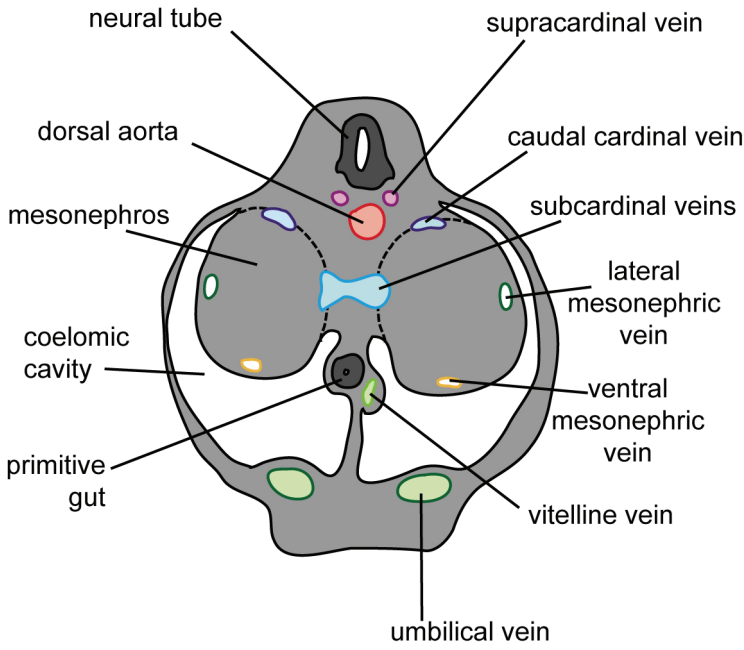

Fig. 3: Schematic representation of a cross-section cranial to the umbilicus of a hypothetical pig embryo to indicate the topographical relationship of all early embryonic veins, labelled on the right side of the image, to the surrounding tissue. The cross-section is hypothetical as not all vessels drawn in the image can simultaneously been found in a single pig embryo during development.

1.2.3.1. The caudal cardinal veins

The cardinal veins are the first group of somatic veins to appear in the embryo (Fig. 4). They first appear bilaterally in porcine embryos smaller than 5mm lateral to the paired dorsal aortae (Butler, 1927; Rüsse, 1991b). Whilst the cranial cardinal veins drain the head region and neck, the caudal cardinal veins, located in the intermediate mesoderm dorsal to the mesonephric ducts, are the main venous return channels of the more caudal body parts (Noden and de Lahunta, 1985). At the level of the heart, the cranial and caudal cardinal veins confluence into the ipsilateral common cardinal vein (Rüsse, 1991b). Both left and right common cardinal veins course in ventral direction to drain together with the paired umbilical and vitelline veins into the sinus venosus of the developing heart (Patten, 1948).

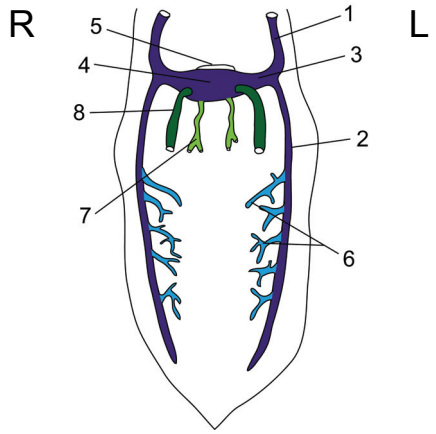

Fig. 4: Ground plan of the veins in a young mammalian embryo, ventral view. 1: left cranial cardinal vein, 2: left caudal cardinal vein, 3: left common cardinal vein, 4: sinus venosus, 5: entrance to the heart, 6: mesonephric branches forming the left subcardinal plexus, 7: right vitelline vein, 8: right umbilical vein. After Patten (1948).

When the intermediate mesoderm on each side in the thoracolumbar region hypertrophies to form the mesonephros or primitive embryonic kidney, the caudal cardinal veins can be found dorsolateral to these organs (Noden and de Lahunta, 1985; Rüsse, 1991b). Each caudal cardinal vein receives segmental tributaries from the dorsal body wall, but its primary function remains the drainage of the mesonephros through tributaries along the lateral and medial surfaces of this voluminous organ (Butler, 1927). In the caudalmost region of the embryo, beyond the caudal ends of the mesonephroi, the caudal cardinal veins, coursing dorsal to the umbilical arteries, shift more laterally to drain the developing hind limb buds (Butler, 1927; Noden and de Lahunta, 1985).

1.2.3.2. The subcardinal veins

In pig embryos of about 5 to 6 mm, a new longitudinal and bilateral symmetric vein pair appear along the ventromedial surface of the mesonephroi (Fig. 5). These so-called subcardinal veins originate as a result of the coalescence of the early mesonephric tributaries

of the caudal cardinal veins which lie medial to the mesonephroi and drain the glomerular region of these organs (Butler, 1927). As the developing mesonephroi grow and bulge towards the midline, the left and right subcardinal veins are brought very close to each other and eventually anastomoses between both veins are formed in the mid-mesonephric region, just ventral to the aorta (Patten, 1948).

Initially, each subcardinal vein drains cranially, at the level of the cranial pole of the mesonephros, into the ipsilateral caudal cardinal vein (Butler, 1927). However, during subsequent development, this connection is lost, and all blood drained by the subcardinal veins is now redirected towards the central subcardinal anastomosis which rapidly increases in size, forming a large venous sinus (Patten, 1948). This sinus is at its turn drained by a newly formed mesenteric vein which connects the right subcardinal vein short after its emergence from the right cranial aspect of the subcardinal anastomosis with the underlying right vitelline vein at the level of the developing liver (Butler, 1927; Patten, 1948). The subcardinal sinus and its vitelline connection gradually evolve into the main passage for the blood returning towards the heart (Fig. 5). As a consequence, the caudal cardinal veins gradually regress, and their mesonephric parts become almost entirely obliterated in the 12-14 mm

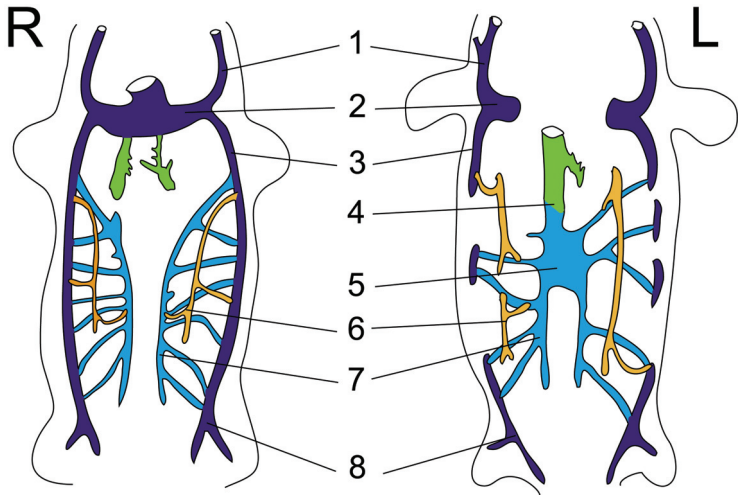

Fig. 5: Schematic representation of the venous pattern in the 5-6 mm (left) and 12-13 mm (right) pig embryo, ventral view (after Patten, 1948). 1: cranial cardinal veins, 2: common cardinal veins, 3: cranial segments of the caudal cardinal veins, 4: subcardinal-vitelline anastomosis, 5: subcardinal sinus, 6: ventral mesonephric veins, 7: subcardinal veins, 8: caudal segments of the caudal cardinal veins.

embryo (Butler, 1927). Cranial to the mesonephroi however, the caudal cardinal veins persist, albeit as much smaller vessels than originally designed (Patten, 1948).

On the other hand, the segments of the caudal cardinal veins caudal to the mesonephroi are still increasing in importance. They collect the blood coming from the tail and the developing hindlimbs. This blood is subsequently passed through several of the aforementioned mesonephric tributaries towards the caudal ends of the ipsilateral subcardinal vein (Butler, 1927).

For the sake of completeness, it must be mentioned that as a unique feature in the pig embryo, at the same time that the subcardinal veins develop, another longitudinal vein pair appears on the ventral surface of the mesonephroi. These left and right ventral mesonephric veins, although of utmost importance in the temporary drainage of the mesonephros itself, do not contribute in the construction of the caudal vena cava and disappear gradually during the next stages of development (Butler, 1927).

1.2.3.3. The supracardinal veins

In the approximately 17-19 mm pig embryo, the supracardinal veins arise as a new bilateral symmetric vein pair in the thoracic and lumbar regions of the body, dorsal and lateral to the aorta, along the ipsilateral sympathetic trunks (Butler, 1927). They are initially solely responsible for the drainage of the dorsal body wall, but during subsequent development, their caudal segment will enter into the construction of the caudal vena cava (Patten, 1948).

In the lumbar region, the supracardinal veins arise at the level of the developing hindlimb, and can be followed in cranial direction until the level of the subcardinal anastomosis. In the thoracic region, the supracardinal veins arise as branches of the remaining cranial segments of the caudal cardinal veins and can be followed to a position slightly cranial of the subcardinal anastomosis. It is not uncommon in the pig that both the thoracic and lumbar segments of these veins fuse with each other to form on each side of the aorta a single continuous channel throughout their entire length (Butler, 1927).

The caudal ends of the lumbar segments of the supracardinal veins connect with the caudal segments of the caudal cardinal veins (Rüsse, 1991b). Blood coming from the hindlimbs and pelvic region is now shifted towards these supracardinal veins, which will subsequently pass it along newly formed supracardinal-subcardinal anastomoses to the large

subcardinal sinus (Patten, 1948). Due to this shift, the role of the caudal segments of the caudal cardinal veins is now reduced to the formation of the iliac veins only (Noden and de Lahunta, 1985).

Butler (1927) described that, at least in the pig and the sheep, an intermediate step is required to shift the venous drainage of the hindlimbs from the caudal cardinal veins to the supracardinal veins. Prior to the development of the supracardinal veins, a lateral mesonephric vein, coursing along the lateral surface of each mesonephros between its caudal pole and the level of the subcardinal anastomosis, arises in the 12-14 mm embryo. As soon as this vein is formed, it takes over the drainage of the hindlimb and pelvic region from the ipsilateral caudal cardinal vein, to pass this task on to the supracardinal vein after its construction in the 17-19 mm embryo (Butler, 1927) (Fig. 6). Remarkably, although Patten (1948) is directly referring to the original investigations by Butler (1927), no sign of these lateral mesonephric veins can be found in its specific work on the development of the pig embryo: the function of the caudal cardinal veins is directly taken over by the supracardinal veins, similar to the condition described in the cat (Huntington and McClure, 1920) and in man (McClure and Butler, 1925).

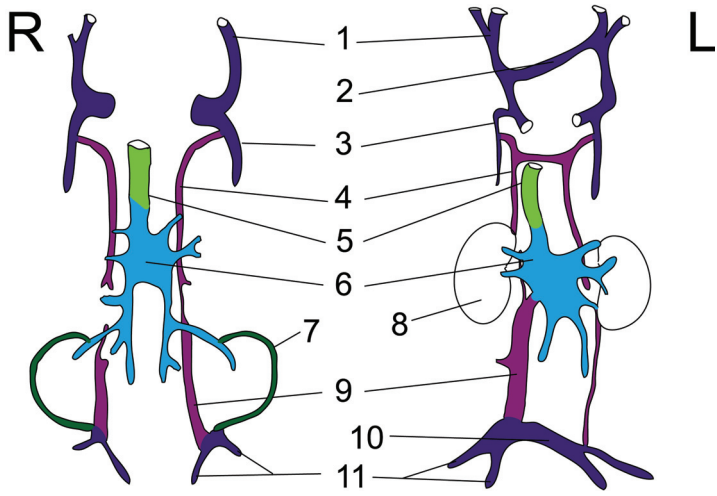

Fig. 6: Schematic representation of the venous pattern in the 16-19 mm (left) and 22-24 mm (right) pig embryo, ventral view (after Butler, 1927; Patten, 1948). 1: cranial cardinal veins, 2: precardial anastomosis, 3: cranial segments of the caudal cardinal veins, 4: thoracic segments of the supracardinal veins, 5: right vitelline segment of the caudal vena cava, 6: subcardinal sinus, 7: left lateral mesonephric vein, 8: right kidney, 9: lumbar segments of the supracardinal veins, 10: iliac anastomosis, 11: internal and external iliac veins.

1.2.3.4. The final construction of the caudal vena cava

In the 22-24 mm embryo, an anastomosis between the left and right common iliac veins is formed (Fig. 6). Next, the lumbar segment of the left supracardinal vein regresses in favour of its right-sided counterpart which further grows and adopts the same diameter as the right vitelline vein draining the subcardinal anastomosis through its mesenteric connection. The thoracic segments of the supracardinal veins interconnect with each other dorsal to the aorta and will, together with the cranial remnants of the caudal cardinal veins eventually evolve into the left azygos and right hemiazygos veins (Butler, 1927; Rüsse, 1991b).

In the 30-35 mm pig embryo (Fig. 7), the construction of the caudal vena cava is nearly complete (Butler, 1927). The right-sided part of the subcardinal sinus has adopted a more tubular shape and is integrated into the final construction of the caudal vena cava, whilst the left-sided segment is transformed into the left renal vein (Patten, 1948).

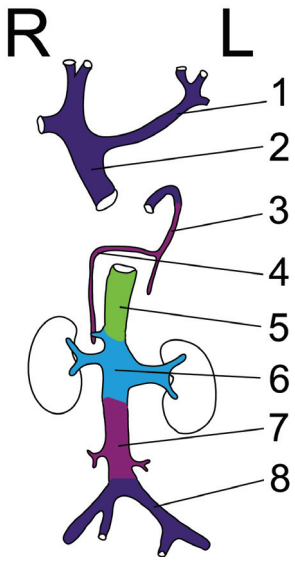

Fig. 7: Schematic representation of the venous arrangement in the 30-35 mm pig embryo, ventral view (after Patten, 1948). Dark blue segments originated from the cardinal veins, pale blue segments from the subcardinal veins, the green segment is derived from the vitelline veins and the purple segment from the supracardinal veins. 1: left brachiocephalic vein, 2: cranial vena cava, 3: left azygos vein, 4: right hemiazygos vein, 5: intrathoracic and hepatic segment of the caudal vena cava, 6: renal segment of the caudal vena cava, 7: infrarenal or lumbar segment of the caudal vena cava, 8: left common iliac vein.

In the adult pig, blood coming from the hindlimbs passes due to the complex construction pattern of caudal vena cava through several venous segments, each belonging to the same channel but characterised by a different origin: the common iliac veins as the remnants of the caudal cardinal veins, the lumbar or infrarenal segment of the caudal vena cava (CVC) built from the right supracardinal vein, the renal segment of the CVC derived from the subcardinal sinus, and the hepatic and thoracic segments of the CVC as a part of the right vitelline vein. When all anastomoses between the original embryonic veins involved in the formation of the CVC are also taken into account, at least 7 different vessels are involved in the final construction of the caudal vena cava (Noden and de Lahunta, 1985).

However, in the next chapter, it will be demonstrated that many aspects of this theory on the development of the caudal vena cava are still controversial, hampering the proper application of this developmental pattern in angiogenesis research.

1.3. Literature

Bahramsoltani, M. and J. Plendl (2007). Different ways to antiangiogenesis by angiostatin and suramin, and quantitation of angiostatin-induced antiangiogenesis. *Acta Pathologica, Microbiologica, et Immunologica Scandinavica* 115, 30-46.

Bailey, A.S. and W.H. Fleming (2003). Converging roads: evidence for an adult hemangioblast. *Experimental Hematology* 31, 987-993.

Baron, M.H. (2003). Embryonic origins of mammalian hematopoiesis. *Experimental Hematology* 31, 1160-1169.

Bautch, V.L., S.D. Redick, A. Scalia, M. Harmaty, P. Carmeliet and R. Rapoport (2000). Characterization of the vasculogenic block in the absence of vascular endothelial growth factor-A. *Blood* 95, 1979-1987.

Butler, E.G. (1927). The relative rôle played by the embryonic veins in the development of the mammalian vena cava posterior. *The American Journal of Anatomy* 39, 267-353.

Carmeliet, P. (2005). Angiogenesis in life, disease and medicine. *Nature* 438, 932-936.

Charnock-Jones, D.S., P. Kaufmann and T.M. Mayhew (2004). Aspects of human fetoplacental vasculogenesis and angiogenesis. I. Molecular regulation. *Placenta* 25, 103-113.

Chen, J.-X., H. Zeng, M.L. Lawrence, T.S. Blackwell and B. Meyrick (2006). Angiopoietin-1 induced angiogenesis is modulated by endothelial NADPH oxidase. *American Journal of Physiology – Heart and Circulatory Physiology* 291, 1563-1572.

Coffin, J.D. and T.J. Poole (1991). Endothelial cell origin and migration in embryonic heart and cranial blood vessel development. *Anatomical Record* 231, 383-395.

Coultas, L., K. Chawengsaksophak and J. Rossant (2005). Endothelial cells and VEGF in vascular development. *Nature* 438, 937-945.

Davis, S., T.H. Aldrich, P.F. Jones, A. Acheson, D.L. Compton, V. Jain, T.E. Ryan, J. Bruno, C. Radziejewski, P.C. Maisonpierre and G.D. Yancopoulos (1996). Isolation of angiopoietin-1, a ligand for the TIE2 receptor, by secretion-trap expression cloning. *Cell* 87, 1161-1169.

Demir, R., Y. Seval and B. Huppertz (2007). Vasculogenesis and angiogenesis in the early human placenta. *Acta histochemica* 109, 257-265.

Döme, B., M.J.C. Hendrix, S. Paku, J. Tóvári ad J. Tímár (2007). Alternative vascularisation mechanisms in cancer: pathology and therapeutic implications. *The American Journal of Pathology* 170, 1-15.

Dor, Y., V. Djonov and E. Keshet (2003). Induction of vascular networks in adult organs: implications to proangiogenic therapy. *Annals of the New York Academy of Sciences* 995, 208-216.

Dyer, M.A., S.M. Farrington, D. Mohn, J.R. Munday, and M.H. Baron (2001). Indian hedgehog activates hematopoiesis and vasculogenesis and can respecify prospective neurectodermal cell fate in the mouse embryo. *Development* 128, 1717-1730.

Fam, N.P., S. Verma, M. Kutryk and D.J. Stewart (2003). Clinician guide to angiogenesis. *Circulation* 108, 2613-2618.

Ferguson, J.E., R.W. Kelley and C. Patterson (2005). Mechanisms of endothelial differentiation in embryonic vasculogenesis. *Arteriosclerosis, Thrombosis, and Vascular Biology* 25, 2246-2254.

Fiedler, U., M. Scharpfenecker, S. Koidl, A. Hegen, V. Grunow, J.M. Smidt, W. Kriz, G. Thurston and H.G. Augustin (2004). The Tie-2 ligand Angiopoietin-2 is stored in and rapidly released upon stimulation from endothelial cell Weibel-Palade bodies. *Blood* 103, 4150-4156.

Folkman, J. (2002). Role of angiogenesis in tumor growth and metastasis. *Seminars in Oncology* 29 (Suppl 16), 15-18.

Furata, C., H. Ema, S.-I. Takayanagi, T. Ogaeri, D. Okamura, Y. Matsui and H. Nakauchi (2006). Discordant developmental waves of angioblasts and hemangioblasts in the early gastrulating mouse embryo. *Development* 133, 2771-2779.

Gilbert, S.F. (2000). Developmental Biology, sixth edition. Sinnauer Associates Inc., Sunderland MA, p. 471-490.

Griffioen, A.W. and G. Molema (2000). Angiogenesis: potentials for pharmacologic intervention in the treatment of cancer, cardiovascular diseases, and chronic inflammation. *Pharmacological reviews* 52, 237-268.

Hanahan, D. (1997). Signaling vascular morphogenesis and maintenance. *Science* 277, 48-50.

Herzog, Y., C. Kalcheim, N. Kahane, R. Reshef and G. Neufeld (2001). Differential expression of neuropilin-1 and neuropilin-2 in arteries and veins. *Mechanisms of Development* 109, 115-119.

Hughes, G.C., M.J. Post, M. Simons and B.H. Annex (2003). Translational physiology: porcine models of human coronary artery disease: implications for preclinical trials of therapeutic angiogenesis. *Journal of Applied Physiology* 94, 1689-1701.

Huntington, G.S. and C.F.W. McClure (1920). The development of the veins in the domestic cat (felis domestica) with especial reference, 1) to the share taken by the supracardinal veins in the development of the postcava and azygos veins and 2) to the interpretation of the variant conditions of the postcava and its tributaries, as found in the adult. *Anatomical Record* 20, 1-30.

Kim, I., H.G. Kim, J.-N. So, J.H. Kim, H.J. Kwak and G.Y. Koh (2000). Angiopoietin-1 regulates endothelial cell survival through the phosphatidylinositol 3'-kinase/Akt signal transduction pathway. *Circulation Research* 86, 24-29.

Kubota, S. And M. Takigawa (2007). CCN family proteins and angiogenesis: from embryo to adulthood. *Angiogenesis* 10, 1-11.

LaRue, A.C., R. Lansford and C.J. Drake (2003). Circulating blood island-derived cells contribute to vasculogenesis in the embryo proper. *Developmental Biology* 262, 162-172.

Lawson, N.D., N. Scheer, V.N. Pham, Ch.-H. Kim, A.B. Chitnis, J.A. Campos-Ortega and B.M. Weinstein (2001). Notch signalling is required for arterio-venous differentiation during embryonic vascular development. *Development* 128, 2675-3683.

Levenberg, S. (2005). Engineering blood vessels from stem cells: recent advances and applications. *Current Opinion in Biotechnology* 16, 516-523.

Loughna, S. and T.N. Sato (2001). A combinatorial role of Angiopoietin-1 and orphan receptor TIE1 pathways in establishing vascular polarity during angiogenesis. *Molecular cell* 7, 233-239.

Maisonpierre, P.C., C. Suri, P.F. Jones, S. Bartunkova, S.J. Wiegand, C. Radziejewski, D. Compton, J. McClain, T.H. Aldrich, N. Papadopoulos, T.J. Daly, S. Davis, T.N. Sato and G.D. Yancopoulos (1997). Angiopoietin-2, a natural antagonist for Tie2 that disrupts in vivo angiogenesis. *Science* 277, 55-60.

Marron, M.B., H. Singh, T.A. Tahir, J. Kavumkal, H.-Z. Kim, G.Y. Koh and N.P.J. Brindle (2007). Regulated proteolytic processing of Tie1 modulates ligand responsiveness of the receptor-tyrosine kinase Tie2. *The Journal of Biological Chemistry* 282, 30509-30517.

McClure, C.F.W. and E.G. Butler (1925). The development of the vena cava inferior in man. *The American Journal of Anatomy* 35, 331-383.

McGeady, T.A., P.J. Quinn, E.S. FitzPatrick and M.T. Ryan (2006). Veterinary Embryology. Blackwell Publishing, Oxford, p. 105-135.

Metheny-Barlow, L. and L.Y. Li (2003). The enigmatic role of angiopoietin-1 in tumor angiogenesis. *Cell research* 13, 309-317.

Milkiewicz, M., E. Ispanovic, J.L Doyle and T.L. Haas (2006). Regulators of angiogenesis and strategies for their therapeutic manipulation. *The International Journal of Biochemistry & Cell Biology* 38, 333-357.

Morisada, T., Y. Kubota, T. Urano, T. Suda and Y. Oike (2006). Angiopoietins and angiopoietin-like proteins in angiogenesis. *Endothelium* 13, 71-79.

Moyon, D., L. Pardanaud, L. Yuan, C. Bréant and A. Eichmann (2001). Selective expression of angiopoietin 1 and 2 in mesenchymal cells surrounding veins and arteries of the avian embryo. *Mechanisms of Development* 106, 133-136.

Naumov, G.N., L.A. Akslen and J. Folkman (2006). Role of angiogenesis in human tumor dormancy: animal models of the angiogenic switch. *Cell Cycle* 5, 1779-1787.

Noden, D. and A. de Lahunta (1985). The embryology of domestic animals: developmental mechanisms and malformations. Williams & Wilkins, London, p. 257-269.

Norrby, K. (2006). *In vivo* models of angiogenesis. *Journal of Cellular and Molecular Medicine* 10, 588-612.

Papetti, M. and I.M. Herman (2002). Mechanisms of normal and tumor-derived angiogenesis. *American Journal of Physiology. Cell Physiology* 282, C947-C970.

Pardanaud, L., D. Luton, M. Prigent, L.-M. Bourcheix, M. Catala and F. Dieterlen-Lièvre (1996). Two distinct endothelial lineages in ontogeny, one of them related to hematopoiesis. *Development* 122, 1363-1371.

Patten, B.M. (1948). Embryology of the pig. McGraw-Hill Book Company, London, p. 240-250.

Perbal, B. (2004). CCN proteins: multifunctional signalling regulators. *Lancet* 363, 62-64.

Ratajska, A. and E. Czarnowska (2006). Vasculogenesis of the embryonic heart contribution of nucleated red blood cells to early vascular structures. *Cardiovascular & Haematological Disorders-Drug Targets* 6, 219-225.

Ribatti, D. (2006). Genetic and epigenetic mechanisms in the early development of the vascular system. *Journal of Anatomy* 208, 139-152.

Ribatti, D. (2007). The discovery of endothelial progenitor cells: an historical review. *Leukemia Research* 31, 439-444.

Ribatti, D., B. Nico, E. Crivellato, A.M. Roccaro and A. Vacca (2007). The history of the angiogenic switch concept. *Leukemia* 21, 44-52.

Rossant, J. and M. Hiraschima (2003). Vascular development and patterning: making the right choices. *Current Opinion in Genetics & Development* 13, 408-412.

Rüsse, I. (1991a). Frühgravität, Implantation und Plazentation. In: Rüsse, I. and F. Sinowatz (editors) Lehrbuch der Embryologie der Haustiere. Verlag Paul Parey, Hamburg, p. 153-218.

Rüsse, I. (1991b). Herz- und Kreislaufsystem. In: Rüsse, I. and F. Sinowatz (editors) Lehrbuch der Embryologie der Haustiere. Verlag Paul Parey, Hamburg, p. 221-246.

Rüsse, I. and F. Sinowatz (1991). Lehrbuch der Embryologie der Haustiere. Verlag Paul Parey, Hamburg, 478 pp.

Sadler, T.W. (1985). Langman's Medical Embryology, fifth edition. Williams & Wilkins, Baltimore, p. 168-169.

Serini, G., D. Ambrosi, E. Giraudo, A. Gamba, L. Preziosi and F. Bussolino (2003). Modeling the early stages of vascular network assembly. *The European Molecular Biology Organization Journal* 22, 1771-1779.

Shalaby, F., J. Rossant, T.P. Yamaguchi, M. Gertsenstein, X.-F. Wu, M.L. Breltman and A.C. Schuh (1995). Failure of blood-island formation and vasculogenesis in Flk-deficient mice. *Nature* 376, 62-66.

Suri, C., P.F. Jones, S. Patan, S. Bartunkova, P.C. Maisonpierre, S. Davis, T.N. Sato and G.D. Yancopoulos (1996). Requisite role of angiopoietin-1, a ligand for the TIE2 receptor, during embryonic angiogenesis. *Cell* 87, 1171-1180.

Thurston, G. (2002). Complementary actions of VEGF and Angiopoietin-1 on blood vessel growth and leakage. *Journal of Anatomy* 200, 575-580.

Ucuzian, A.A. and H.P. Greisler (2007). In vitro models of angiogenesis. *World Journal of Surgery* 31, 654-663.

Urness, L.D., L.K. Sorensen and D.Y. Li (2000). Arteriovenous malformations in mice lacking activin receptor-like kinase-1. *Nature Genetics* 26, 328-331.

Velazquez, O.C. (2007). Angiogenesis and vasculogenesis: inducing the growth of new blood vessels and wound healing by stimulation of bone marrow-derived progenitor cell mobilization and homing. *Journal of Vascular Surgery* 45, 39A-47A.

Wang, H.U., Z.-F. Chen and D.J. Anderson (1998). Molecular distinction and angiogenic interaction between embryonic arteries and veins revealed by ephrin-B2 and its receptor Eph-B4. *Cell* 93, 741-753.

Ward, N.L. and D.J. Dumont (2002). The angiopoietins and Tie2/Tek: adding to the complexity of cardiovascular development. *Seminars in Cell & Developmental Biology* 13, 19-27.

Yancopoulos, G.D., S. Davis, N.W. Gale, J.S. Rudge, S.J. Wiegand and J. Holash (2000). Vascular-specific growth factors and blood vessel formation. *Nature* 407, 242-248.

Ye, L., H.Kh. Haider, S. Jiang, R.S. Ran, W.Ch. Toh, R.W. Ge and E.K.W. Sim (2007). Angiopoietin-1 for myocardial angiogenesis: a comparison between delivery strategies. *European Journal of Heart Failure* 9, 458-465.

Yuan, H.T., C. Suri, D.N. Landon, G.D. Yancopoulos and A.S. Woolf (2000). Angiopoietin-2 is a site-specific factor in differentiation of mouse renal vasculature. *Journal of the American Society of Nephrology* 11, 1055-1066.

CHAPTER 2:
PROBLEMS AND SCIENTIFIC AIMS

2.1. Questioning the existing supracardinal model

2.2. Scientific aims

2.3. Literature

Based on:

Cornillie, P. and P. Simoens (2005). Prenatal development of the caudal vena cava in mammals: review of the different theories with special reference to the dog. *Anatomia, Histologia, Embryologia* 34, 364-372.

Cornillie, P., T. Baten and P. Simoens (2006). Retrocaval ureter in a cat. *The Veterinary Record* 159, 24-25.

CHAPTER 2: PROBLEMS AND SCIENTIFIC AIMS

2.1. Questioning the existing supracardinal model

2.1.1. Introduction

Despite the presence of a commonly accepted and widely used model describing the development of the caudal vena cava as depicted in the previous chapter, several items of this developmental pattern both in man and domestic animals are still controversial. In particular, the origin of the lumbar segment of the caudal vena cava is equivocally described. At least five different theories describing the building plan of the caudal vena cava in man or domestic animals can be found in recent papers and current textbooks. Due to these inconsistencies, more certainty about the exact developmental pattern of the caudal vena cava is needed before it can be used as a model to study the factors controlling the physiological stabilization or regression of existing blood vessels in animal models.

One possible way to clarify some aspects on this matter is by carefully studying the congenital malformations and anatomical variations of the venous system as found in man or domestic animals. In fact, teratology offers a useful tool to explain some specific stages in normal embryonic development, as an anatomical variation is often reflecting a normally transient embryonic configuration that for some reason failed to further evolve into the final adult composition. Additionally, malformations of the caudal vena cava can also be explained by an alternative course of development, in which the share of a certain embryonic vein in the construction of the adult caudal vena cava is taken over by another vein, secondary to the failure of the former vessel to become properly constructed.

In the following sections, the differences between the five existing theories on the development of the caudal vena cava as well as some possible explanations for these inconsistencies will be discussed. Subsequently, descriptions of some anatomical variations of the cranial and caudal vena cava will be matched with the current theories on the development of the venous system in an attempt to rule out some ambiguities on this matter. A number of alternative venous configurations in the dog and cat as personally observed during two years teaching practical courses of Anatomy at the department of

Morphology, Ghent University, will serve as a basis for this analysis, completed with some data from literature.

2.1.2. Alternative theories on the development of the caudal vena cava

The five different models discussed in this section are, up to a certain level, quite similar to each other. However, next to some minor discrepancies, they all have a different viewpoint about the origin of the caudalmost segment of the caudal vena cava, situated caudal to the renal veins and often referred to as the infrarenal or lumbar segment of the caudal vena cava. Each of these theories will be named below according to the original embryonic vein which is considered as the precursor of that particular part of the caudal vena cava. Successively, the main characteristics of the supracardinal model, the caudal cardinal model, the sacrocardinal model, the lateral sympathetic model and the subcardinal model will be discussed. A general overview of all 5 theories is given in figure 8.

2.1.2.1. The supracardinal model (Fig. 8A)

The supracardinal model is the most common theory (Bass et al., 2000), and both the official Nomina Embryologica (1983) and Nomina Embryologica Veterinaria (2006) are based upon this model. It is well documented in recent papers (Hunt et al., 1998; Bass et al. 2000; Sandercoe and Brooke-Cowden, 2003) and in many textbooks (Patten, 1948; Arey, 1974; Patten and Carlson, 1974; Noden and de Lahunta, 1985; Rüsse and Sinowatz, 1991; Carlson, 1994; Barone, 1996; McGeady et al., 2006). All these descriptions refer directly or indirectly to the original work of Huntington and McClure (1920) who studied feline embryos, McClure and Butler (1925) who examined human embryos and Butler (1927) who investigated embryos of different species including the pig, sheep and bat. The major characteristics of this model have elaborately been discussed in section 1.2.3.. Compared to the different other theories, especially the concept that the azygos veins and the infrarenal part of the caudal vena cava both arise from the embryonic supracardinal veins is a typical and unique feature of the supracardinal model.

According to Butler (1927), the supracardinal model applies for all mammalian species in which the activity of the mesonephroi persists over a comparatively long period during embryonic development, as the size and functional life span of the mesonephroi are important for the development of the veins in the caudal part of the embryo. Furthermore, in

embryos of species such as the pig which have highly functional and long-lasting mesonephroi, additional veins such as the ventral and lateral mesonephric veins develop temporarily to assure an adequate drainage of the very large mesonephroi (Butler, 1927). In the cat, which has smaller but still functional mesonephroi (Noden and de Lahunta, 1985), the developmental pattern of the venous system most closely resembles the supracardinal model as shown in fig. 8A (Huntington and McClure, 1920).

2.1.2.2. The caudal cardinal model (Fig. 8B)

The caudal cardinal model was initially proposed by Hochstetter in 1893 and has later on been refined by Butler (1927). In contrast to the other theories discussed further in this section, this model does not question the accuracy of the supracardinal model. It is merely an extension of the latter towards mammalian species in which the mesonephroi barely develop, such as rabbits, in which the functional period of the mesonephroi lasts only 5 days (Leeson and Baxter, 1957) and rats, in which the mesonephroi remain functionless. In these species, the right caudal cardinal vein takes a greater share in the development of the caudal vena cava because the supracardinal venous plexus is formed only during a small period of development and never gives rise to two prominent longitudinal channels in the lumbar region (Butler, 1927).

The right caudal cardinal vein is less privileged than the right supracardinal vein to construct the caudal part of the caudal vena cava, because its initial anatomical position is lateral and ventral to the ipsilateral metanephros. The right ureter impedes the easy transition of the caudal cardinal vein towards its final position which is dorsal and medial to the right kidney. According to Hochstetter (1893), a periureteric venous ring is formed in the rabbit on the course of the caudal cardinal vein in a first step to bypass the ureter. In a second phase, the ventral segment of the ring degenerates, allowing the further migration of the caudal cardinal vein towards its final destination (Fig. 9). The dorsal (or medial) segment of the periureteric ring is allegedly of supracardinal origin (Fig. 8Bb) (Butler, 1927).

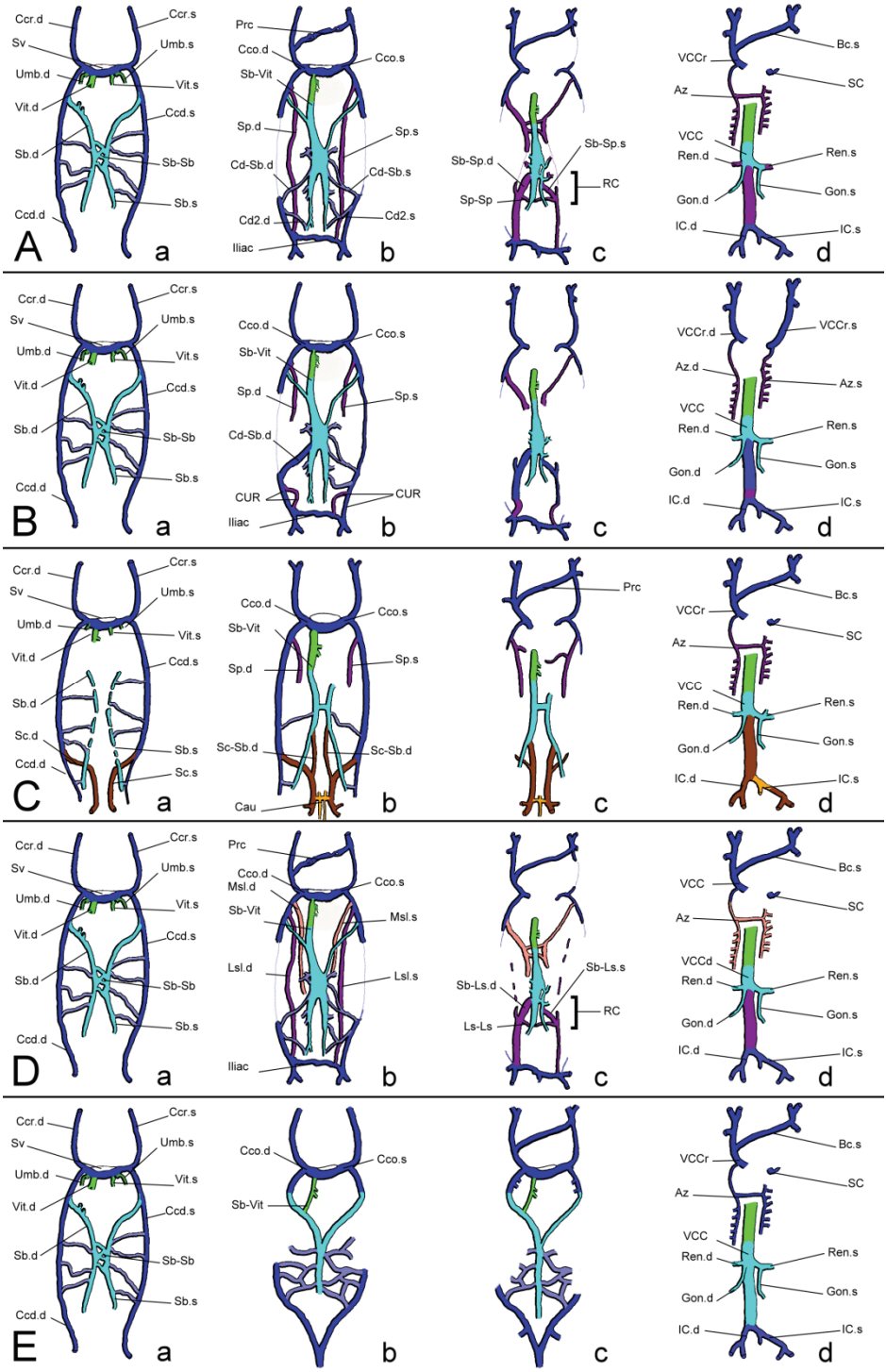
Ccr.d
Ccr.s
Sv
Umb.s
Umb.d
Vit.s
Vit.d
Ccd.s
Sb.d
Sb-Sb
Sb.s
Ccd.d
A
a
Prc
Cco.d
Cco.s
Sb-Vit
Sp.d
Sp.s
Cd-Sb.d
Cd-Sb.s
Cd2.d
Cd2.s
Iliac
b
Sb-Sp.s
Sb-Sp.d
RC
Sp-Sp
c
VCCr
Bc.s
SC
Az
VCC
Ren.d
Ren.s
Gon.d
Gon.s
IC.d
IC.s
d
B
CUR
C
Sc.d
Sc-Sb.d
Sc.s
Cau
VCCr.d
VCCr.s
Az.d
Az.s
D
Msl.d
Msl.s
Lsl.d
Lsl.s
Sb-Ls.s
Sb-Ls.d
Ls-Ls
VCCd
E

Fig. 8: Schematic drawing of the five models discussed in this section.

A: Supracardinal model
B: Caudal cardinal model
C: Sacrocardinal model
D: Lateral sympathetic model
E: Subcardinal model

a: Primary stage
b: Intermediate stage
c: Secondary stage
d: Final stage (staging after Grünwald, 1938)

Az	Vena azygos
Az.d	Vena azygos dextra
Az.s	Vena azygos sinistra
Bc.s	Vena brachiocephalica sinistra
Cau	Venae caudales
Ccd.d	Vena cardinalis caudalis dextra
Ccd.s	Vena cardinalis caudalis sinistra
Cco.d	Vena cardinalis communis dextra
Cco.s	Vena cardinalis communis sinistra
Ccr.d	Vena cardinalis cranialis dextra
Ccr.s	Vena cardinalis cranialis sinistra
Cd2.d	Right mesonephric branch of the caudal cardinal vein
Cd2.s	Left mesonephric branch of the caudal cardinal vein
Cd-Sb.d	Right caudal cardinal-subcardinal anastomosis
Cd-Sb.s	Left caudal cardinal-subcardinal anastomosis
CUR	Periureteric venous ring
Gon.d	Vena gonadalis dextra
Gon.s	Vena gonadalis sinistra
IC.d	Vena iliaca communis dextra
IC.s	Vena iliaca communis sinistra
Iliac	Iliac anastomosis (Arey, 1974)
Lsl.d	Right lateral sympathetic line vein
Lsl.s	Left lateral sympathetic line vein
Ls-Ls	Lateral sympathetic vein anastomosis
Msl.d	Right medial sympathetic line vein
Msl.s	Left medial sympathetic line vein
Prc	Anastomosis precardinalis
RC	Renal collar = circumaortic venous ring
Ren.d	Vena renalis dextra
Ren.s	Vena renalis sinistra
Sb.d	Vena subcardinalis dextra
Sb.s	Vena subcardinalis sinistra
Sb-Sb	Anastomosis subcardinalis
Sb-Ls.d	Right subcardinal-lateral sympathetic vein anastomosis
Sb-Ls.s	Left subcardinal-lateral sympathetic vein anastomosis
Sb-Sp.d	Anastomosis subsupracardinalis dextra
Sb-Sp.s	Anastomosis subsupracardinalis sinistra
Sb-Vit	Anastomosis subcardinalis-vitellina
SC	Sinus coronarius
Sc.d	Vena sacrocardinalis dextra
Sc.s	Vena sacrocardinalis sinistra
Sc-Sb.d	Anastomosis sacrosubcardinalis dextra
Sc-Sb.s	Anastomosis sacrosubcardinalis sinistra
Sp.d	Vena supracardinalis dextra
Sp.s	Vena supracardinalis sinistra
Sp-Sp	Anastomosis supracardinalis
Sv	Sinus venosus
Umb.d	Vena umbilicalis dextra
Umb.s	Vena umbilicalis sinistra
VCCr	Vena cava cranialis
VCCr.d	Vena cava cranialis dextra
VCCr.s	Vena cava cranialis sinistra
VCC	Vena cava caudalis
Vit.d	Vena vitellina dextra
Vit.s	Vena vitellina sinistra

A particular feature of the caudal cardinal model is the persistence of the left cranial cardinal vein and the absence of the precardinal anastomosis, resulting in both a left and a right cranial vena cava in the adult, in contrast to what is shown in the other models. This characteristic is illustrated in figure 8B, which is based on the vein development in the rabbit. Like in rodents such as the mouse, rat and hamster, a double cranial vena cava is the normal anatomical configuration in this species (Popesko et al., 1992a & 1992b).

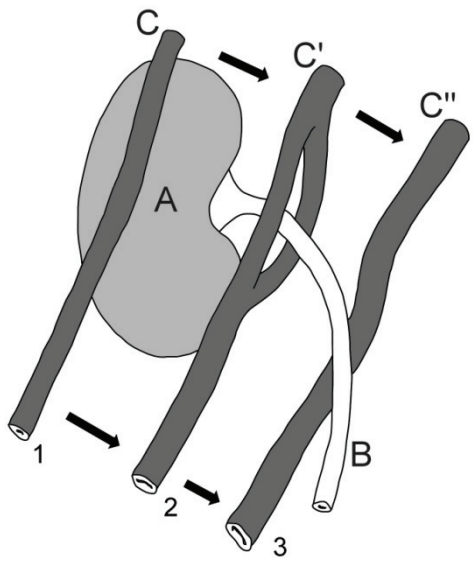

Fig. 9: Schematic compilatory drawing of the migration of the right caudal cardinal vein during embryonic development in the rabbit according to Hochstetter (1893) and Butler (1927) (ventral view). A. right metanephros, B: ureter, C - C' - C'': right caudal cardinal vein. 1: Initial location of the caudal cardinal vein ventral and lateral to the metanephros. 2: Vascular migration in medial direction and formation of a periureteric vascular ring. 3: Loss of the ventral half of the periureteric ring and further migration towards the final position of the caudal vena cava.

2.1.2.3. The sacrocardinal model (Fig. 8C)

In a reaction to the publication of the supracardinal model by the group of Huntington, McClure and Butler (cfr. supra), Grünwald (1938) presented the sacrocardinal model which is often referred to in German handbooks (Starck, 1975; Michel, 1986; Schnorr, 1989), and also in Langman's Medical Embryology by Sadler (1985).

Grünwald (1938), who studied the venous development in human embryos, never found the supracardinal veins reaching the lumbar region. Instead, in this region he observed a new pair of veins, which he named the left and right sacrocardinal veins and which he described as important participants in the construction of the caudal vena cava (Fig. 8C). The role of the supracardinal veins in this model is reduced to the formation of the azygos and hemi-azygos veins. Furthermore, Grünwald (1938) also highlights the previously neglected

importance of the caudal veins (Fig. 8C: Cau) in the formation of an anastomosis between the left and right venous channels that lie caudal in the embryo and contribute to the construction of the left common iliac vein. A final major difference between both theories is the fact that in the sacrocardinal model the subcardinal veins do not merge with the ipsilateral caudal cardinal veins cranial to the mesonephroi. Until a connection is established between the right subcardinal vein and the hepatic veins, the subcardinal system does not take part in the direct drainage of blood from the hind quarters and abdomen towards the heart.

Besier and Stofft (1977), Fasel and Ludwig (1988) and Forte et al. (2002) explained some anatomical variations of the caudal vena cava in human patients by means of the sacrocardinal model. Fasel and Ludwig (1988) were familiar with both the supracardinal and sacrocardinal model. In an attempt to clear the ambiguities on this topic, they performed a new study on the development of the venous system in the human embryo and confirmed the sacrocardinal origin of the infrarenal part of the caudal vena cava as described by Grünwald (1938). The same conclusion was drawn ten years later by Petrenko (1998).

2.1.2.4. The lateral sympathetic model (Fig. 8D)

This model is very similar to the supracardinal model, except for the origin of the azygos veins which is attributed to a new pair of veins named the medial sympathetic or azygos line veins. Therefore, the supracardinal veins in this model are usually designated as lateral sympathetic line veins. The names of these two different vein pairs are derived from their relative location inside the embryo as the former lie medial and the later are situated lateral to the developing sympathetic trunk.

More detailed descriptions of this model can be found in papers by Loughna and Sato (1991), Rahalkar (2002) and Trubač et al. (2002) and in several handbooks (Dierickx, 1969; Williams et al., 1993). We could trace this theory back to Gladstone (1929), who further referred to Sabin (1915), Reagan and Robinson (1926) and Reagan and Tribe (1926).

2.1.2.5. The subcardinal model (Fig. 8E)

This last theory is the oldest of the five models discussed. According to Butler (1927), it has initially been proposed by Rathke (1838). Balinsky (1981) used this model to exemplify the transformation of the veins in embryos of terrestrial vertebrates, based on observations of developing pig embryos.

According to this theory, the left and right subcardinal veins fuse and form one large vessel along the midline of the embryo. The entire caudal vena cava is believed to arise almost entirely from this vessel, except for its hepatic segment which originates from the right vitelline vein. Furthermore, the azygos vein is said to be a remnant of the right caudal cardinal vein. Additional vessels such as the supracardinal or sacrocardinal veins are not described in this model. This theory has been rejected by Butler (1927) when presenting the supracardinal model, and Grünwald (1938) also reported never to have seen an entire fusion of the left and right subcardinal veins.

2.1.2.6. Discussion

The discrepancies between the different theories about systemic vein development in mammalian embryos can be ascribed to several reasons, including interspecies variations, methodological and technical restrictions, and nomenclatory confusions.

The anatomical configuration of the venous system in adult mammals differs considerably from one species to another. This variation implies that the venous development in the embryo is characterised by species-specific pathways. Two examples of vascular arrangements dissimilar to the situation in man and common domestic animals are the duplication of the cranial vena cava as a normal arrangement in the rabbit and some rodents (Popesko et al., 1992a & 1992b), and the double caudal vena cava which is a regular finding in whales and dolphins (Barone, 1996). However, these alternative configurations have been reported many times as uncommon variations of the venous system in man (Bass et al., 2000) and in several domestic animals including the dog (*see section 2.1.3.*). Furthermore, there are many similarities between the variations of the venous system reported in man and those seen in domestic animals. This supports the idea that there is a common blueprint for the developmental pattern of the venous system in all mammals, while only later in embryonic development species-specific modifications are responsible for the particular characteristics of the various anatomical configurations. The major features that are common in all five models form the basic blueprint and are listed in Table 1.

In the comparative study of Butler (1927) both the sacrocardinal and caudal cardinal model are described and linked to species-specific developmental features, in particular to the functionality of the mesonephroi. Species-specificity however does not solely account for the differences between the five models, as evidenced by the fact that for the human species three different models have been described, viz. the supracardinal, lateral sympathetic and sacrocardinal model.

The controversial statements about the development of the caudal segment of the caudal vena cava can partly also be ascribed to technical limitations of ancient embryologic procedures. Three-dimensional reconstructions of embryos were usually based on wax models that were moulded after serial histological cross-sections from paraffin embedded

embryos (Grünwald, 1938). This technique had many disadvantages. Perpendicular cross-sections were necessary to make a reliable reconstruction, and loss or damage by cracking or folding of any cross-section was detrimental for the entire procedure (Grünwald, 1938). Furthermore, because early embryos are strongly curved, only a specific segment of the embryo, depending on its orientation in the paraffin block, could be cut into cross-sections perpendicular to the longitudinal axis. To solve this problem, several embryos of the same age were oriented differently in the paraffin blocks, and only the perfectly perpendicular cross-sections were compiled in the right order to reconstruct a stretched virtual embryo. This method required a large amount of embryos to be sectioned. In most cases the embryos came from different laboratories and were fixated and stained in different ways (McClure and Butler, 1925; Butler, 1927; Grünwald, 1938). Moreover, it was found that embryos of the same length did not necessarily have the same developmental age nor an identical venous configuration (McClure and Butler, 1925). Furthermore, exact measurements could not be performed on the wax plates, as they needed to be polished before reconstruction (Grünwald, 1938). Only the use of an ocular graticule to calculate the distance between a specific vessel and the imaginary midline of the embryo during light microscopic observation of the sections could provide some reliable numerical data.

Table 1: Common features of the five different models.

- Early embryonic vein configuration is initially bilaterally symmetric.
- During the development of the caudal vena cava, the left venous channels regress and the blood flow is shifted towards the right side of the body.
- The complete differentiation from a bilaterally symmetric system to a single right-sided caudal vena cava is first established in the segments cranial to the metanephroi, and only later on in the region caudal to the kidneys.
- The hepatic and intrathoracic segments of the caudal vena cava are derived from the right vitelline vein.
- An anastomosis between the right subcardinal vein and the cranial segment of the right vitelline vein is established very early in development.
- The caudal cardinal veins disappear together with the regression of the mesonephroi.
- The subcardinal veins, in particular the right subcardinal vein, take over the main venous drainage after regression of the caudal cardinal veins.

The problems encountered in the wax model technique can be avoided by modern techniques such as microvascular corrosion casting (Ozerdem et al., 2002) and non-invasive 3D microtomography technologies such as micro-Computerized Tomography (Sasov and Van

Dyck, 1998), micro-Magnetic Resonance Imaging (Schneider et al., 2003) and Optical Projection Tomography (Sharpe, 2003). These methods can give novel, highly qualitative and more reliable insights in the embryonic development of the venous system in different species and make it worth to reinvestigate this topic.

A critical analysis of the descriptions by the different authors also indicates that observations of a specific vascular arrangement were not always interpreted uniformly. This can be illustrated by comparing some of the original lateral view drawings of the development of the venous system in the region of the metanephros (Fig. 10). This indicates that the sacrocardinal veins described by Grünwald (1938) correspond to the caudal parts of the caudal cardinal veins as described by Huntington and McClure (1920), McClure and Butler (1925) and Butler (1927). The term “sacrocardinal veins” was introduced by Grünwald (1938) in order to differentiate between the primitive caudal cardinal veins which course ventral to the umbilical arteries in 4 mm embryos and the sacrocardinal veins which course dorsal to the umbilical arteries in the elder embryo. In his concept, the caudal segments of the caudal cardinal veins remain located on the ventral side of the umbilical arteries and they correspond with the veins that were described by McClure and Butler (1925) as the caudal mesonephric branches of the caudal cardinal veins.

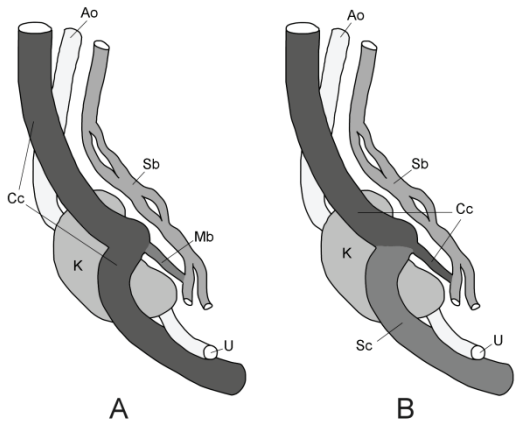

Fig. 10: Right-lateral views of the intermediate embryonic vein system (see Fig. 3 column b) in the human embryo (upright position), showing the different nomenclature used for naming the caudalmost segment of the cardinal vein system. A: Supracardinal model redrawn after McClure and Butler (1925). B: Sacrocardinal model redrawn after Grünwald (1938). Ao: aorta, Cc: right caudal cardinal vein, K: right metanephros, Mb: mesonephric branch of the caudal cardinal vein, Sb: right subcardinal vein, Sc: right sacrocardinal vein, U: umbilical artery.

The discussion whether the embryonic sympathetic trunk is accompanied by a single supracardinal vein (Fig. 8A) or the paired lateral and medial sympathetic line veins (Fig. 8D), can be another example of a different interpretation of the same observations. Most early embryonic veins are no single straight tubes carrying the blood towards the heart, but they are initially formed as irregular venous plexuses which have several cross-sections on any histological slide. The various venous lumina surrounding the sympathetic trunk are considered as a single entity in the supracardinal model, whilst in the lateral sympathetic model a differentiation is made between the lumina at the lateral side and those at medial side of the sympathetic trunk. This subdivision is based upon the observation that in the abdominal region most of the blood passes through the lateral part of this plexus, contrary to the situation in the thoracic region.

A number of contradictions between some specific statements by the different authors remain unclear. Butler (1927) linked the developmental pattern of the venous system with the functional development of the mesonephroi in the embryo. The functional development of the mesonephroi is further correlated with the type of placental barrier (Noden and de Lahunta, 1985). As a human embryo can rely on a highly specialised, thin-layered haemochorial placenta to filter its metabolic waste products (Ramsey, 1982), it has no need for an endogenous filtering and storage system like the mesonephros and allantois (Engle, 1986; Moritz and Wintour, 1999). The mesonephroi therefore never show any functional excretory activity during human embryogenesis (Gilbert, 2000). Based on these facts and the aforementioned theory of Butler (1927), one can deduce that the developmental pattern of the venous system in man is in accordance with the caudal cardinal model. However, McClure and Butler (1925) and Butler (1927) reported that the veins in the human embryo develop according to the supracardinal model.

In the supracardinal model, the caudal cardinal veins course dorsal to the umbilical arteries (Fig. 8A). Grünwald (1938) rejected this supracardinal model and proposed the sacrocardinal model as an alternative because he observed in 4 mm embryos that the primitive caudal cardinal veins course ventral to the umbilical arteries. However, in an independent study of human embryos of the same age, Gladstone (1929) had reported that the caudal cardinal veins are situated dorsal to the umbilical arteries.

Further comparative studies are needed to elucidate these conflicting reports as well as to confirm or deny the existence of the supracardinal veins in the lumbar region. There is

also need for more precise data on possible species-specific characteristics such as the presence of a circumaortic venous ring or renal collar (Fig. 8Ac), which is the normal adult configuration in monotremes (Barone, 1996) but may partly persist as a congenital anomaly in man (Macchi et al., 2003). This feature is not described yet in the canine embryo nor as an anomalous configuration in the adult dog. Furthermore, Butler (1927) explicitly mentioned that a renal collar is not formed during the embryonic development in the pig as the dorsal limb of this ring is completely lacking in this species.

2.1.3. Anatomical variations of the venous system

2.1.3.1. Case descriptions

Anatomical variations of the venous system have been reported repeatedly in man and domestic animals. These reports include not only malformations of the large systemic veins, which are the focus of this chapter, but also of the portal and pulmonary venous system. In man, the combined incidence rate of inferior vena cava malformations in symptomatic and asymptomatic patients is 2.9% - 6.6%, and even amounts to 13.4 - 16.7% when taking into account the malformations of its major tributaries such as the renal veins (Chuang et al., 1974; Bass et al., 2000). Persistence of the left superior vena cava is the most common thoracic vein anomaly in man and occurs in 0.3% - 0.5% of the general population (Tang et al., 2004). Anomalies of the cranial vena cava have also been reported quite often in dogs (Evans, 1993). They are commonly associated with other congenital defects, but in rare cases they may occur as isolated malformations (Fernandez del Palacio et al., 1997). In contrast, malformations of the caudal vena cava in dogs are considered to be rare, but significant epizootic data in domestic animals are lacking (Reis and Tepe, 1956; Barthez et al., 1996). The variety and prevalence of these malformations can largely be attributed to the complexity of the developmental process of the venous system in the mammalian embryo (Sadler, 1985).

In 120 dog cadavers that were dissected for educational purposes at the Department of Morphology in the Faculty of Veterinary Medicine of Ghent University between 2002 and 2004, eight variations of the caudal or cranial vena cava were observed as single congenital anomalies. All of these malformations have been described in literature before (Table 2).

Conversely, during similar dissections on cats, a retrocaval ureter was found in an adult, unneutered male cat (Fig. 11). This variation, supposed to be caused by a developmental anomaly of the caudal vena cava, is a well-known condition of clinical relevance in man (Bass et al., 2000; Perimenis et al., 2002) and has also been experimentally induced in the rabbit (Scortichini et al., 1986). However, this finding in the cat is the first and only reported case of an uncomplicated retrocaval ureter in domestic animals to date, whereas almost simultaneously with our own report, Doust et al. (2006) described the first case of a retrocaval or circumcaval ureter accompanied by an intrahepatic portosystemic shunt associated with clinical symptoms in a dog.

The anomaly in the cat was characterised by a medial deviation of the right ureter which crossed the caudal vena cava dorsally at the level of the 5th lumbar vertebra. The right ureter subsequently emerged between the caudal vena cava and the abdominal aorta, and coursed back in lateral direction across the ventral surface of the caudal vena cava. It resumed its normal anatomical location along the psoas musculature and continued caudally towards the urinary bladder. Neither a dilation of the proximal part of the right ureter nor apparent signs of urinary tract inflammation were present.

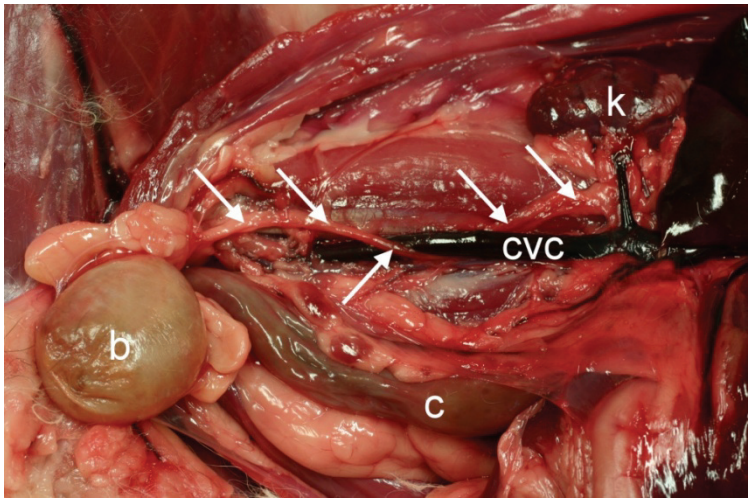

Fig. 11: Ventral view of a right retrocaval ureter (arrows) in a domestic cat. b: urinary bladder, c: colon, k: right kidney, cvc: caudal vena cava.

Table 2: Vein anomalies observed in dogs during routine anatomical dissections at the Department of Morphology in the Faculty of Veterinary Medicine (Ghent University), in a period of two years.

Case #	Dog Breed	Age	Major anomalies	References to similar cases
1	Mongrel	Adult	Duplication of the caudal vena cava, caudal to the mesenteric root.	Heinze, 1965; Krahmer, 1969; Weir, 1970
2	Mongrel	Adult	Continuation of the abdominal part of the caudal vena cava into the right azygos vein. The caudal vena cava was deviated to the right and coursed over the ventral side of the right kidney. Double right renal vein	May, 1960; Wallace, 1960; Ingham, 1969; Vitums, 1972; Martin and Gerrity, 1983; Barthez et al., 1996
3	Unknown	7 weeks	Continuation of the abdominal part of the caudal vena cava into the right azygos vein. The caudal vena cava was deviated to the right and coursed over the ventral side of the right kidney.	
4	Border Collie	4 months	Stenosis of the caudal vena cava at the level of the liver. Dilation of the caudal vena cava caudal to the stenosis with several connections to the azygos vein. Additional portal vein hypoplasia with pre-hepatic porto-caval shunts resulting in hepatoencephalopathy.	Hunt et al., 1998; Harder et al., 2002
5	Dogo Argentino	Adult	Persistent left cranial vena cava in absence of a normal right cranial vena cava.	Fernandez del Palacio et al., 1997
6	German Shepherd	Adult	Persistent left cranial vena cava additional to its normal right-sided counterpart.	Krahmer, 1964; Jacobs et al., 1983; Fernandez del Palacio et al., 1997
7	German Shepherd	Adult	Left costocervical vein draining directly into the coronary sinus.	Buchanan, 1963; Nam et al., 2003
8	German Shepherd	Adult	Left costocervical vein draining directly into the coronary sinus.	

2.1.3.2. Discussion

Despite the present doubts on the accuracy of the currently most accepted model describing the embryonic development of the caudal vena cava, the supracardinal theory is still often used to explain the numerous variations of the caudal vena cava observed in human clinical practice (Bass et al., 2000; Minniti et al., 2002; Nagashima et al., 2006; Hashmi and Smaroff, 2007). Due to the great similarity between the anomalies observed in man and those found in domestic animals, many of the available hypotheses on the ontogeny of these variations in man are also used to explain the alternative configurations observed in the dog and cat.

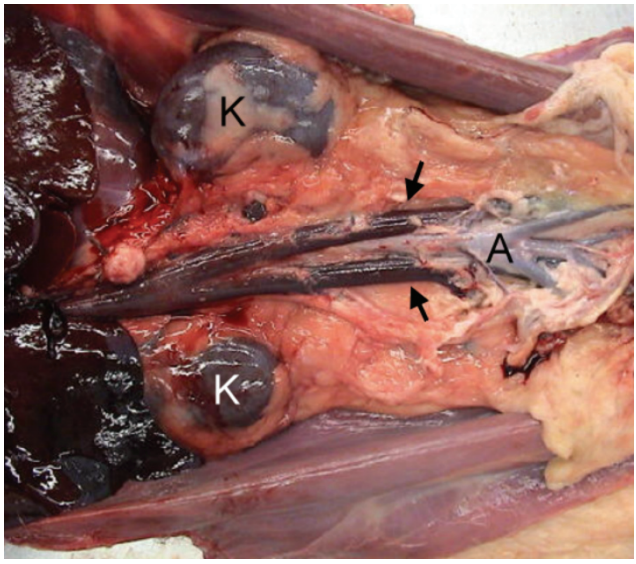

Fig. 12: Ventral view of a double caudal vena cava in a dog (case # 1). The arrows point at both limbs of the caudal vena cava. A: caudal end of the abdominal aorta, K: kidneys.

In many cases, this model can provide sufficient answers to unravel the alternative pathways that lie at the base of the observed variations. Hence, the duplication of the caudal vena cava (Case #1, Fig. 12) can easily be explained by the persistence of both the right and left supracardinal vein in the adult, whereas a left cranial vena cava (Cases #5 & 6, Fig. 13)is most likely the result of the persistence of the left cranial cardinal vein (Bass et al., 2000). However, these malformations can also be explained by any of the four other models

discussed in section 1.2.3., as all theories describe the gradual transition from a bilateral symmetric venous network towards a unilateral right-sided system in which the persistence of a left-sided vein is can be a possible variation.

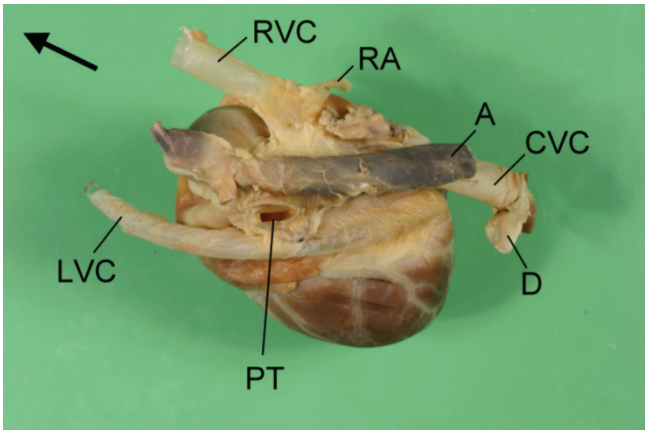

Fig. 13: Dorsal view of the plastinated heart of a German Shepherd with a double cranial vena cava (Case # 6). The arrow is pointing in cranial direction. A: aorta, RA: right azygos vein, CVC: caudal vena cava, D: diaphragm, LVC: left cranial vena cava, RVC: right cranial vena cava, PT: pulmonary trunk.

In cases in which the persistence of a left-sided vessel cannot be indicated as a possible cause of the anomaly, such as in cases #2 and #3 (Figs. 14 & 15) in which an anomalous caudal vena cava courses along the ventral side of the right kidney, perforates the diaphragm close to the vertebral column and continues in the thorax as the right azygos vein, more controversy about the exact ontogeny of this malformation can be found in literature. May (1960) and Wallace (1960), by using the supracardinal model to explain this anomaly, believed that this variation is due to the persistence of the right supracardinal vein along its entire length. Likely, these authors may have developed their hypothesis based on the many schematic representation in papers and textbooks displaying just a concise summary of original supracardinal model. In many of these summaries, the relation of the embryonic veins to the different organs has been omitted and only the construction plan of the venous in itself is displayed. As the right supracardinal vein is held responsible for the construction of both the azygos vein as the infrarenal part of the caudal vena cava, persistence of this vessel along its entire length is at first sight certainly an acceptable explanation for the present type of anomaly. However, in the original descriptions by McClure and Butler (1925) and Butler (1927), it is clearly indicated that the supracardinal veins are located dorsal to the developing

kidneys. Based on these facts, the hypothesis by May (1960) and Wallace (1960) is rather implausible, as the anomalous vena cava observed in these cases was coursing ventral to the right kidney.

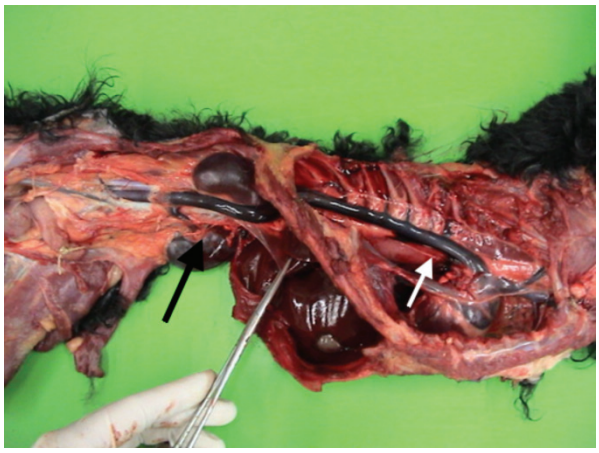

Fig. 14: Right view of an abnormal caudal vena cava in a dog (Case # 2). The abdominal part of the caudal vena cava (black arrow) is deviated to the right and crosses the cranial pole of the right kidney. After perforating the diaphragm between the right crus of the diaphragm and the vertebral column, it continues in the thorax as an enlarged azygos vein (white arrow).

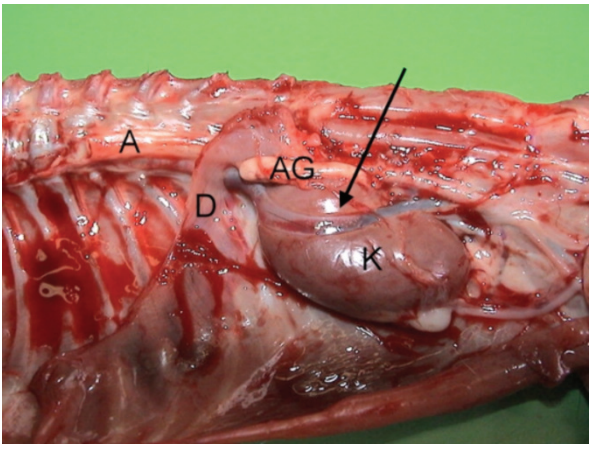

Fig. 15: Left view of an abnormal caudal vena cava in a 7 weeks old pup (Case # 3). The abdominal part of the caudal vena cava is deviated to the right (arrow) and overlaps the ventral and medial side of the right kidney (K). After passing between the right crus of the diaphragm (D) and the vertebral column, it continues directly into the right azygos vein. A: thoracic aorta, AG: Adrenal gland.

Other authors (Lohse et al., 1976; Barthez et al., 1996) interpreted the azygos continuation of the caudal vena cava as being caused by the persistence of the entire right caudal cardinal vein. However, again due to some topographical inconsistencies, a number of arguments against this second hypothesis can be raised. It has been mentioned before that the caudal cardinal vein is a less privileged vein to construct the caudal vena cava as it is originally located ventral to the kidney and lateral to the ipsilateral ureter. During the complex remodelling of the venous system, all embryonic vessels have the tendency to migrate towards the axial midline of the embryo. As a consequence and due to its relative position to the urinary tract, a persisting right caudal cardinal vein will sweep the right ureter along its migratory path towards the midline and entrap the ureter between itself, the vertebral column and the aorta (Fig. 16) (Bass et al., 2000). Therefore, persistence of the right caudal cardinal vein, and more specifically its lumbar segment, is more believed to be

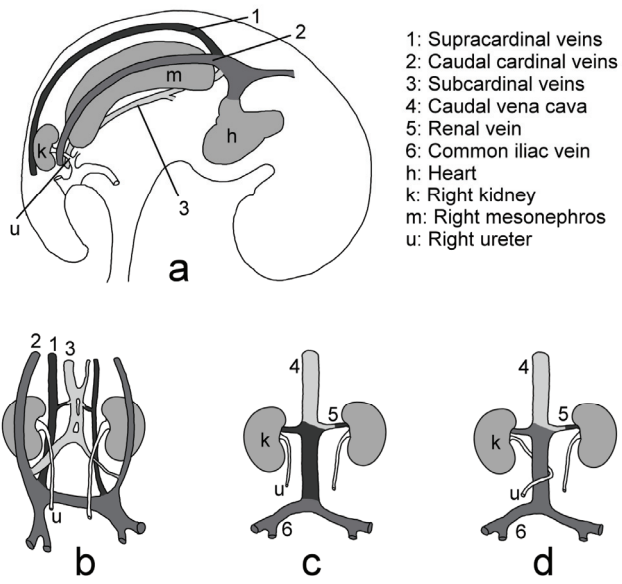

Fig. 16: a: Right lateral view of the veins of the cardinal system in the feline embryo (according to Huntington and McClure, 1920). b: Ventral view of the primitive veins in the lumbar region of the cat embryo. c: Ventral view of the normally developed feline caudal vena cava of which the infrarenal segment is formed by the right supracardinal vein. d: Ventral view of a right retrocaval ureter encircling the infrarenal segment of the caudal vena cava which is formed by the persisting right caudal cardinal vein.

the direct cause leading to the condition of a retrocaval ureter (Bass et al., 2000; Gundeti et al., 2006). On the other hand, some authors have recently suggested that not the caudal cardinal vein but rather a persisting right subcardinal vein is involved in the occurrence of a retrocaval ureter (Perimenis et al., 2002; Soundappan and Barker, 2004).

A third hypothesis on the ontogeny of the azygos continuation of the caudal vena cava can be found in the works of Ingham (1969), Vitums (1972), Martin and Gerrity (1980) and McClure and Constantinescu (1987). These authors consider this anomaly as the result of a failed anastomosis between the right subcardinal and vitelline veins. As in this case the blood coming from the hindquarters of the embryo cannot be passed to the heart via the intrathoracic segment of the caudal vena cava, a newly formed connection with the azygos veins is assumed to take up this task.

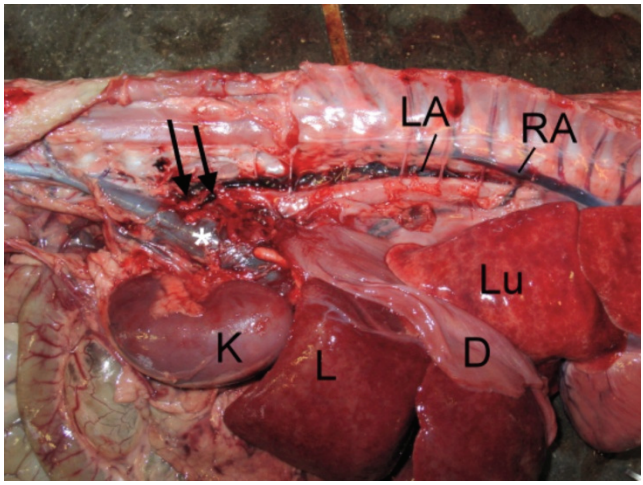

Fig. 17: Right view of a stenotic caudal vena cava in a Border Collie (Case # 4). Caudal to the stenosis, the caudal vena cava is dilated (*) and drains via various anastomoses (arrows) into the left hemiazygos vein (LA). The latter has been exposed by pulling the thoracic aorta ventrally. D: Diaphragm, K: Left kidney, L: Liver, Lu: lung, RA: Right azygos vein.

Remarkably, Hunt et al. (1998) and Harder et al. (2002) have attributed the latter explanation to a totally different anomaly, similar to our case # 4 (Fig. 17), in which a stenotic, blind-ending caudal vena cava dilates at the level of the liver and is connected with the azygos vein by several small vessels which pass through the diaphragm. However, this apparently conflicting situation of two different anomalies with the same explanation does

not necessarily mean that both hypotheses cannot coexist. The former situation can result from a primary agenesis of the subcardinal-vitelline anastomosis, while in the latter case this anastomosis may have developed normally, but was interrupted later in development due to a thromboembolic event, forcing the blood to find another way back to the heart (Achiron et al., 2000).

On the other hand, the co-existence of three completely different theories to explain the same venous anomaly is highly suggestive for the speculative nature of these kind of hypotheses, of which their individual plausibilities are only nourished by the imprecision and incompleteness of our current knowledge on the morphological and physiological developmental mechanisms of the caudal vena cava in the embryo.

2.2. Scientific aims

The controversies on the identity of the specific embryonic vein contributing to the formation of the lumbar segment of the caudal vena cava as well as the conflicting hypotheses on the exact ontogeny of some congenital variations of the venous system clearly indicate that the exact development of the vena cava in man and domestic animals is a topic that is not yet entirely elucidated.

Therefore, as a general objective of this study, an in-depth investigation on the morphological development of the caudal vena cava in the pig embryo as a model was performed with the purpose of clarifying some specific controversial aspects between the different currently circulating theories. In this respect, special attention went out to the visualisation of the topographical organisation of the developing vascular network in relation to the different surrounding organs and tissues.

As previous investigations on the developmental pattern of the caudal vena cava were hampered by the technical limitations of the applied protocols, a more advanced approach based on recently developed technology had to be designed to overcome these specific limitations.

Furthermore, this investigation is not only intended to acquire more insights in the developmental pattern of the caudal vena cava that also can present more profound explanations for the different variations and congenital vascular defects observed in domestic animal species, a major purpose is also to provide a suitable model in which the presence and effects of different modulators of vascular development can be studied on a molecular level.

2.3. Literature

Achiron, R., J. Hegesh, S. Yagel, S. Lipitz, S.B. Cohen and Z. Rotstein (2000). Abnormalities of the fetal central veins and umbilico-portal system: prenatal ultrasonographic diagnosis and proposed classification. *Ultrasound in Obstetrics and Gynecology* 16, 539-548.

Arey L.B. (1974). Developmental Anatomy, a Textbook and Laboratory Manual of Embryology, seventh revised edition. W. B. Sauders Company, Philadelphia, p. 360-370.

Balinsky, B.I. (1981). An Introduction to Embryology, fifth edition. Saunders College Publishing, Philadelphia, p. 505-508.

Barone, R. (1996). Anatomie comparée des Mammifères domestiques, Tome cinquième, Angiologie. Editions Vigot, Paris, p. 454-459, p. 651.

Barthez, P.Y., L.M. Siemens and P.D. Koblik (1996). Azygos continuation of the caudal vena cava in a dog : radiographic and ultrasonic diagnosis. *Veterinary Radiology and Ultrasound* 37, 354-356.

Bass, J.E., M.D. Redwine, L.A. Kramer, P.T. Huynh and J.H. Harris (2000). Spectrum of congenital anomalies of the inferior vena cava: cross-sectional imaging findings. *Radiographics* 20, 639-652.

Besier, H. and E. Stofft (1977). Zum Venensystem im Retroperitonealbereich (Beitrag zur Persistenz des primitiven Vena cava-Systems). *Anatomischer Anzeiger* 142, 175-179.

Buchanan, J.W. (1963). Persistent left cranial vena cava in dogs: angiocardiography, significance and coexisting anomalies. *Journal of the American Veterinary Radiology Society* 4, 1-8.

Butler, E.G. (1927). The relative role played by the embryonic veins in the development of the mammalian vena cava posterior. *American Journal of Anatomy* 39, 267-353.

Carlson, B.M. (1994). Human Embryology and Developmental Biology. Mosby - Year Book Inc., Saint-Louis, p. 382-383.

Chuang, V.P., C. Ernesto Mena and P.A. Hoskins (1974). Congenital anomalies of the inferior vena cava. Review of embryogenesis and presentation of a simplified classification. *British Journal of Radiology* 47, 206-213.

Dierickx, K. (1969). Embryologie van mens en eutheria. Leerboek ten behoeve van studenten in de menselijke en de dierlijke geneeskunde. Wetenschappelijke Uitgeverij E. Story-Scientia P.V.B.A., Gent, Handboek pp. 223-228, Atlas p. 75.

Doust, R.T., S.P. Clarke, G. Hammond, C. Paterson and A. King (2006). Circumcaval ureter associated with and intrahepatic portosystemic shunt in a dog. *Journal of the American Veterinary Medical Association* 228, 389-391.

Engle W.D. (1986). Development of fetal and neonatal renal function. *Seminars in Perinatology* 10, 113-124.

Evans, H.E. (1993). Veins. In: Evans H.E. (Editor), Miller's Anatomy of the Dog. W. B. Saunders Company, Philadelphia PA, p. 682-716.

Fasel, J. and K.S. Ludwig (1988). Eine partiell verdoppelte Vena cava inferior: klinische, makroskopische und embryologische Anatomie. *Gegenbaurs Morphologisches Jahrbuch* 134, 143-153.

Fernadez del Palacio, M.J., L. Bernal, A. Bayón and V. Luis Fuentes (1997). Persistent left cranial vena cava associated with multiple congenital anomalies in a six-week-old puppy. *Journal of Small Animal Practice* 38, 526-530.

Forte, F., C. Farina, E. Bronzetti, S. Carbotta, S. Germani, G. Virgili and G. Vespasiani (2002). Clinical implications of left ovarian vein incomplete duplicity with embryonic intersubcardinal anastomosis-derived branches. *Surgical and Radiologic Anatomy* 24, 64-67.

Gilbert, S.F. (2000). Developmental Biology, sixth edition. Sinauer Associates Inc., Sunderland, MA, p. 460.

Gladstone, R. (1929). Development of the inferior vena cava in the light of recent research, with especial reference to certain abnormalities, and current descriptions of the ascending lumbar and azygos veins. *Journal of Anatomy* 64, 70-93.

Grünwald, P. (1938). Die Entwickelung der Vena cava caudalis beim Menschen. *Zeitschrift für Mikroskopisch-Anatomische Forschung* 43, 275-331.

Gundeti, M.S., P.G. Duffy and I. Mushtaq (2006). Robotic-assisted laparoscopic correction of pediatric retrocaval ureter. *Journal of Laparoendoscopic and Advanced Surgical Techniques part A* 16, 422-424.

Harder, M.A., D. Fowler, J.W. Pharr, K.A. Tryon and C. Shmon (2002). Segmental aplasia of the caudal vena cava in a dog. *Canadian Veterinary Journal* 43, 365-368.

Hashmi, Z.A. and G.G. Smaroff (2007). Dual inferior vena cava: two inferior vena cava filters. *The Annals of Thoracic Surgery* 84, 661-663.

Heinze, W. (1965). Agenesis renis unilateralis, Verdoppelung der V. cava caudalis und Persistenz von nephrogenem Gewebe bei einem Hund. *Anatomischer Anzeiger* 116, 92-98.

Hochstetter, F. (1893). Beiträge zur Entwickelung des Venensystems der Amnioten, (3) Säuger. *Morphologisches Jahrbuch* 20, Bd. 4, Heft S, 543-648. (Cited by Butler, 1927).

Hunt, G.B., C.R. Bellenger, R. Borg, K. Ruth Youmans, P.L.C. Tisdall and R. Malik (1998). Congenital interruption of the portal vein and caudal vena cava in dogs: six case reports and a review of the literature. *Veterinary Surgery* 27, 203-215.

Huntington, G.S. and C.F.W. McClure (1920). The development of the veins in the domestic cat (*Felis domestica*) with especial reference, 1) to the share taken by the supracardinal veins in the development of the postcava and azygos veins and 2) to the interpretation of the variant conditions of the postcava and its tributaries, as found in the adult. *Anatomical Record* 20, 1-30.

Ingham, B. (1969). An unusual configuration of the posterior vena cava in a Beagle. *Zeitschrift für Versuchstierkunde* 11, 276-278.

Jacobs, G., G.R., Bolton and B.J. Watrous (1983). Echocardiographic features of dilated coronary sinus in a dog with persistent left cranial vena cava. *Journal of the American Veterinary Medical Association* 182, 407-408.

Krahmer, R. (1964). Über eine paarige V. cava cranialis beim Schäferhund. *Anatomischer Anzeiger* 115, 354-357.

Krahmer, R. (1969). Über einige Gefäßanomalien beim Hund (*Canis familiaris*). *Anatomischer Anzeiger* 124, 496-508.

Leeson, T.S. and J.S. Baxter (1957). The correlation of the structure and function in the mesonephros and metanephros of the rabbit. *Journal of Anatomy* 91, 383-390.

Lohse, C.L., R.R. Selcer and P.F. Suter (1976). Hepatoencephalopathy associated with situs inversus of abdominal organs and vascular anomalies in a dog. *Journal of the American Veterinary Medical Association* 168, 681-688.

Loughna, S. and T.N. Sato (2001). A combinatorial role of Angiopoietin-1 and orphan receptor TIE1 pathways in establishing vascular polarity during angiogenesis. *Molecular cell* 7, 233-239.

Macchi, V., A. Parenti and R. De Caro (2003). Pivotal role of the sub-supracardinal anastomosis in the development and course of the left renal vein. *Clinical Anatomy* 16, 358-361.

Martin, J.E. and L.W. Gerrity (1980). Azygos continuation of the caudal vena cava in the dog. *Southwestern Veterinarian* 33, 155-157.

May, N.D.S. (1960). Absence of the prerenal segment of the posterior vena cava of the dog. *Australian Veterinary Journal* 36, 67-68.

McClure, C.F.W and E.G. Butler (1925). The development of the vena cava inferior in man. *American Journal of Anatomy* 35, 331-383.

McClure, R.C. and G.M. Constantinescu (1987). An uncommon right azygos vein and caudal vena cava in the dog. *Anatomia, Histologia, Embryologia* 16, 84.

McGeady, T.A., P.J. Quinn, E.S. FitzPatrick and M.T. Ryan (2006). Veterinary Embryology. Blackwell Publishing, Oxford, p. 105-135.

Michel, G. (1986). Kompendium der Embryologie der Haustiere, Vierte, überarbeitete Auflage. Gustav Fisher Verlag, Stuttgart, pp. 259-263.

Minniti, S., S. Visentini and C. Procacci (2002). Congenital anomalies of the venae cavae: embryological origin, imaging features and report of three new variants. *European Radiology* 12, 2040-2055.

Moritz, K.M. and E.M. Wintour (1999). Functional development of the meso- and metanephros. *Pediatric Nephrology* 13, 171-178.

Nagashima, T., J. Lee, K. Andoh, T. Itoh, K. Tanohata, M. Arai and T. Inoue (2006). Right double inferior vena cava: report of 5 cases and literature review. *Journal of Computer Assisted Tomography* 30, 642-645.

Nam, Y.S., C.H. Lee, D.W. Chung, Y.S. Yoon, H.S. Lee and I.S. Lee (2003). Left costocervical vein malformation with anomalous ramification of aortic arch in a dog. *Journal of Veterinary Science* 4, 205-208.

Noden, D.M. and A. de Lahunta (1985). The Embryology of Domestic Animals. Williams & Wilkins, Baltimore, p. 257-269, p. 312.

Nomina Embryologica (1983). In: Nomina Anatomica: fifth edition, Nomina Histologica: second edition and Nomina Embryologica: second edition / Prepared by Subcommittees of the International Anatomical Nomenclature Committee. Williams & Wilkins, Baltimore, p. E 22.

Nomina Embryologica Veterinaria (2006), 2nd edition. Prepared by the International Committee on Veterinary Embryological Nomenclature, Ghent, p. 16. http://www.wava-amav.org/Downloads/nev_2006.pdf

Ozerdem, U., W.L. Charbano and W.B. Stallcup (2002). Plastic casting of embryonic, placental and tumor vasculature in the mouse. *Microvascular Research* 64, 486-490.

Patten, B.M. (1948). Embryology of the pig. McGraw-Hill Book Company, London, p. 240-250.

Patton, B.M. and B.M. Carlson (1974). Foundations of Embryology, third edition. McGraw-Hill Book Company, New York, p. 554-565.

Perimenis, P., K. Gyftopoulos, A. Athanasopoulos, V. Pastromas and G. Barbalias (2002). Retrocaval ureter and associated abnormalities. *International Urology and Nephrology* 33, 19-22.

Petrenko, V.M. (1998). Morfogenez kornei nizhnei poloi veny v embryogeneze cheloveka. *Morfologiia* 114, 56-59.

Popesko, P., V. Rajtová and J. Horák (1992a). A Colour Atlas of the Anatomy of Small Laboratory Animals, Volume one: Rabbit - Guinea Pig. Wolfe Publishing Ltd., London, p. 77.

Popesko, P., V. Rajtová and J. Horák (1992b). A Colour Atlas of the Anatomy of Small Laboratory Animals, Volume two: Rat - Mouse – Hamster. Wolfe Publishing Ltd., London, p. 53, 141 & 206.

Rahalkar, M.D. (2002). Dr. N. G. Gadekar Memorial Oration. 55th conference of IRIA, Kolkata. *Indian Journal of Radiology and Imaging* 12, 109-114.

Ramsey E.M. (1982). The Placenta, Human and Animal. Praeger Publishers, New York, p. 65-75.

Rathke, H. (1838). Ueber den Bau und die Entwickelung des Venensystems der Wirbelthiere. *Dritter Bericht über das naturwissenschaftliche Seminar bei der Universität zu Königsberg*, 1838. (Cited by Butler, 1927).

Reagan, F.P. and A. Robinson (1926). The later development of the inferior vena cava in man and in carnivora. *Proceedings of the Anatomical Society of Great Britain and Ireland, Journal of Anatomy* 61, 482. (Cited by Gladstone, 1929).

Reagan, F.P. and M. Tribe (1926). The early development of the postrenal vena cava in the rabbit. *Proceedings of the Anatomical Society of Great Britain and Ireland, Journal of Anatomy* 61, 480. (Cited by Gladstone, 1929).

Reis, R.H. and P. Tepe (1956). Variations in the pattern of renal vessels and their relation to the type of posterior vena cava in the dog (*Canis familiaris*). *American Journal of Anatomy* 99, 1-15.

Rüsse, I. and F. Sinowatz (1991). Lehrbuch der Embryologie der Haustiere. Verlag Paul Parey, Berlin, p. 231-235.

Sabin, F.L. (1915). On the fate of the posterior cardinal veins, and their relation to the development of the vena cava and azygos in the embryo pig. *Contributions to Embryology* III-7, 5. (Cited by Gladstone, 1929).

Sadler, T.W. (1985). Langman's Medical Embryology, fifth edition. Williams & Wilkins, Baltimore, p. 203-209.

Sandercoe, G.D. and G.L. Brooke-Cowden (2003). Developmental anomaly of the inferior vena cava. *ANZ Journal of Surgery.* 73, 356-360.

Sasov, A. and D. Van Dyck (1998). Desktop X-ray microscopy and microtomography. *Journal of Microscopy* 191, 151-158.

Schneider J.E., S.D. Bamforth, S.M. Grieve, K. Clarke, S. Bhattacharya and S. Neubauer (2003). High-resolution, high throughput magnetic paragraph sign resonance imaging of mouse embryonic paragraph sign anatomy using a fast gradient-echo sequence. *MAGMA* 16, 43-51.

Schnorr, B. (1989). Embryologie der Haustiere, ein Kurzlehrbuch, 2., neu bearbeitete Auflage. Ferdinand Enke Verlag, Stuttgart, p. 193-194.

Scortichini, B.H., J.A. John-Greene, J.F. Quast and K.S. Rao (1986). Teratologic evaluation of dermally applied diethylene glycol monomethyl ether in rabbits. *Fundamental and Applied Toxicology* 7, 68-75.

Sharpe, J. (2003). Optical projection tomography as a new tool for studying embryo anatomy. *Journal of Anatomy* 202, 175-181.

Soundappan, S.V. and A.P. Barker (2004). Retrocaval ureter in children: a report of two cases. *Pediatric Surgery International* 20, 158-160.

Starck, D. (1975). Embryologie, ein Lehrbuch auf allgemein biologischer Grundlage, 3., neubearbeitete und erweiterte Auflage. Georg Thieme Verlag, Stuttgart, p. 560-567.

Tang, E.W.H., W.Y. Cheung, C.M. Ho and A.W.C. Yip (2004). What abnormality is evident on the chest X-ray after placement of the central venous catheter? *Hong Kong Medical Journal* 10, 65-66.

Trubač, R., M. Hribernik and L. Páč (2002). Congenital interruption of the inferior vena cava with hemiazygos continuation. *Scripta Medica (Brno)* 75, 291-302.

Vitums, A. (1972). Anomaly of the vena cava caudalis in a dog. *Zentralblatt für Veterinärmedizin Reihe* C 1, 149-152.

Wallace, C.R. (1960). Absence of posterior vena cava in a dog. *Journal of the American Veterinary Medical Association* 136, 27-28.

Weir, E.C. (1970). Venous anomalies in the abdomen of a dog. *Veterinary Record* 86, 582.

Williams P.L., R. Warwick, M. Dyson and L. M. Bannister (1993). Gray's Anatomy, 37th edition, reprint. Churchill Livingstone, Edinburgh, p. 219-226.

CHAPTER 3: MATERIALS AND METHODS

3.1. Introduction

3.2. Computer assisted three-dimensional reconstruction

3.3. Corrosion casting

3.4. Discussion

3.5. Literature

Based on:

Cornillie P., W. Van den Broeck and P. Simoens (2008). Three-dimensional reconstruction of the remodelling of the systemic vasculature in early pig embryos. *Microscopy Research and Technique* 71, 105-111.

Cornillie P., W. Van den Broeck and P. Simoens (2008). Origin of the infrarenal part of the caudal vena cava in the pig. *Anatomia, Histologia, Embryologia,* accepted.

The critical reflections on the applied methodology are based on:

Cornillie P., W. Van den Broeck and P. Simoens (2005). Computer assisted three-dimensional reconstruction of the developing caudal vena cava in the pig embryo. *Third Meeting of the Young Generation of Veterinary Anatomists, Ghent-Antwerp, July 13-15, 2005.*

Cornillie P., W. Van den Broeck, P. Simoens (2007). Application of computer assisted three-dimensional visualization techniques in histology, medical computer tomography and nuclear magnetic resonance imaging. *Proceedings of the Fourth Meeting of the Young Generation of Veterinary Anatomists, Ljubljana, July 8-10, 2007*. Published in: *Slovenian Veterinary Research* 44, 46.

CHAPTER 3: MATERIALS AND METHODS

3.1. Introduction

In the past decades, several different types of image acquisition and advanced 3D-visualisation techniques in the microscopic area have been developed. Computer graphics technologies currently allow researchers to explore, manipulate and rotate 3D shapes of biological specimens without the need to build real physical (scale) models to understand the full 3D complexity of the structures they study (Sharpe, 2003). The raw data for these three-dimensional images may come either from non-invasive 3D microscopical scanning technologies or from invasive techniques, in which the specimen of interest first must be deconstructed (e.g. serial-sectioned) before a 3D-image can be reconstructed (Whiten et al., 1998; Sharpe, 2003).

Both types of approaches have their own advantages and intrinsic weaknesses. The final choice of the applied technique in a certain research will largely depend on the specific aims of study, tolerability of the technical limitations of the preferred procedure, financial resources, infrastructural possibilities, available time and equipment, and the presence of skilled personnel. By weighing all these factors, it has been opted to investigate the morphological characteristics of the developing caudal vena cava in the pig embryo by means of relatively more time consuming invasive techniques rather than by making use of one of the less morphologically disrupting non-invasive applications that are currently available.

In the next sections, detailed protocols of the computer assisted three-dimensional reconstruction procedure starting from histological serial sections as well as the microvascular corrosion casting technique applied in the present research will be described. Subsequently, the specific reasons why these approaches were chosen above the currently available non-invasive three-dimensional visualisation techniques will be argued in the finalizing technical discussion section.

3.2. Computer assisted three-dimensional reconstruction

3.2.1. Embryo collection

Twelve embryos ranging from 3.73 - 6.82 mm Crown-Rump Length (CRL) were collected from the uterus of a sow slaughtered for financial reasons at the local abattoir (Eeklo, Belgium) 18 days after artificial insemination. On various other occasions, 56 embryos and foetuses, equally distributed within the range of 6.30 - 40 mm CRL (corresponding with a gestational age from 18 to 37 days p.c. (Evans and Sack, 1973)), were collected from several gravid porcine uteri in local abattoirs (Lokeren, Eeklo, Zele and Zedelgem, Belgium) within 15 minutes after exsanguination of pregnant sows without known history.

3.2.2. Fixation and tissue processing

Immediately after dissection of the uteri, the embryos were separated from their extra-embryonic membranes and CRL measurements were made by means of sliding callipers. In a pilot study only involving the specimens smaller than 20 mm CRL, embryos from each uterus were distributed at random into two groups and individually immersed in 30 ml fixative solution. The first group of 19 embryos was fixed overnight in a 4% 0.1 M PBS buffered paraformaldehyde solution, whilst the remaining 18 embryos were fixed in Bouin's solution (75 ml saturated aqueous picric acid, 25 ml 40% formaldehyde and 5 ml glacial acetic acid) for between four and 16 hours depending on their size, according to Kaufman (1992). Paraformaldehyde-fixed embryos were washed in distilled water and submersed in a 50% ethanol solution for 2.5 hours. All embryos were subsequently dehydrated in a series of alcohols (70% ethanol, 80% ethanol, 94% ethanol, and isopropyl alcohol), cleared in xylene and impregnated with paraffin under vacuum by means of an automated system (Shandon Citadel 1000 histokinette, 20-hour cycle duration).

In later studies on embryos and foetuses larger than 20 mm CRL, all specimens were submerged in 30 ml Bouin's fixative solution for 24 hours and subsequently dehydrated, cleared and impregnated with paraffin by using a Microm STP-420D tissue processor (Prosan nv, Belgium). Prior to fixation, specimens larger than 27.5 mm CRL were transectioned and only their caudal halves were further processed for histological investigation.

The specimens were embedded in paraffin blocks (Microm EC 350-1 embedding station, Prosan nv, Belgium) so that the head of the embryos or cranial part of the

hemisectioned foetuses was the first structure to be transected. Serial sections, each 8 µm thick, were made using a Microm HM360 rotation microtome (Prosan nv, Belgium) equipped with a cool-cut object clamp. A record was kept of the slices that could not be harvested. The collected sections were first stretched on a 50% ethanol bath and subsequently transferred to a 2% gelatine bath that was heated to 48 °C to allow a better adhesion to the microscopy glass slides. Sections were stained with haematoxylin and eosin by a Sakura linear stainer II and further processed according to standard laboratory protocols.

3.2.3. Selection of the embryos for reconstruction

The quality of a variable number of slices of all sectioned specimens was assessed using an Olympus BX61 light microscope. Based on this evaluation, nine embryos and foetuses of 3.7, 4.6, 10.0, 12.0, 18.0, 20.0, 22.5, 27.6, and 36.7 mm CRL respectively, all fixed in Bouin's solution, were selected for three-dimensional reconstruction. For each of the reconstructed specimens, two additional embryos or foetuses with comparable CRLs as their reference specimen were serially sectioned and served as control samples. In cases where the two-dimensional histological aspects of the control serial sections could not provide sufficient information about the reliability of the three-dimensional data in the reconstructed reference embryo, the corresponding regions of the control specimens were also visualized three-dimensionally. The remaining embryos and foetuses were also serially sectioned at a regular interval of 160 µm or less, and served as control samples as well, but they were only evaluated microscopically without any software-guided assistance.

3.2.4. Acquisition of the digital images

All slices of the specimens selected for reconstruction were evaluated using the Olympus BX61 light microscope. A record was kept of all slices that were not suitable for three-dimensional reconstruction due to technical artefacts such as folds and cracks. All remaining sections were provided with a unique number written in permanent ink on the cover slip next to each individual section on the glass slice for further reference. Subsequently, these sections where photographed with an Olympus DP50 digital camera mounted on the microscope with either a 4x magnifying objective lens, resulting in a digital image with a pixel size of 5.0 x 5.0 µm (embryos of 3.7 and 10.0 mm CRL), or a 2x magnifying objective lens, resulting in a digital image with a pixel size of 10.05 x 10.05 µm (all other specimens). In the larger embryos, several pictures had to be taken in order to cover each

section in its entirety. By means of the multiple image alignment module (MIA) of the analySIS docu 3.2 software (Olympus Soft Imaging Solutions) linked to the microscope, these individual images were automatically merged into one single picture. A white border of invariable dimension was added to every digital image of each embryo in which MIA had been used to ensure a constant width and height of every picture as required by the reconstruction software.

All images of each embryo were saved in jpeg format in separate folders containing 101 pictures. The last picture in every folder was identical to the first picture of the next folder (e.g. 0-100, 100-200, etc.). The smallest embryo yielded 383 pictures, whilst 2339 pictures were finally used for the reconstruction of the 22.5 mm embryo, the largest specimen that was entirely visualised in 3D.

3.2.5. Three-dimensional reconstruction

3.2.5.1. Data input

For every folder of 101 pictures, a plain text file containing the pixel size of the images, the filename of each picture, along with the relative distance of each individual slice to the position of the first section through the embryo (in increments of 8 µm except at the level where specific sections were lost) was created to load these 'bricks' of 101 pictures in stacked slices file format into the Amira 4.0.1 (Mercury Computer Systems SA) application. Initially, not all bricks were loaded at the same time to avoid overloading the computer's memory capacity (1GB DDR 2 SDRAM 533 MHz, on a Pentium 4, 3.40 GHz, Windows XP Professional SP2). For the specimens of 20 mm and larger, the computer's RAM memory was upgraded to 3 GB to be able to cope with such a large amount of data.

3.2.5.2. Image alignment

All slices within a brick were aligned to each other using the automated least squares alignment mode of the AlignSlices module (standard settings)(Fig. 18). No external landmarks or reference points were used to perform this alignment. Correctness of alignment was checked manually and adjusted where necessary. Image alignment quality of at least 95% was achieved in the majority of the cases, and the minimal quality level threshold was set at 85%. Alignment attempts that fell below this quality threshold were abandoned. Instead, the slice to be aligned was matched with a nearby but not adjacent higher numbered reference slice, until an alignment quality of 85% or more was achieved. Subsequently, all slices

between the current slice and the fix reference slice were aligned to this reference slice as well, even if the highest quality of alignment level did not reach 85%. The aligned slices were resampled in high-quality mode into an Amira mesh file format.

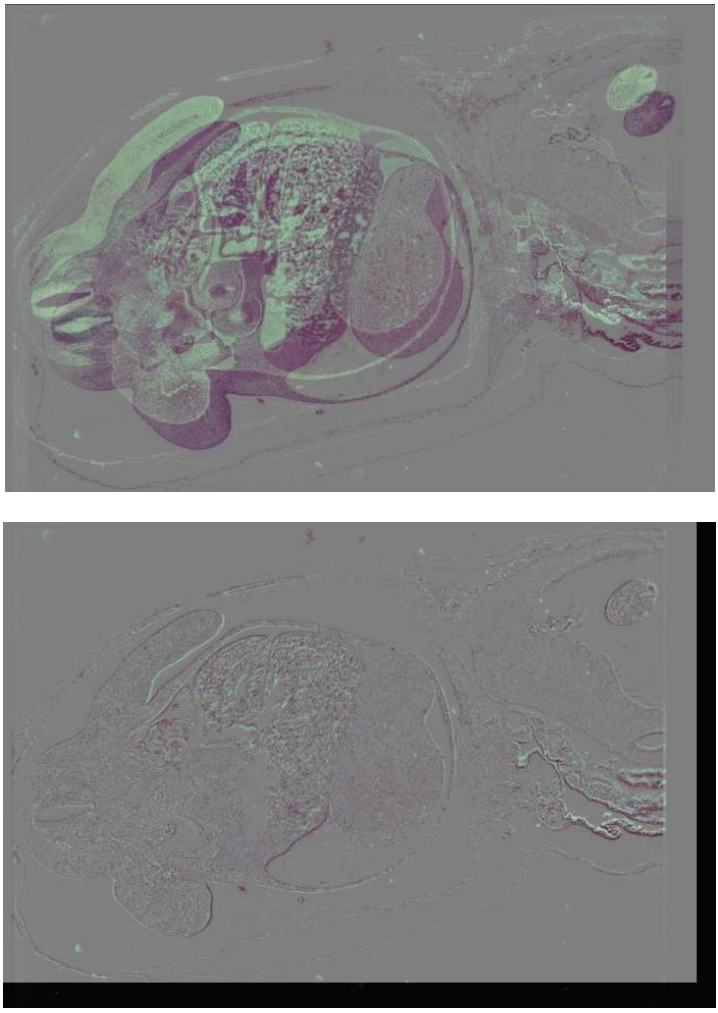

Fig. 18: Example of the image alignment between two consecutive sections of the 12.0 mm embryo without using external references or landmarks. The colour image of the first section is superimposed with the negative colour image of the next slice, and the average colour of the overlapping pixels is displayed on the screen (top image). During the subsequent automated process of image alignment, the superimposed image is shifted and rotated until the average colour of as many displayed pixels as possible is the 50% grey value (bottom image). In this case, image alignment quality was 95.6%.

3.2.5.3. Casting

Before step image segmentation could be performed, every pixel of each slice had to be assigned a certain numerical value. In the typical black-and-white medical images, such as Computed Tomography (CT) or Magnetic Resonance Imaging scans (MRI), this value is related to the grey-tone value of the pixel, and is automatically assigned by the Amira software.

Histological sections however are multicoloured images. In computer technology, a colour pixel is typically attributed four different values according to the four channels in the RGBA colour chart: Red, Green, Blue and Alpha. Whilst the first three channels represent the basic colours of a computer screen, the Alpha-value indicates the transparency of the item. Amira allows selecting the value of one of these channels or an average of all colour channels as the reference value to assign to a certain pixel. Based on this assigned pixel value, the image on screen is turned into a grey-tone image, with a pixel value of 0 being represented in black and pixels that are assigned the number 255 being visualised in white.

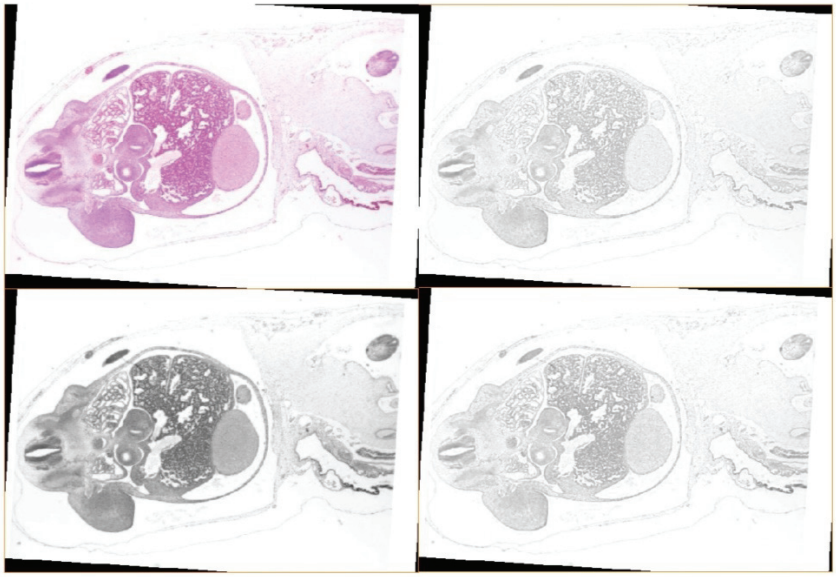

Fig. 19: Outcome of the different casting options. Top left: native image of a section through the hepatic region of a 12.0 mm pig embryo. Top right: casted image based on the red colour channel. Bottom left: casted image based on the green colour channel. Bottom right: casted image based on the blue colour channel. Image casting based on the alpha channel or average colour channels is not displayed. In the present study, casting based on the green colour channel was chosen.

In the present study, to enhance the contrast of the resulting grey-tone images from the haematoxylin- and eosin-stained slices, channel 1 (green) was selected as the reference colour channel by using the standard settings of the Castfield module in the amira software (Fig. 19).

3.2.5.4. Image segmentation

During image segmentation, each pixel of every slice was assigned to a certain "material", corresponding with important histological structures identified on the pictures (Fig. 20). In every specimen, the arterial and venous lumina as well as the contours of the gonads, mesonephroi and metanephroi were labelled. In embryos smaller than 20mm, also

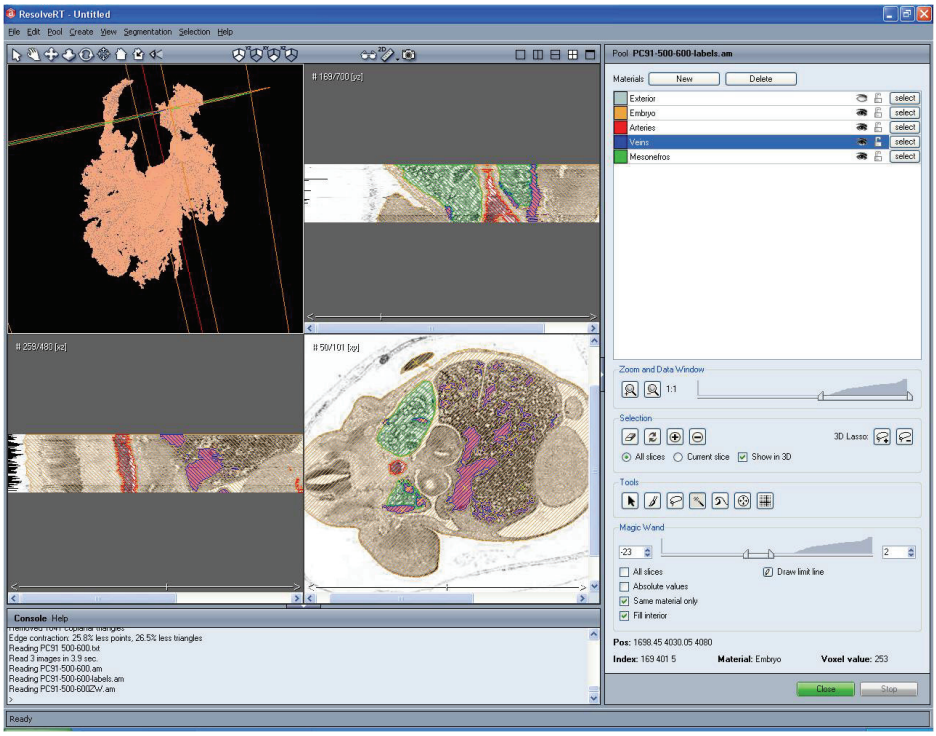

Fig. 20: Image segmentation module of the Amira 4.0.1. software. The material list together with the segmentation tools are displayed on the right of the screen. On the left side, regions of interest can be highlighted in red on the native section (bottom right) or on the virtual compilation of all sections along the xz-axis (bottom left) and yz-axis (top right). Related regions in the consecutive slices can be indicated as well and are in real-time displayed in three dimensions in the top left screen. Voxels that have been assigned to a certain material are shaded in the corresponding colour. Yellow crosses on the bottom right screen indicate pixels that have been labelled manually, whilst the surrounding pixels of the same material were automatically assigned to this material by using the magic wand tool and appropriate pixel value thresholds.

the contours of the embryo were drawn. In larger specimens, labelling of the exterior surface was not performed to save the computer's memory during the reconstruction phase. On the other hand, in these specimens of 20 mm and larger, the lymphatic system, sympathetic trunks and urinary tracts were labelled in addition, as these structures are of vital importance in the current discussion on the topographical organisation of the developing caudal vena cava in this range of embryos and foetuses.

Wherever possible, structures were labelled semi-automatically – e.g. the contours of the embryo and mesonephroi were drawn using the 2D "auto trace edges" -lasso tool every ten sections. The sections in-between were subsequently labelled through the interpolation command of the segmentation editor. At the level of the liver, intrahepatic venous lumina were highly contrasting with the surrounding dark hepatic tissue, which made it possible to label this vascular network using the 3D magic wand selection mode and appropriate pixel value (contrast) thresholds. Likewise, the aortic lumen was directly labelled in 3D. By selecting the fill interior option, it was ensured that blood residues in the centre of the lumen, often being represented by "darker" pixel values below the preset threshold were also labelled as being part of the vascular lumen. Semi-automatic labelling was usually followed by applying the "smooth edges" and "remove islands" functions (standard settings). In order to incorporate the vascular wall within the selection of the veins and arteries, the edges of the labelled vascular lumina were allowed to expand with an arbitrary number of one pixel (grow command, two-dimensional mode).

Sections which, due to technical artefacts, lacked some parts of the embryo and slices that could not sufficiently be aligned were also labelled through interpolation of the labelled segments on the adjacent or nearby slices (Fig. 21).

All labelled vessels were checked for continuity on the previous and next digital slice. As at the level of the mesonephroi it was hard to determine on the digital images whether a certain lumen was lined with a vascular endothelium or a mesonephric tubule epithelium, correct labelling of the venous lumina at the level of these organs was confirmed by comparing the original histological slices with the labelled digital images.

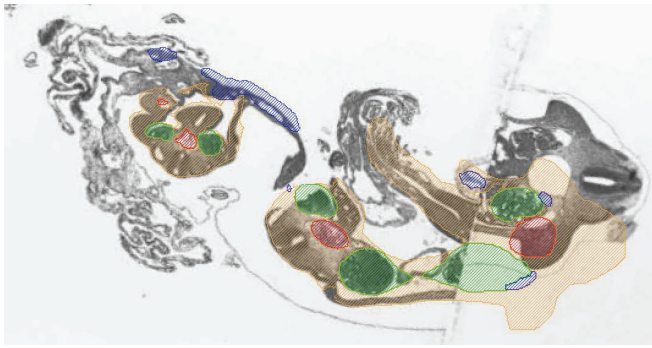

Fig. 21: Example of interpolation of the segmentation data from adjacent slices to label a torn section of a 4.5 mm embryo. On the right side of the section, image labels do not follow the contours of the displaced part of the section but are based on a calculated image by interpolating the segmentation data from the previous and next section.

3.2.5.5. Resampling

To save memory for the three-dimensional reconstruction, the voxel size of all bricks containing 101 labelled sections was down-sampled by a factor of 2 in every direction (x, y and z) using the resample module. In most cases, this resulted in a final voxel size of 20.1 x 20.1 x 16 µm.

3.2.5.6. Surface generation

A three-dimensional image was created from each of the bricks of labelled sections. During this process, an initial smoothing was performed based on the existing weights of the down-sampled bricks. All resulting surfaces were closed after ensuring that the cross-sectioned parts of the embryo extending beyond the top and bottom slice of one brick were not regarded as exterior surfaces by using the extra material option of the SurfaceGen computing module. All surfaces were built from triangles of which the edge length was at least 0.4 times the down-sampled voxel size. The obtained three-dimensional images were not subjected to any kind of smoothing or compaction as it was experienced that small tubular structures such as blood vessels tended to shrink and disappear in the final 3D image in cases where smoothing had been applied. The bricks containing the three-dimensional surfaces, visualised through the Surfaceview module, were aligned manually using the transform editor of each dataset.

3.2.6. Evaluation

After alignment of the entire embryo, the CRLs of the entirely reconstructed virtual embryos were measured by means of the Amira 3D measurement tool. Evaluation of the vascular network was performed in stereo view using red-cyan stereo glasses. Findings in the virtual embryos, in particular the orientation of the vessels to each other and to the reconstructed organs, were compared with the histological slices of the reference embryos of a similar CRL. Because of the twisted shape of the 4.6 mm embryo, it was very hard to compare the findings in the virtual 3D embryo with the 2D histological slices of the reference embryos. Therefore, a three-dimensional reconstruction was made of the vasculature surrounding the mesonephroi in the caudal half of a 4.7 mm reference embryo according to the aforementioned protocol in order to validate the initial conclusions. For similar reasons, two control embryos of the 27.6 mm reference embryo were also reconstructed.

As especially in the larger embryos and foetuses the raw images were harder to interpret and because it was found that for these specimens a single reconstruction is not always representative for all embryos of the same age, the general layout of the developing venous system was drawn in diagram based on the findings in the reconstructed reference embryo as well as the control embryos with similar sizes using the Adobe CS3 Illustrator software.

3.3. Microvascular corrosion casting

To complete the series of developmental stages of the caudal vena cava, corrosion casts were made of the nearly end-stage vascular system in six 9 cm foetuses (corresponding to a gestational age of 46 days p.c. (Evans and Sack, 1973)) obtained from gravid uteri collected in a commercial slaughterhouse in Zele, Belgium. To prevent desiccation and damage of the fresh specimens during transport, the foetuses were only removed from their intact foetal membranes and surrounding uterus after arrival at the department of Morphology, Ghent University.

After measurement of the crown-rump length, an umbilical artery in the umbilical cord still attached to the foetus was catheterized with a 25G flexible catheter under stereomicroscopic guidance. The catheter together with some umbilical cord tissue was pinned onto a piece of cardboard-covered polystyrene foam. At the point where the catheter entered the umbilical artery, a drop of cyanoacrylate glue was applied to seal off the lumen of the umbilical artery surrounding the catheter. The catheterised umbilical artery was flushed with 1 ml isotonic fluid (0.9% NaCl). During this procedure, the correct placement of the catheter was checked and the second umbilical artery was clamped. The umbilical vein was left open and served as natural drainage.

The resin to be injected was prepared by mixing 5 ml Batson's #17 monomer base solution (Polysciences Inc., Warrington, Pennsylvania (USA)), a pinch of red pigment and 0.75 ml Batson's #17 catalyst. Immediately after adding two drops of Batson's #17 anatomical corrosion kit promoter, the resin was injected through the catheter with gentle pressure using 2 ml plastic syringes until filling of subcutaneous veins was observed or intraperitoneal leakage of the resin was discovered. To damp sudden pressure changes caused by the manual injection, an air bubble was left in the syringe barrel between the resin to be injected and the tip of the plunger. Extra care was taken not to inject this small amount of air through the catheter into the foetus.

Half an hour after injection of the Batson's, the foetuses were submerged for 24 hours in a 25% potassium hydroxide solution. Subsequently, the corroded specimens were washed in running tap water for 8 hours, rinsed in 3 litres of distilled water and air-dried overnight in a vented hood. The air-flow passing through the drying corrosion casts was needed to prevent the branches of the cast from sticking together.

The dorsal parts of the casted abdominal aorta and caudal vena cava were exposed by carefully clipping away the small vessels supplying the vertebral column and dorsal muscles and studied under an Olympus SZX7 stereomicroscope.

3.4. Discussion

Concomitant with the application of invasive three-dimensional reconstruction techniques, a number of unavoidable technical artefacts are certain to interfere with the final image quality. As these artefacts are predominantly associated with preparatory deconstructive phases of tissue fixation and sectioning, many of these obstacles can simply be avoided by the use non-invasive 3D microscopical techniques such as Optical Projection Tomography (OPT), micro Magnetic Resonance Imaging (μMRI), Optical Coherence Tomography (OCT) or micro Computed Tomography (μCT), which allow the scanning of an entire specimen without disruption of its original configuration.

Although some of these applications have initially been taken into consideration to be used in the present study, it was finally chosen to continue exclusively with the invasive technique of serial sectioning and subsequent reconstruction to investigate the development of the caudal vena cava in the pig embryo. Whilst in the next chapter an appraisal will be given of the artefacts encountered in this study by following this approach, in the present section, the anticipatory measures that were taken to minimize these adverse effects will be discussed first. Subsequently, a short overview will be given of all items that have led to the elimination of the different non-invasive 3D microscopical techniques that are currently applied in embryonic research as a potential approach method in the present study.

3.4.1. Artefacts and final image quality

To minimize the adverse effects of the inevitable technical artefacts on the final image quality, a threefold strategy was followed: (1) analysing the critical steps in image reconstruction (2) minimizing the global incidence of technical artefacts and (3) when they occur, minimizing their impact on the final image reconstruction.

The most critical step during reconstruction turned out to be the image alignment. Bad alignment was not only detrimental for the 3D surface generation, most technical artefacts during the preparatory phases directly affected the alignment process specifically. Furthermore, bad alignment of the slices was difficult to resolve in the subsequent steps of reconstruction, and could only partially be bypassed by using the interpolation option in the segmentation step as explained earlier.

To avoid as many problems as possible at this specific bottleneck, the disruptive effects of the fixative solutions due to tissue dehydration and shrinkage were closely monitored. Although paraformaldehyde is commonly used for embryo fixation and histological processing (Zucker et al., 1999), its use was abandoned during the study as it turned out to have too many disruptive effects (see section 4.1.1.). Furthermore, during sectioning, stretching of the individual section on a hot plate was banned as the high temperature of the plate could cause the paraffin to melt and deliquesce, resulting in an unequally overstretched section. Throughout the staining procedure, the colour baths were frequently changed, to avoid gradual colour loss in the consecutive slices. Although less affecting the image alignment, colour variations were highly interfering with the semi-automated image segmentation.

Also the Amira reconstruction software was specifically chosen for its versatile ability to align histological slices and its capacity to deal with lost slices. A special algorithm was designed to help deciding whether a certain slightly damaged section was suitable for reconstruction or not (Fig. 22). Even the colour of the ink used to number the consecutive slices was determinative for a successful image alignment, as when a part of this number written next to the slice was accidently incorporated in the digital image of the section, the software experienced more difficulties to disregard this spot during its alignment attempts when black ink was used instead of red ink.

A second major critical point was the image smoothing that can be performed during or after the creation of the three-dimensional surface. As it was experienced that especially tubular structures tended to shrink and disappear from the image during this process, smoothing was abandoned and only the unaltered three-dimensional surface was evaluated in this study.

By carefully monitoring these several critical control points, the incidence of technical artefacts intervening with the final evaluation could be reduced to a certain minimum and readable and reliable three-dimensional images could be produced. However, this approach could not eliminate the second most commonly described disadvantage of this invasive 3D microscopical technique (Sharpe, 2003), namely its rather time-consuming and labour intensive character.

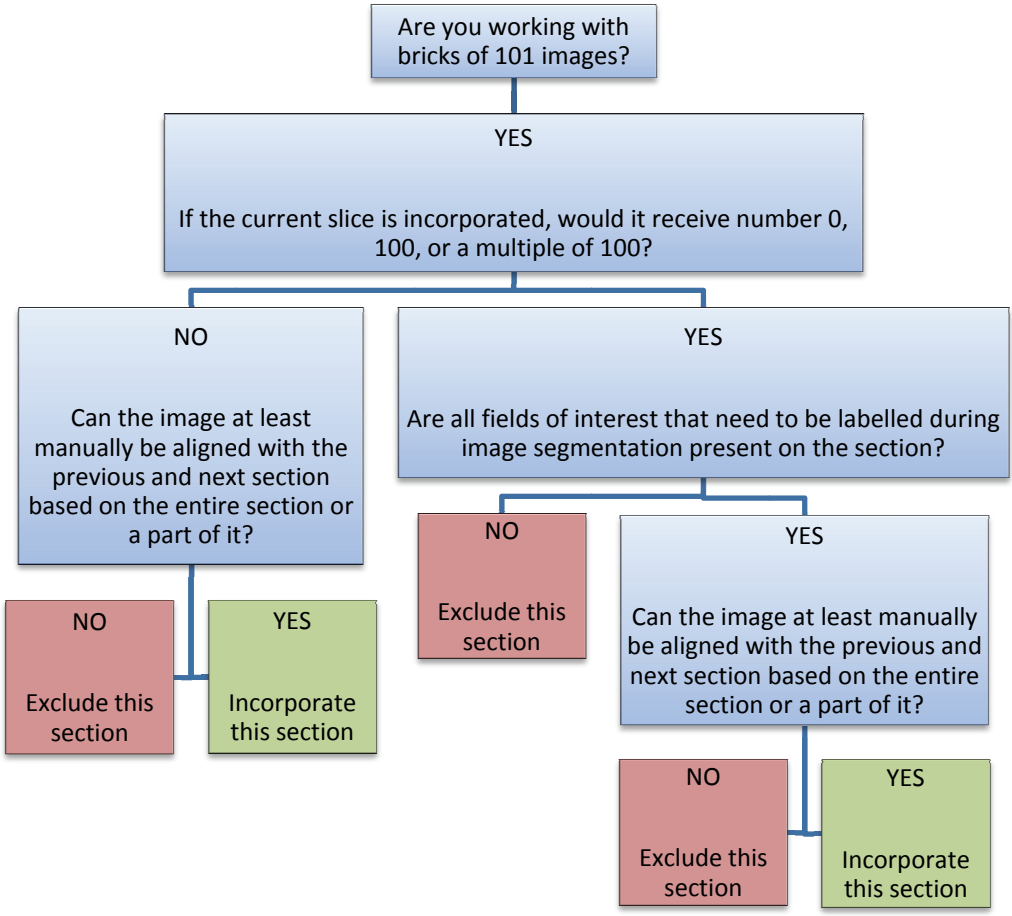

Fig. 22: Example of an algorithm used to determine whether a slightly damaged histological section could be used for three-dimensional reconstruction, illustrating the determinative character of the image alignment step. The intermediate step that was specially created for sections that might receive the numbers 0, 100 or a multiple of 100 had to be inserted because for these sections, bypassing the effects of a bad image alignment by using the interpolation option during subsequent image segmentation could not be performed (these image would become the first or last image of a certain brick of 101 slices and cannot dispose of both a previous and next section to have the segmentation data interpolated from).

3.4.2. Elimination of non-invasive three-dimensional techniques

Non-invasive 3D microscopy has many advantages compared to the invasive techniques (table 3 on page 87), especially in cases in which the detailed topographical anatomy of embryos is to be studied. The most important benefit is the fact that embryos can be studied in toto, without the need to cut them into smaller parts or sectioning them. This way, technical artefacts associated with sectioning and subsequent reconstruction from two-dimensional images substantially affecting the 3D-image quality can be avoided. Furthermore, non-invasive techniques are less time consuming and less labour-intensive (Sharpe, 2003; Davies and Armstrong, 2006).

One of the currently more and more frequently applied non-invasive 3D visualisation techniques in embryology is Optical Projection Tomography (OPT). The principle of this application is quite similar to the technology of the typical medical CT-scanners, but rather by scanning the object with X-rays, optical laser light in the visible or ultraviolet range of the electromagnetic spectrum is passed through the rotating specimen of interest, and the transmitted beams are captured on a CCD camera chip. Using the same back-projection algorithm as for medical CT scans, virtual sections and a three-dimensional image on microscale can be computed (Sharpe, 2003). In fact, this technique has already successfully been applied to study the vascular development in the mouse embryo (Coultas et al., 2005). However, as OPT has only very recently been developed (Sharpe et al., 2002), this new technology was not yet commercially available at the start of the present study. Furthermore, current OPT-scanners (Bioptonics® 3001) can only handle specimen smaller than 10 mm in diameter and 15 mm in length, whilst the construction of the infrarenal part of the caudal vena cava in the pig embryo, which is the main focus of this study, only takes place in embryos ranging between 20 and 35 mm in length.

A non-invasive tool that can visualise larger soft-tissue specimens in 3D is micro-Magnetic Resonance Imaging (µMRI). Micro-MRI is not hampered by the opacity of sample and has already successfully been used to study embryonic morphological development (Tyszka et al., 2005). It relies on identical principles as the medical MRI scanners. However, to achieve a higher resolution in the micrometer range, more powerful magnets have to be used than the commonly used 0.2 till 3 Tesla magnets in diagnostic imaging. Whereas a typical µMRI scanner can achieve a magnetic force of 7 Tesla, µMRI scanners that are utilized to scan embryos have to be equipped with a giant magnet of 17.6 T and more to achieve a resolution

of about 10 µm (Poelman and Hogers, 2004). This equipment, having a magnetic force of approximately 360,000 times the earth's magnetic field strength, is not only in itself very expensive, also the installation of a specialised infrastructure housing the equipment requires a huge financial effort (Jakob, 2004).

Also Optical Coherence Tomography (OCT) has been proven to be of significant value in 3D morphological studies in embryos (Boppart et al., 1996; Yelbuz et al., 2002). This technology relies on the same principle as medical B-mode 3D ultrasonography, but instead of analysing the reflection of emitted ultrasound waves, the coherence between the emitted and reflected visible light waves is analysed and translated into a 3D image (Masters and Böhnke, 2002). Yelbuz et al. (2002) reported in their study a resolving power of 27x27x22 µm, which is sufficient to study the large vascular architecture in the developing embryo. However, the virtual sections produced by OCT have the typical appearance of a common B-mode ultrasonogram: whilst for the human eye it is very easy to distinguish the different structures on the picture, a computer has, due to the grainy aspect of the image and the unclear, rugged boundaries between the different projected tissues, the greatest difficulties to identify the various tissues, which is pernicious for the subsequent segmentation process in the 3D reconstruction. Furthermore, high costs of the equipment combined with a low penetration dept into the specimen are also drawbacks for the practical application of the OCT-scanner.

A last non-invasive 3D microscopic technique that has been considered for application in the present study is the micro-Computed Tomography (µCT). Although this application is, similar to the medical CT-scanners, based on X-ray technology, it has already successfully been used to study the microscopic architecture of soft tissues such as lung alveoli (Litzlbauer et al., 2006). However, attempts to visualise the vascular architecture in 10 mm embryos using a high-resolution Skyscan 1072 µCT scanner ended in rather disappointing results as only the embryo's exterior and central nervous system could be reconstructed from the virtual sections (Fig. 23). Infusion of contrast media to opacify the vessels could have been a solution (Langheinrich et al., 2004; Butcher et al., 2007), but clear visualisation of the surrounding developing organs would have remained problematic.

For the reasons described above, the application of non-invasive 3D microscopy was no longer considered as an option in the present study. The technique of three-dimensional reconstruction of embryonic tissues starting from histological serial sections has been

developed since the second half of the 1990ies (Verbeek et al., 1995; Whiten et al, 1998) and is currently still a widely used application (Yasuda et al., 2007). In the current research, the technical horizons of this application have even be broadened and limits have been extended, as never before, such a large amount of slices and different tissues were used and labelled in a single reconstruction.

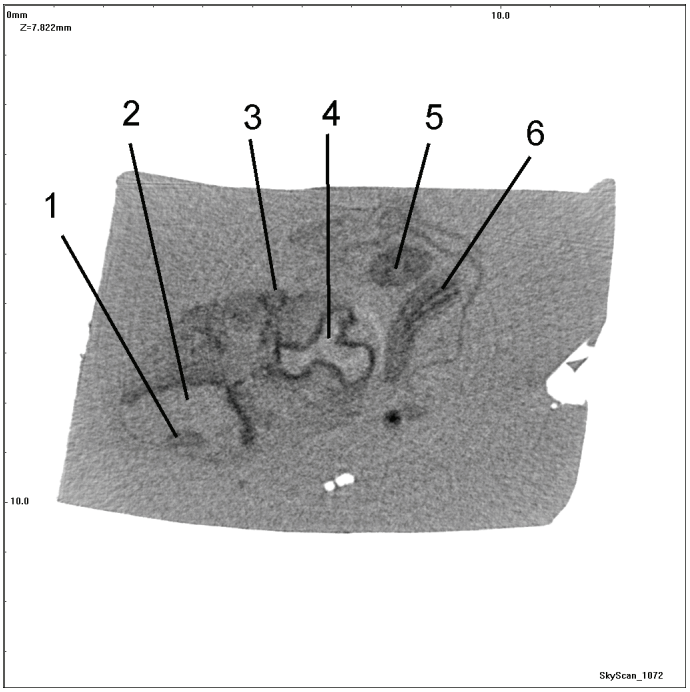

Fig. 23: Virtual micro-computed tomography section through a 13 mm cat embryo embedded in a block of paraffin, obtained by using a Skyscan 1072 µCT scanner. Only the contours of the embryo and some parts of the central nervous system could be visualised: 1: plexus choroideus of the metenchephalon, 2: metencephalon, 3: optic vesicle, 4: telencephalon, 5: left hindlimb bud, 6: tail. Image courtesy of Skyscan, Kontich, Belgium.

Table 3: Comparison between the different three-dimensional microscopic techniques described in the present section. The data is obtained from the manufacturer's information sheets and from the references in the main text. The figures in the last column are based on personal experiences.

	OPT	**µMRI**	**OCT**	**µCT**	**Histological serial sections**
Example device	Bioptonics 3001	Bruker Avance 750 WB 17.6 T	Thorlabs OCMP 1300 SS	Skyscan 1072	Olympus BX61 and DP50 camera
Maximum resolution	4-28 µm	7.8 µm	15 µm (transverse) 9 µm (axial)	5-10 µm	200 nm (transverse) 4 µm (axial)
Maximum sample diameter	10 mm	89 mm	1-3 mm	15 mm	unlimited
Maximum sample size	15 mm	Several cm	10 mm	30 mm	unlimited
Sampling time	30 minutes	14 hours	30 seconds	15 minutes - 2 hours	Days - weeks - months
Costs	Moderate	Very high	High	Moderate	Low
Availability / application	First model launched in 2007	Only in highly specialised laboratory environment	In specialised laboratory and clinical environment	Wide range of types and models available	Widely available
Invasive	No	No	No	No	Yes
Sample preparation (embryology)	Clarification and staining	None	None	Injection of contrast agents	Paraffin embedding, serial sectioning and staining

3.5. Literature

Boppart, S.A., M.E. Brezinski, B.E. Bouma, G.J. Tearny and J.G. Fujimoto (1996). Investigation of developing embryonic morphology using optical coherence tomography. *Developmental Biology* 177, 54-63.

Butcher, J.T., D. Sedmera, R.E. Guldberg and R.R. Markwald (2007). Quantitative volumetric analysis of cardiac morphogenesis assessed through micro-computed tomography. *Developmental Dynamics* 236, 802-809.

Coultas, L., K. Chawengsaksophak and J. Rossant (2005). Endothelial cells and VEGF in vascular development. *Nature* 438, 937-945.

Davies, J.A. and J.E. Armstrong (2006). The anatomy of organogenesis: novel solutions to old problems. *Progress in Histochemistry and Cytochemistry* 40, 165-176.

Evans, H.E. and W.O. Sack (1973). Prenatal development of domestic and laboratory animals: growth curves, external features and selected references. *Anatomia, Histologia, Embryologia* 2, 11-45.

Jakob, P. (2004). Resolution, limitations and strengths of micro-MRI (up to 17.6 Tesla). *Workshop Non-Invasive 3D Microscopy*, 21st August 2004, Antwerp.

Kaufman, M.H. (1992). The atlas of mouse development. Academic Press, London, p. 3.

Langheinrich, A.C., R.M. Bohle, A. Breithecker, D. Lommel, W.S. Rau (2004). Micro-computed tomography of the vasculature in parenchymal organs and lung alveoli. *RöFo : Fortschritte auf dem Gebiete der Röntgenstrahlen und der Nuklearmedizin* 176, 1219-1225.

Litzlbauer, H.D., C. Neuhaeuser, A. Moell, S. Greschus, A. Breithecker, F.E. Franke, W. Kummer and W.S. Rau (2006). Three-dimensional imaging and morphometric analysis of alveolar tissue from microfocal X-ray computed tomography. *American Journal of Physiology. Lung Cellular and Molecular Physiology* 291, L535-L545.

Masters, B.R. and M. Böhnke (2002). Three-dimensional confocal microscopy of the living human eye. *Annual Review of Biomedical Engineering* 4, 69-91.

Poelman, R.E. and B. Hogers (2004). MicroMRI in embryology. *Workshop Non-Invasive 3D Microscopy*, 21st August 2004, Antwerp.

Sharpe, J., U. Ahlgren, P. Perry, B. Hill, A. Ross, J. Hecksher-Serensen, R. Baldock and D. Davidson (2002). Optical projection tomography as a tool for 3D microscopy and gene expression studies. *Science* 296, 541-545.

Sharpe, J. (2003). Optical projection tomography as a new tool for studying embryo anatomy. *Journal of Anatomy* 202, 175-181.

Tyszka, J.M., S.E. Fraser and R.E. Jacobs (2005). Magnetic resonance microscopy: recent advances and applications. *Current Opinion in Biotechnology* 16, 93-99.

Verbeek, F.J., D.P. Huijsmans, R.J. Baeten, N.J. Schoutsen and W.H. Lamers (1995). Design and implementation of a database and program for 3D reconstruction from serial sections: a data-driven approach. *Microscopy Research and Technique* 30, 496-512.

Whiten, S., S.D. Smart, J.C. McLachlan and J.F. Aiton (1998). Computer-aided interactive three-dimensional reconstruction of the embryonic human heart. *Journal of Anatomy* 193, 337-345.

Yasuda, M., S. Yamada, C. Uwabe, K. Shiota and Y. Yasuda (2007). Three-dimensional analysis of inner ear development in human embryos. *Anatomical Science International* 82, 156-163.

Yelbuz, T.M., M.A. Choma, L. Thrane, M.L. Kriby and J.A. Izatt (2002). Optical coherence tomography: a new high-resolution imaging technology to study cardiac development in chick embryos. *Circulation* 106, 2771-2774.

Zucker, R.M., E.S. Hunter III and J.M. Rogers (1999). Apoptosis and morphology in mouse embryos by confocal laser scanning microscopy. *Methods* 18, 473-480.

CHAPTER 4: RESULTS

4.1. Vascular development in the 3.7-18.0 mm pig embryo

4.2. Development of the infrarenal part of the porcine caudal vena cava in the late embryonic and early foetal period

4.3. Literature

Based on:

Cornillie P., W. Van den Broeck and P. Simoens (2008). Three-dimensional reconstruction of the remodelling of the systemic vasculature in early pig embryos. *Microscopy Research and Technique* 71, 105-111.

Cornillie P., W. Van den Broeck and P. Simoens (2008). Origin of the infrarenal part of the caudal vena cava in the pig. *Anatomia, Histologia, Embryologia,* accepted.

CHAPTER 4: RESULTS

4.1. Vascular development in the 3.7-18.0 mm pig embryo

4.1.1. General remarks

The histological morphology of the paraformaldehyde-fixed embryos was severely altered making them unsuitable for reconstruction. In particular, the neural tube and pericardial cavity suffered from disproportional expansion and subsequent rupture.

In contrast, the internal morphology of the Bouin's-fixed embryos was well conserved, and therefore no substantial difficulties were encountered during slice alignment and 3D-reconstruction (Fig. 24). However, a difference was noticed between the CRL measurements before fixation (values expressed in mm) and after virtual three-dimensional reconstruction (values expressed in mm between brackets): 3.7 mm (3.2 mm), 4.6 mm (measurement not possible), 10.0 mm (6.3 mm), 12.0 mm (8.6 mm) and 18.0 mm (16.4 mm). On the microscopic slices of the reference embryos, cross-sections of the vessels observed in the reconstructed embryos of a comparable CRL were found in a similar orientation relative to the mesonephroi, metanephroi and gonads.

4.1.2. Vascular configuration in the 3.7 mm embryo

The external morphology after three-dimensional reconstruction of the smallest embryo of the series was characteristic of an embryo that had suffered from recent intra-uterine death and which had passed through the initial phases of embryonic resorption. Moreover, at the moment of removal from the uterus, the tail part of the embryo had become detached from the rest of the body and was lost. However, the internal morphology, including the major vessels, still could be seen. The ventral aortae emerging from the truncus arteriosus clearly branched into two discernible pairs of branchial arch arteries (first and second pair), each connected with the ipsilateral dorsal aorta. At the level of the liver, both dorsal aortae fused into a single abdominal aorta. The arterial system was bilaterally flanked by the cranial and caudal cardinal veins which drained into the sinus venosus of the heart through the left and right common cardinal veins. The caudal cardinal veins coursed dorsolateral to the corresponding mesonephroi. As the tail part of the embryo was missing,

the relative position of the caudal cardinal veins to the umbilical arteries could not be assessed.

4.1.3. Vascular configurations in the 4.6 and 4.7 mm embryos

Initial remodelling of the basic vascular pattern, as described in the 3.7 mm embryo, had occurred in this specimen. The branchial arch system now contained three pairs of arteries which could be identified as the second, third and fourth pharyngeal arch arteries (Fig. 25).

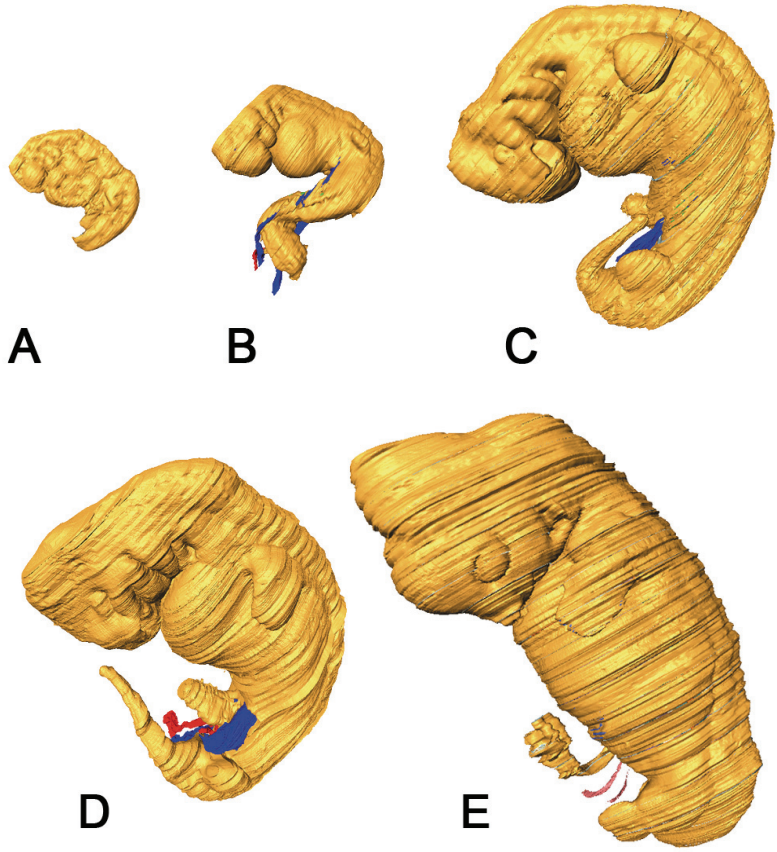

Fig. 24: Reconstruction images of the pig embryos of 3.7 mm (A), 4.6 mm (B), 10.0 mm (C), 12.0 mm (D) and 18.0 mm (E) crown-rump length.

Both caudal cardinal veins were identifiable as voluminous vessels dorsolateral to the cranial-most fourth part of the mesonephroi and as much smaller vessels dorsal to the caudal half of these organs. At the level of the second quarter of the mesonephroi, the left caudal cardinal vein was absent whilst its right counterpart had been partially interrupted. Blood from the caudal-most parts of the caudal cardinal veins had deviated along the medial wall of the mesonephroi to the newly formed subcardinal veins which were located ventromedial to the mesonephroi and ventral to the aorta. Both subcardinal veins were about 1,000 µm in length and had no contact with each other. They drained into the cranial segment of the

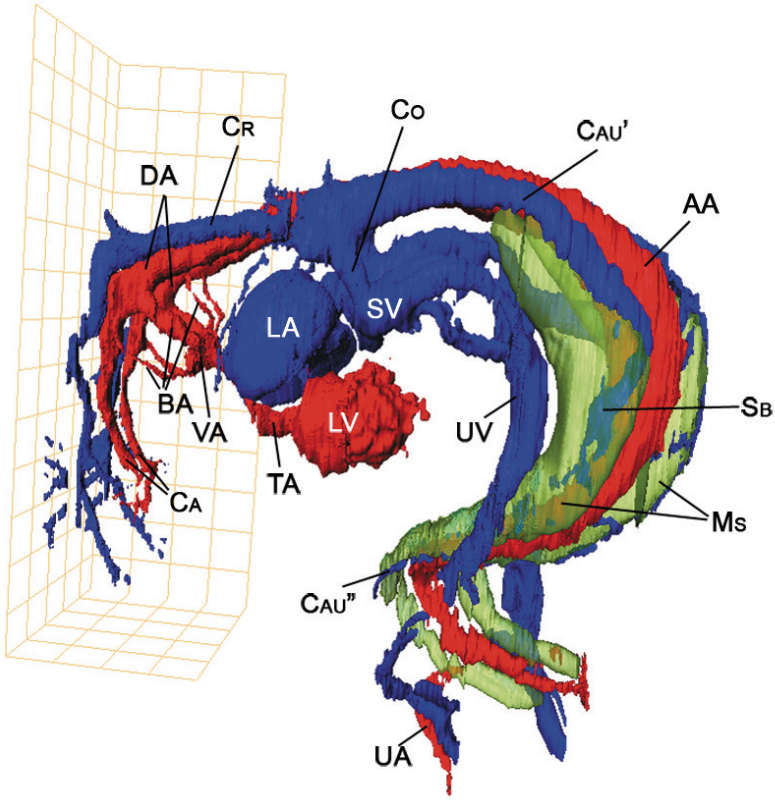

Fig. 25: Left lateral view of the vasculature surrounding the mesonephroi in the 4.6 mm pig embryo. The arterial system is displayed in red, the venous system in blue and the mesonephroi in transparent green. Grid unit = 250 µm x 250 µm. AA: abdominal aorta, BA: branchial arch arteries, CA: carotid arteries, CAU': left caudal cardinal vein (cranial segment), CAU": left caudal cardinal vein (caudal segment), CO: left common cardinal vein, CR: left cranial cardinal vein, DA: dorsal aortae, LA: left atrium, LV: left ventricle, MS: mesonephros, SB: left subcardinal vein, SV: sinus venosus, TA: truncus arteriosus, UA: left umbilical artery, UV: left umbilical vein, VA: ventral aorta.

ipsilateral caudal cardinal veins along the dorsomedial border of the mesonephroi. Medial to the cranial-most quarter of the mesonephroi, several separate venous sacs were present in a metameric configuration. They each drained individually along the dorsomedial wall of the mesonephroi into the cranial part of the caudal cardinal vein.

Due to their very narrow diameter, the caudal-most segments of the caudal cardinal veins could not be seen at the level of the umbilical arteries in the three-dimensional reconstructions of the 4.6 mm embryo. Only the mesonephroi were still identifiable in this region. They were located dorsal and lateral to the umbilical arteries which branched off from the abdominal aorta (Figs. 25 and 29A). In the three-dimensional reconstruction of the caudal half of the 4.7 mm reference embryo, the caudal cardinal veins were more voluminous in this specific region and clearly coursed dorsal to the mesonephroi overlying the umbilical arteries (Fig. 26). In this reference embryo, the subcardinal veins extended more caudally and were also identifiable in the first half of the reconstructed caudal part of the embryo. In this region, they were connected to the ipsilateral caudal cardinal veins through at least five individual anastomoses along the dorsomedial wall of the mesonephroi.

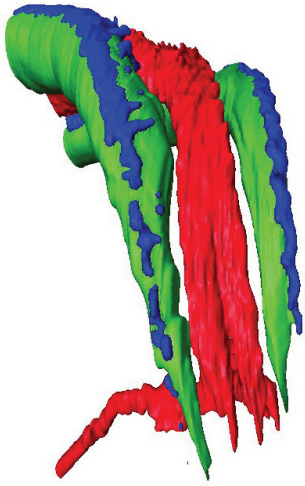

Fig. 26: Caudodorsal view on the vasculature and mesonephroi in the caudal half of a 4.7 mm pig embryo. The mesonephroi (green) and overlying caudal cardinal veins (blue) could be visualised dorsal to the terminal branching of the aorta in both left and right umbilical artery (red).

4.1.4. Vascular configurations in the 10.0 and 12.0 mm embryos

The bilateral third, fourth and sixth branchial arch arteries could be seen in both the 10.0 mm and 12.0 mm embryos. The dorsal aorta was still paired cranial to the transverse septum. Caudally, the aorta branched into both umbilical arteries which, in contrast with the situation in the earlier embryos, were now located caudal to the caudal poles of the mesonephroi in the 10.0 mm embryo and caudodorsal to the mesonephroi in the 12.0 mm embryo.

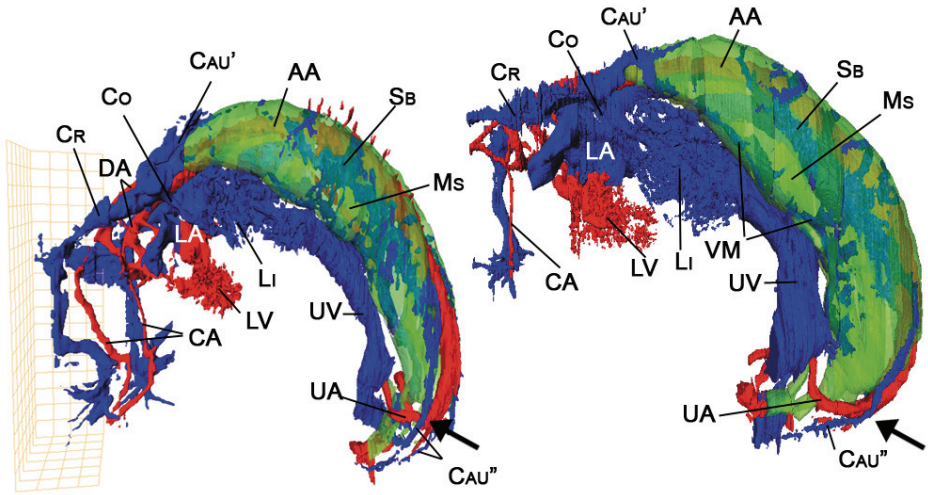

Fig. 27: Left lateral views of the process of dorsal deviation of the caudal cardinal veins. Grid unit = 250 µm x 250 µm. **Left**: Reconstruction of the vascular system in the 10.0 mm embryo with a straight caudal cardinal vein at the level of the umbilical arteries (arrow). **Right**: Reconstruction of the vascular system in the 12.0 mm embryo showing the dorsal displacement of the caudal cardinal veins (arrow). AA: abdominal aorta (medial to the mesonephros), CA: carotid arteries, CAU': left caudal cardinal vein (cranial segment), CAU": left caudal cardinal vein (caudal segment), CO: left common cardinal vein, CR: left cranial cardinal vein, DA: dorsal aortae, LA: left atrium, LI: venous vasculature of the liver, LV: left ventricle, MS: mesonephros, SB: fused left and right subcardinal vein (medial to the mesonephros), SV: sinus venosus, TA: truncus arteriosus, UA: left umbilical artery, VM: left ventral mesonephric vein (cranial and caudal segment).

The caudal cardinal veins were interrupted in the mid-region of the mesonephroi. Their caudal-most segments were clearly located dorsal to the umbilical arteries, coursed dorsolateral to the caudal third part of the mesonephroi, and drained along the dorsomedial surface of these organs in the subcardinal veins. In the 12.0 mm embryo, the caudal cardinal veins appeared to be locally displaced in the dorsal direction by the umbilical arteries (Figs. 27 and 29C).

The cranial segments of the caudal cardinal veins were located dorsolateral to the cranial third part of the mesonephroi and drained into the ipsilateral common cardinal veins. The middle third part of both mesonephroi was drained by several separate veins which emerged at the lateral surface of the mesonephroi and curved transversely around their dorsal surface, merging at a perpendicular angle with the subcardinal veins at the medial surface of the mesonephros ventral to the aorta.

The subcardinal veins were the most dominant somatic venous channels. The middle third segments of the left and right subcardinal veins were fused with each other in the midline of the embryo. The cranial segments of the subcardinal veins were no longer connected to the caudal cardinal veins. Instead, the right subcardinal vein drained all the blood from the subcardinal system through a newly formed anastomosis with the cranial part of the underlying right vitelline vein towards the sinus venosus of the heart.

In the 12.0 mm embryo, an additional longitudinal vein coursed along the ventral side of each mesonephros. Each of both these longitudinal ventral mesonephric veins could be subdivided into two segments. Their cranial segments drained smoothly into the caudal cardinal veins cranial to the mesonephroi, whilst the caudal segments drained into the subcardinal system along both the ventromedial and the dorsolateral surfaces of the mesonephroi, thereby creating a venous ring encircling each mesonephros (Fig. 29C). In the 10.0 mm embryo, short venous segments at the ventral side of the mesonephroi could be observed although not yet organised as longitudinal channels draining into the caudal cardinal or subcardinal veins.

4.1.5. Vascular configuration in the 18.0 mm embryo

In the 18.0 mm embryo, the arterial system had adapted its configuration as found in the end-term foetus: the aorta was present as a single tube which could be subdivided in the ascending aorta emerging from the left ventricle, the aortic arch receiving the ductus arteriosus (Botalli), and the thoracic and abdominal parts of the descending aorta. The pulmonary trunk arising from the right ventricle could be visualised up to the level of the two pulmonary arteries, whilst its major branch was the ductus arteriosus which served as a short cut between the pulmonary and systemic circulations.

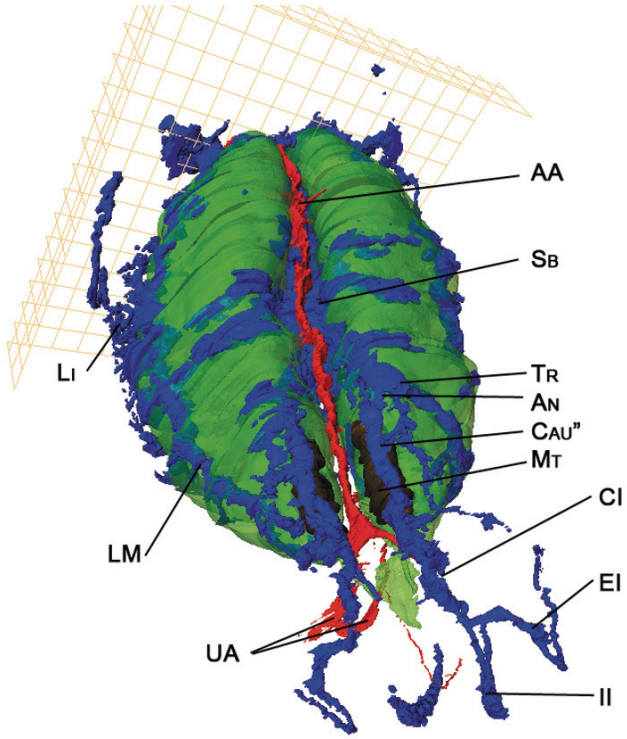

Fig. 28: Caudodorsal view of the reconstructed vascular system of the 18 mm pig embryo in relation to the excretory organs. Grid unit = 250 µm x 250 µm. AA: abdominal aorta, An: anastomosis between the right caudal cardinal vein and the caudalmost tributary of the subcardinal system, CAU": right caudal cardinal vein (caudal segment), CI: right common iliac vein, EI: right external iliac vein, II: right internal iliac vein, LI: venous vasculature of the liver, LM: left lateral mesonephric vein, MT: right metanephros, SB: fused left and right subcardinal vein, TR: caudalmost mesonephric tributary of the subcardinal veins, UA: umbilical arteries.

On the other hand, the configuration of somatic veins was still in a transient embryonic stage, although severe adaptations could be observed to the basic pattern, as described above. At the level of the mesonephroi, the caudal cardinal veins as well as the

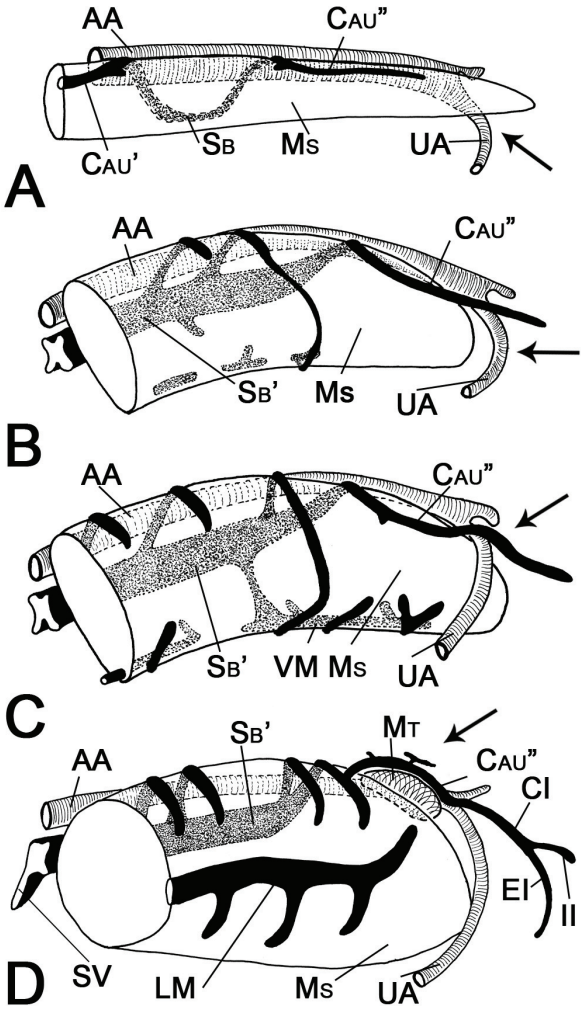

Fig. 29: Schematic compilation of the migration of the umbilical arteries to the mesonephroi (arrows) and subsequent dorsal deviation of the caudal cardinal veins in the pig embryo. Left lateral view on the caudal half of the 4.6 mm embryo (A), 10.0 mm embryo (B), 12.0 mm embryo (C) and 18.0 mm embryo (D). AA: abdominal aorta, CAU': left caudal cardinal vein (cranial segment), CAU": left caudal cardinal vein (caudal segment), CI: left common iliac vein, EI: left external iliac vein, II: left internal iliac vein, LM: left lateral mesonephric vein, MS: Left mesonephros (caudal part), MT: left metanephros, SB: left subcardinal vein, SB': fused left and right subcardinal veins, SV: subcardinal-vitelline anastomosis, UA: left umbilical artery, VM: left ventral mesonephric vein.

longitudinal ventral mesonephric veins were completely absent. The subcardinal system was further developed and collected several individual veins emerging from the dorsolateral surfaces of the caudal half of the mesonephroi. Caudal to the mesonephros, remainders of the caudal cardinal veins could be observed dorsal to the developing metanephroi. These veins in the lumbar region collected the blood from the internal and external iliac veins. Craniolateral to the metanephroi, they curved with sharp angles in a ventrolateral direction and joined the caudal-most mesonephric tributaries of the subcardinal veins (Figs. 28 and 29D).

Along the entire lateral surface of each mesonephros, a new longitudinal vein could be observed which drained cranially into the ipsilateral common cardinal vein. This lateral mesonephric vein received tributaries from the ventrolateral parts of the mesonephros.

4.1.6. Discussion

The present findings on the fate and origin of the veins in the mesonephric region are in overall agreement with the observations described in both the supracardinal and the sacrocardinal models depicting the development of the caudal vena cava. Veins typical for the pig, such as the ventral and lateral mesonephric veins as reported by Butler (1927), were also observed. However, in contrast with the conclusions of the latter author, the lateral mesonephric veins in the 18 mm embryo in the present study extended along the entire lateral surface of the mesonephroi rather than being restricted to the caudal third only.

Whereas most existing theories agree upon the pattern of vascular remodelling at the level of the mesonephroi, there are many conflicting theories as regards the fate of the more caudally located veins that will eventually build the infrarenal part of the caudal vena cava. Although the supracardinal and sacrocardinal models reflect a different opinion as concerns the origin and fate of the embryonic veins which are involved in the construction of this segment of the caudal vena cava, they both claim that these specific vessels are located in a more dorsal plane than the veins surrounding the mesonephroi, and therefore must be a new pair of vessels different from the caudal cardinal or subcardinal veins (Cornillie and Simoens, 2005). However, observations in the present study suggest that the veins in this specific region are most probably the residual parts of the caudal cardinal veins which have been displaced dorsally during development, due to the downward migration of the mesonephroi in relation to the umbilical arteries (Fig. 29). Because these veins extend beyond the caudal end of the mesonephroi, they are incapable of following the relocation of these organs as they are hampered by the umbilical arteries branching from the aorta. This relative deviation in dorsal direction is further expanded on by the development of the metanephroi in the space which is bordered ventrally by the mesonephroi, caudally by the umbilical arteries and dorsally by the caudal cardinal veins. This eventually results in the configuration described for the so-called supracardinal veins in the late 17-19 mm pig embryo by Butler (1927), or the sacrocardinal veins in the early 9 mm human embryo by Grünwald (1938). Despite the interspecies differences in CRL and the developmental stage of the vascular architecture at that specific time, the appearance of the more dorsally located venous segments coincides remarkably with the species-specific time of metanephric development, as reported by Sadler (1985), Rüsse (1991) and Carlson (1994). This strengthens the suggested hypothesis of the relocation of pre-existing vessels.

The use of three-dimensional reconstruction software made it possible to evaluate the vascular architecture and its relative position to other organs during development without disruption of the spatial arrangement of the embryo. Unlike previous investigations into the anatomy of the embryonic venous system, each histological section through a single embryo could be used for evaluation. Earlier studies relied solely on cross-sections that were exactly perpendicular. As early embryos are C-shaped, several embryos of the same age, each differently orientated in the paraffin blocks, were needed to reconstruct a virtually stretched embryo suitable for evaluation (Grünwald, 1938). Undoubtedly, this artefact must have obscured some vital information on the spatial arrangement of the venous system, and most likely formed the basis for the various contradicting hypotheses on the development of the caudal vena cava. Although the use of state-of-the-art reconstruction software offers a closer approach to the real-life configuration, it still relies on intermediate steps such as tissue fixation and sectioning which influence the size and morphology of the reconstructed image. Indeed, embryos tended to shrink and obtained an even more curved shape during fixation and tissue processing, while disruption of specific tissues could be observed, depending on the fixative. Variations in the degree of stretching of the paraffin sections prior to mounting them on glass slides negatively influenced correct alignment of the consecutive slices.

The disadvantages of using histological sections for three-dimensional reconstruction have however not impeded the search for an explanation for the disparities between the supracardinal and sacrocardinal models. In the present study, it has clearly been shown that the paired veins located dorsally in the lumbar region are in fact the caudal cardinal veins which have been displaced due to the shift of the umbilical arteries relative to the developing metanephroi. The specific time at which these veins assume their more dorsal position must not been regarded as related to a specific developmental stage of the venous architecture, as suggested by authors of the different models, but merely as being influenced by the time of development of the metanephroi.

However, this specific time of appearance is not the only discrepancy between the existing theories on the development of the caudal vena cava. According to Huntington and McClure (1920) and Butler (1927), the caudal supracardinal veins, which correspond to the displaced caudal cardinal veins in the present study, will temporarily form a connection with the veins building the azygos system in the thorax, whilst Grünwald (1938) definitely stated that he had never observed such a connection. Because this transitory fusion is said to occur

later than the 17-19 mm stage in porcine embryos (Butler, 1927), further research in older embryos is still necessary to clarify the latter point of disagreement and finally to be able to map the exact process of vascular development and regression of the somatic veins in the pig model.

4.2. Development of the infrarenal part of the porcine caudal vena cava in the late embryonic and early foetal period

4.2.1. General remarks

The terminology in this section is derived from the descriptions of Butler (1927) for the venous system and Sabin (1909) for the lymphatic system and has, where necessary, been adapted to the official nomenclature listed in the Nomina Embryologica Veterinaria (2006). The only exception is the name used to indicate the longitudinal pair of veins that is directly involved in the construction of the infrarenal part of the caudal vena cava. To allow an unbiased approach, it was preferred to refer to these veins in the present chapter by using the purely descriptive topographical term "sublumbar veins" so that afterwards, in the discussion, a proper evaluation of the true identity and homology of these veins can be performed. The numbers between brackets in the next sections refer to the anatomical structures labelled accordingly in the following schematic figures.

4.2.2. Venous pattern in the lumbar region of the 20.0 mm embryo

The anatomical configuration of the venous system in the lumbar region (Fig.30) did not differ much from the situation in the 18.0 mm embryo described in section 4.1.5. The blood returning from the hindquarters of the embryo was collected by the left and right common iliac veins (7), whilst the blood coming from each mesonephros was mainly drained by the ipsilateral subcardinal vein (4-5-6) coursing along the medial surface of the organ.

Both common iliac veins (7) did not meet each other at the level of the terminal aortic branching. Instead, they were each continued cranially by the sublumbar veins (8), which curved over the dorsal surface of the ipsilateral developing metanephros. Along their entire length, the sublumbar veins were located lateral to the sympathetic trunks. Craniomedial to the metanephroi, each sublumbar vein was connected through a vertical slit-like anastomosis (9) with the ipsilateral subcardinal vein (6) medial to the mesonephros. Cranial to the reception of the sublumbar veins, the midsections of the left and right subcardinal veins were fused, forming a large subcardinal anastomosis (5) ventral to the aorta (1).

Unlike the situation in the 18.0 mm embryo, the lateral mesonephric veins (11), coursing in a shallow groove along the lateral surface of the mesonephroi, anastomosed

caudally with the ipsilateral common iliac veins (7). Furthermore, they were connected with the subcardinal veins at the level of the subcardinal anastomosis (5) by a single branch (12) coursing perpendicularly over the dorsal surface of the ipsilateral mesonephros.

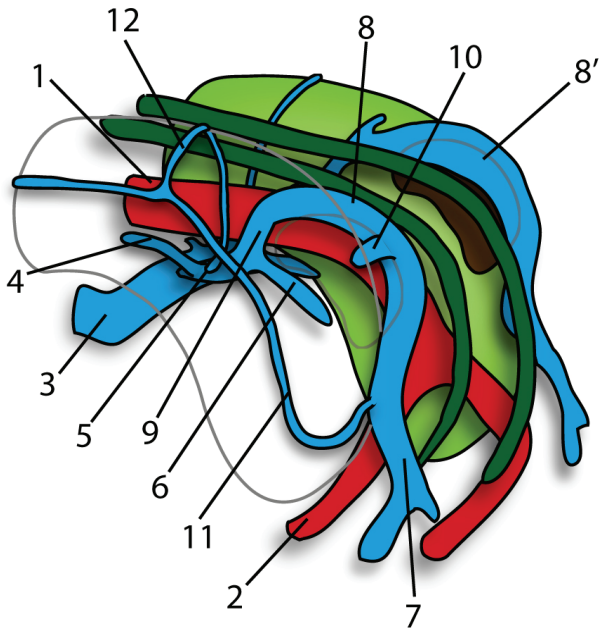

Fig. 30: Schematic representation of the developing vascular system in the caudal half of a 20 mm embryo after removal of the left mesonephros and metanephros (drawn in contours), left lateral view. Colour codes: red: arterial system, blue: venous system, dark green: sympathetic trunk, pale green: mesonephros (partially displayed), brown: right metanephros / kidney. Numbers followed by an accent (') indicate right-sided structures. 1: aorta, 2: umbilical artery, 3: cranial part of the caudal vena cava, 4: cranial segment of the subcardinal vein, 5: subcardinal anastomosis, 6: caudal segment of the subcardinal vein, 7: common iliac vein, 8: sublumbar vein (longitudinal segment), 9: sublumbar vein (vertical segment), 10: cranial abdominal vein, 11: lateral mesonephric vein, 12: anastomosis between 11 & 5.

4.2.3. Venous pattern in the 22.5 mm embryo

Apart from the lumbar region (Fig. 32), the thoracic (Fig. 31) and abdominal parts of this embryo were also reconstructed in detail. Cranial to the heart and aortic arch (23), the large anastomosis (17) between the left and right cranial cardinal veins (14') could clearly be identified. Between this anastomosis and the left common cardinal vein (13), the left cranial cardinal vein was still present and equal in size and diameter as its right counterpart. In the angle between the left and right jugular (20') and cephalic (19') veins, the jugular lymphatic

sacs (21') could clearly be visualized, as well as the subclavian sacs (22') draining into these. On the other hand, there was no sign of a thoracic duct draining into one of the jugular sacs.

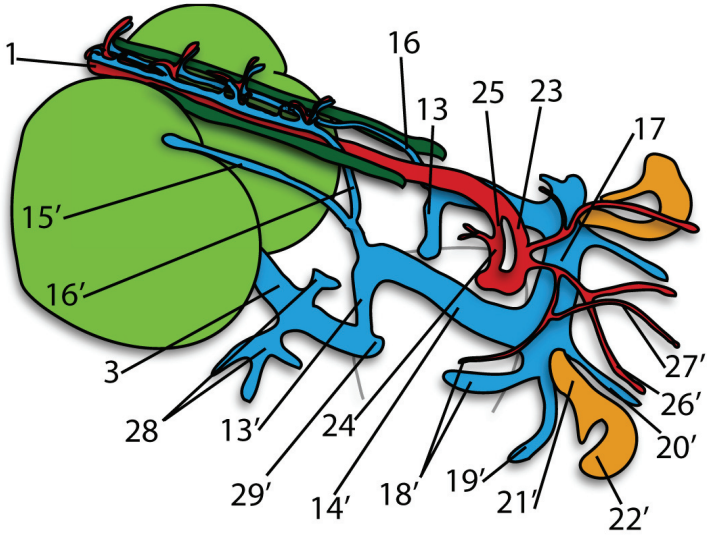

Fig. 31: Schematic representation of the developing vascular system in the thoracic region of a 22.5 mm pig embryo, right lateral view. Colour codes: red: arterial system, blue: venous system, orange: lymphatic system, dark green: sympathetic trunk, pale green: mesonephros (partially displayed). Numbers followed by an accent (') indicate right-sided structures. 1: aorta, 3: cranial part of the caudal vena cava, 13: common cardinal vein, 14: cranial cardinal vein, 15: caudal cardinal vein, 16: supracardinal vein, 17: precardial anastomosis between 14 & 14', 18: subclavian artery and vein, 19: cephalic vein, 20: jugular vein, 21: jugular lymphatic sac, 22: subclavian lymphatic sac, 23: aortic arch, 24: pulmonary trunk, 25: ductus arteriosus (Botalli), 26: common carotid artery, 27: vertebral artery, 28: hepatic veins, 29: sinus venosus.

Unlike its left counterpart, the right caudal cardinal vein was still present (15'). It emerged from the cranial and dorsal aspect of the right mesonephros, coursed lateral to the ipsilateral sympathetic trunk and entered the right common cardinal vein. Its function appeared to be restricted to the drainage of the mesonephros only, as along its further course in the thorax, it did not receive any more tributaries.

Dorsolateral to the thoracic aorta and medial to the sympathetic trunks, the left and right supracardinal veins (16 & 16') collected the blood from the vertebral column and the

dorsal regions of the body. Numerous anastomoses between both these longitudinal veins were present across the dorsal border of the aorta. The cranial ends of the supracardinal veins bent in ventral and lateral direction to cross the ipsilateral sympathetic trunks ventrally. The right supracardinal vein (16') subsequently entered in the right caudal cardinal vein (15') whilst the left supracardinal vein (16) drained directly into the left common cardinal vein (13). The caudal ends of the supracardinal veins extended further in the abdomen. They could be discerned until the level of the cranial poles of the metanephroi, where they dissipated into an indefinable capillary plexus.

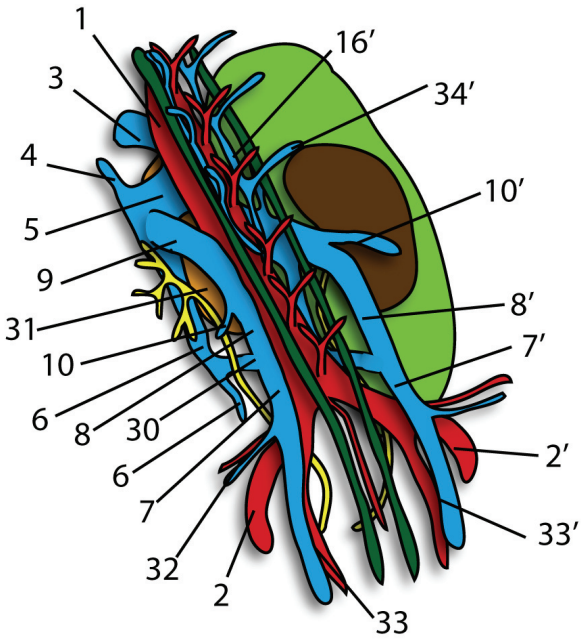

Fig. 32: Schematic representation of the developing vascular system in the 22.5 mm pig embryo, left dorsolateral view on the lumbar region after removal of the left mesonephros and metanephros. Colour codes: red: arterial system, blue: venous system, orange: lymphatic system, yellow: urinary tract, dark green: sympathetic trunk, pale green: mesonephros (partially displayed), brown: right metanephros / kidney. Numbers followed by an accent (') indicate right-sided structures. 1: aorta, 2: umbilical artery, 3: cranial part of the caudal vena cava, 4: cranial segment of the subcardinal vein, 5: subcardinal anastomosis, 6: caudal segment of the subcardinal vein, 7: common iliac vein, 8: sublumbar vein (longitudinal segment), 9: sublumbar vein (vertical segment), 10: cranial abdominal vein, 16: supracardinal vein, 30: anastomosis between 6 & 8, 31: retroperitoneal mesenteric lymph sac, 32: external iliac artery and vein, 33: internal iliac artery and vein, 34: third lumbar vein.

In the caudal half of the embryo (Fig. 32), the venous architecture was further elaborated and modified. The lateral mesonephric veins as observed in younger embryos were completely regressed and the only drainage routes for the common iliac veins (7) were now the longitudinal sublumbar veins (8). These veins still coursed lateral to the sympathetic trunks but they were no longer located dorsal to the metanephroi due to the relative cranial and lateral migration of these developing kidneys. Instead, the sublumbar veins (8) were now located dorsal to dorsolateral to the ipsilateral ureters. The veins coursing transversely over the dorsal surface of the kidneys could be identified as the left and right cranial abdominal veins (10). Both these veins entered along with the suprarenal veins and some undefined somatic tributaries into the vertical segment of the ipsilateral sublumbar veins (9), which in turn merged with the expanded subcardinal anastomosis (5). The caudal segments of the left and right subcardinal veins (6) extended further caudally and were both connected with the overlying sublumbar vein (8) through at least one anastomosis (30) which emerged from their dorsal aspect and coursing medial to the ipsilateral ureter.

Ventral to the aorta and the subcardinal anastomosis (5), a large, single retroperitoneal mesenteric lymphatic sac (31) was located between the cranial and caudal mesenteric artery. Other large lymphatic structures in this region such as the cysterna chyli were still absent.

4.2.4. Venous pattern in the lumbar region of the 27.6 mm embryo

The embryos within the range of 27.5 and 30.0 mm were difficult to interpret and hard to reconstruct due to intensive state of reorganization of the venous and lymphatic systems in the lumbar and pelvic regions. Moreover, some remarkable differences were found between the reference embryo and the control embryos. Unless otherwise stated, the descriptions below refer to the 27.6 mm embryo (Fig. 34).

Intense remodelling activities were found in the region between the left kidney and aorta and were characterized by the presence of numerous cross-sections through a plexus of veins and lymphatic vessels (Fig. 33). As a result, a patent left sublumbar vein could no longer be observed in the 27.6 mm embryo, though its former existence was still testified by the presence of some large blood-filled venous spaces (35). However, in a 27.5 and one of the three 30.0 mm control embryos, the left sublumbar vein was still present as a single continuous vessel.

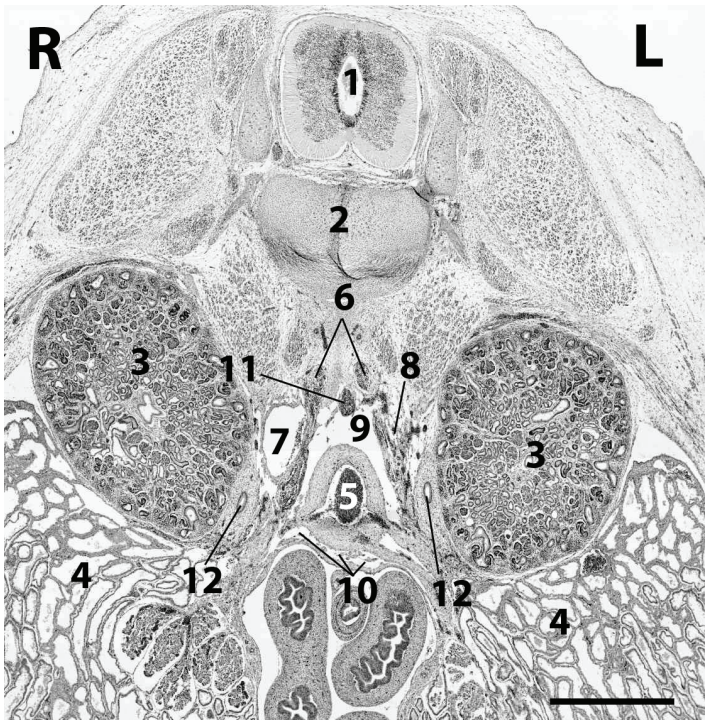

Fig. 33: Cranial view of a cross-section at the level of the fourth lumbar vertebral body in a 30.0 mm embryo (control embryo of the 27.6 mm reference embryo). Scale bar = 1 mm. 1: neural tube, 2: fourth lumbar vertebral body, 3: metanephroi, 4: mesonephroi, 5: aortic lumen filled with blood, 6: sympathetic trunks, 7: right sublumbar vein (caudal vena cava), 8: area with numerous cross-sections through blood-filled or lymphatic capillaries, 9: lymphatic extension of the mesenteric lymphatic sac encircling the aorta and constructing the cysterna chyli, 10: retroperitoneal mesenteric lymphatic sac, 11: blood-filled common trunk of the fourth lumbar arteries, 12: ureter.

In all embryos of this group, the retroperitoneal mesenteric lymphatic sac (31) displayed several outgrows (36) along the left and right lateral wall of the aorta. In the largest control embryos (30.0 mm), these outgrows fused dorsal to the aorta to form the cysterna chyli (Fig. 33). The left-sided outgrow was dominating in volume. Furthermore, a left and right lumbar lymphatic trunk, located medial to the ipsilateral ureter and umbilical artery, drained into the caudal part of the mesenteric sac (not drawn in Fig. 34).

In the reference embryo and larger control embryos, an anastomosis between the left and right common iliac veins could be observed (37). It was located across the dorsal border of the aorta and surrounded the common trunk of the sixth lumbar arteries (38) that arose as

a dorsal branch from the aorta. In the 27.5 mm control embryo, both common iliac veins were connected with each other by small venules that did not display the characteristics of a full functional anastomosis.

The supracardinal veins (16) were present as two longitudinal channels just dorsal to the aorta. They extended caudally until the level of the hilus of the kidneys.

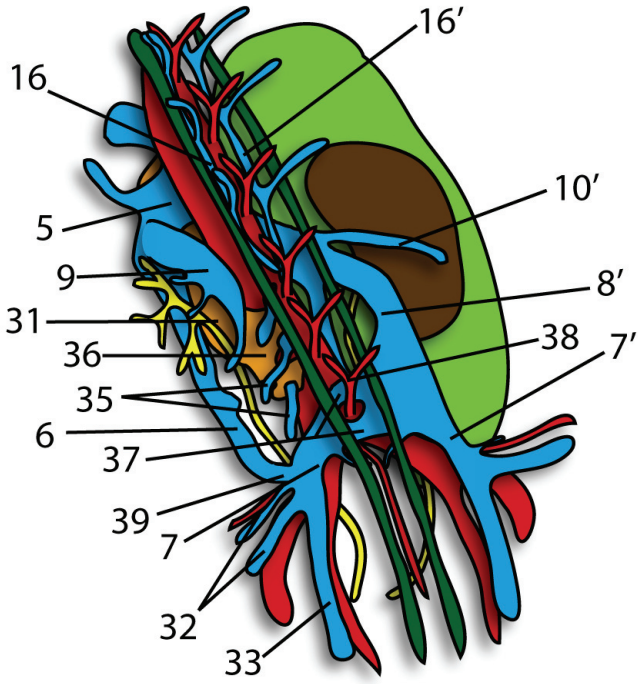

Fig. 34: Schematic representation of the developing vascular system in the 27.6 mm pig embryo, left dorsolateral view on the lumbar region after removal of the left mesonephros and metanephros. Colour codes: red: arterial system, blue: venous system, orange: lymphatic system, yellow: urinary tract, dark green: sympathetic trunk, pale green: mesonephros (partially displayed), brown: right metanephros / kidney. Numbers followed by an accent (′) indicate right-sided structures. 5: subcardinal anastomosis, 6: caudal segment of the subcardinal vein, 7: common iliac vein, 8: sublumbar vein (longitudinal segment), 9: sublumbar vein (vertical segment), 10: cranial abdominal vein, 16: supracardinal vein, 31: retroperitoneal mesenteric lymph sac, 32: external iliac artery and vein, 33: internal iliac artery and vein, 35: remnants of the left sublumbar vein, 36: periaortic extensions of the mesenteric lymphatic sac, 37: iliac anastomosis, 38: sixth lumbar artery, 39: caudalmost anastomosis between 6 & 7.

The caudal segments of the individual subcardinal veins (6) closely approached the ipsilateral common iliac veins (7) and sometimes an anastomosis between these veins was formed. The presence of such an anastomosis (39) was a variable finding: it was only seen on the left hand side in the reference embryo and on the right hand side in a reconstructed 27.5 mm control embryo. In a third control embryo (30.0 mm), such an anastomosis could not be observed on either side. When present, and in contrast with the other anastomoses between the subcardinal veins and the overlying common iliac or sublumbar veins, this caudal anastomosis was located lateral to the ipsilateral ureter.

4.2.5. Venous pattern in the lumbar region of the 36.7 mm foetus

In this early foetal stage (Fig. 36), the anastomosis between the left and right common iliac veins (37) was further elaborated. It could now clearly be subdivided into a cranial and caudal part, both separated from each other by the common trunk of the sixth lumbar arteries (38). Cranial to this iliac anastomosis, the left sublumbar vein was absent and

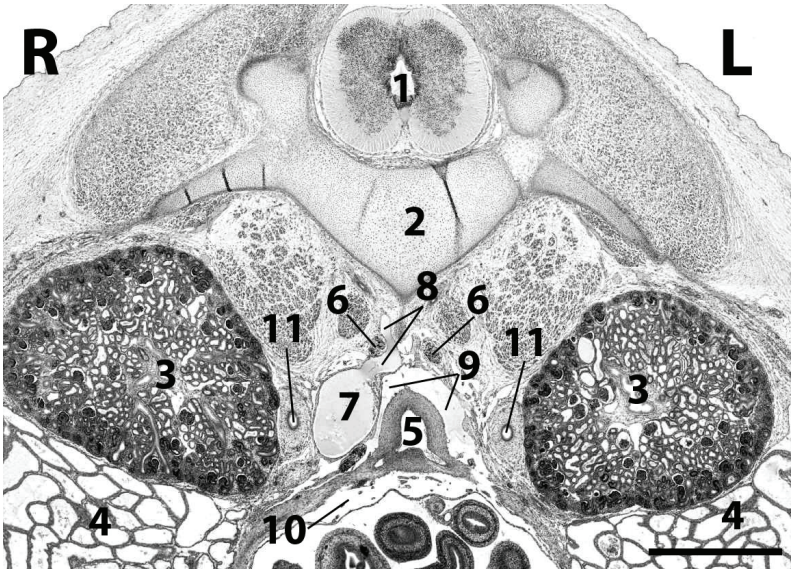

Fig. 35: Cranial view of a cross-section at the level of the fourth lumbar vertebral body in a 36.7 mm embryo. Scale bar = 1 mm. 1: neural tube, 2: fourth lumbar vertebral body, 3: metanephroi, 4: mesonephroi, 5: aortic lumen, 6: sympathetic trunks, 7: right sublumbar vein (caudal vena cava), 8: fourth lumbar vein situated along the medial and ventral aspect of the right sympathetic trunk, 9: lymphatic extension of the mesenteric lymphatic sac encircling the aorta and constructing the cysterna chyli, 10: retroperitoneal mesenteric lymphatic sac, 11: ureter.

the space it occupied previously was now taken in by the large lymphatic connection (36) between the retroperitoneal mesenteric sac (31) and the cysterna chyli (40).

The only functional remnant of the left sublumbar vein was its vertical segment (9), just prior to its confluence with the subcardinal anastomosis (5). It served as the left renal vein (41) by collecting a dorsal and ventral branch emerging from the hilus of the left kidney. This left renal vein also collected the left cranial abdominal vein (10) which coursed transversely over the dorsal surface of the left kidney. The right sublumbar vein (8') was prominent and very similar to the infrarenal part of the adult caudal vena cava. Just before

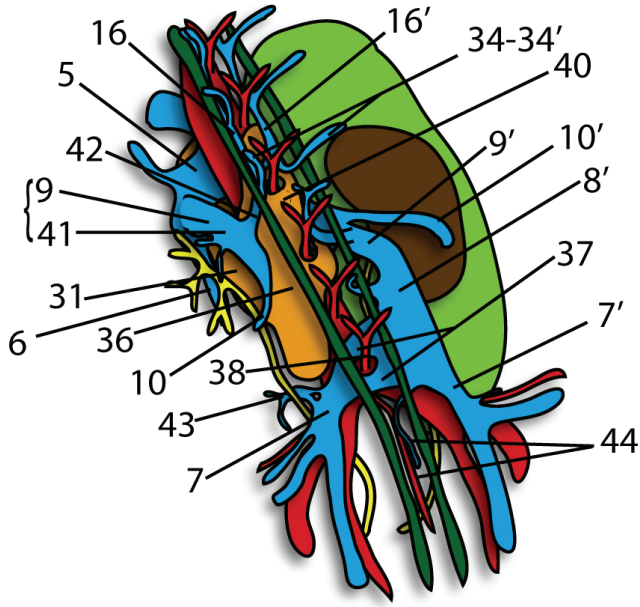

Fig. 36: Schematic representation of the developing vascular system in the 36.7 mm pig foetus, left dorsolateral view on the lumbar region after removal of the left mesonephros and metanephros. Colour codes: red: arterial system, blue: venous system, orange: lymphatic system, yellow: urinary tract, dark green: sympathetic trunk, pale green: mesonephros (partially displayed), brown: right metanephros / kidney. Numbers followed by an accent (') indicate right-sided structures. 5: subcardinal anastomosis, 7: common iliac vein, 8: sublumbar vein (longitudinal segment), 9: sublumbar vein (vertical segment), 10: cranial abdominal vein, 16: supracardinal vein, 31: retroperitoneal mesenteric lymph sac, 34: third lumbar vein, 36: periaortic extensions of the mesenteric lymphatic sac, 37: iliac anastomosis, 38: sixth lumbar artery, 40: cysterna chyli, 41: renal artery and vein, 42: anastomosis between 10 & 16, 43: mesonephric branch of 7, 44: median sacral artery and vein.

entering the subcardinal anastomosis (5), it received both the dorsal and ventral vein emerging from the right kidney as well as the right cranial abdominal vein (10').

Dorsal to the aorta and medial to the sympathetic trunks, the supracardinal veins (16-16') constructing the azygos system collected the first three lumbar vein pairs draining the overlying vertebral column and the dorsal aspects of the body. At the level of the third lumbar vein (34), the caudal end of the left supracardinal vein (16) was connected through a ventrolateral anastomosis (42) with the left cranial abdominal vein (10). Similar to the fourth lumbar vein pair, the left and right fifth lumbar veins merged in the midline of the foetus to form a common trunk. This trunk first coursed ventrally between the left and right sympathetic trunks and subsequently turned horizontally to continue in lateral direction, crossing the right sympathetic trunk ventrally, before entering into the right sublumbar vein (Fig. 35). The sixth and seventh lumbar vein pair drained each with a short common trunk in the iliac anastomosis or median sacral vein, respectively (not drawn in Fig. 36).

The caudal segments of the subcardinal veins (6) along the medial surface of the mesonephroi were largely regressed. The caudal part of each mesonephros was now drained by a single branch (43) which joined the common iliac vein (7).

4.2.6. Corrosion casting of the 9 cm foetus

Both the arterial and venous systems of all injected foetuses were filled with the polymer. Conversely, the lymphatic system had not been filled with Batson's and was corroded away along with all other soft tissues of the foetuses (Fig. 38). Caudal to the renal arteries, the aorta was still supplying some mesonephric glomeruli through a number of bilateral mesonephric arteries (45).

The caudal vena cava had reached its final configuration (Fig. 37). It collected both common iliac veins (7) just cranial to the sixth lumbar artery (38). The most caudal segment of the caudal vena cava was initially located dorsal to the aorta, but more cranially, it shifted towards the right ventrolateral side of the aorta and crossed the right renal artery (41') ventrally. It was continued by the hepatic and intrathoracic segments of the caudal vena cava (3) before finally reaching the right atrium of the heart.

The left azygos vein could be followed from the heart to the level of the eighth intercostal space. More caudally, the right hemiazygos vein (16a') collected both the left and

right intercostal veins and the first three lumbar veins. The caudal end of the right hemiazygos vein was connected through a ventrolateral anastomosis (42') with the right cranial abdominal vein.

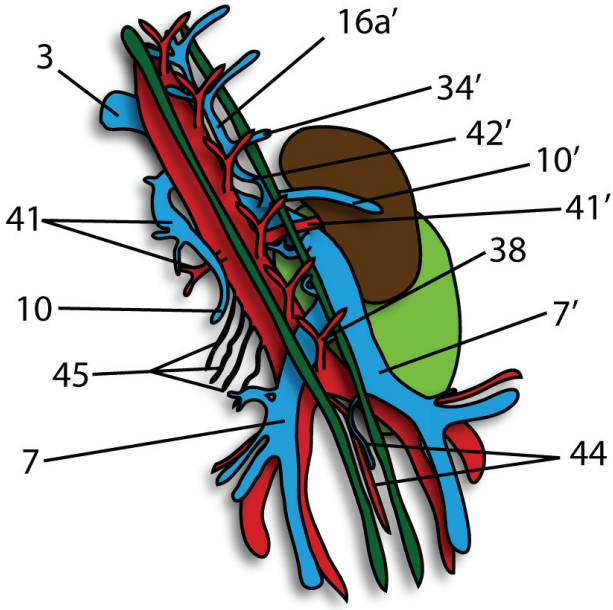

Fig. 37: Schematic representation of the developing vascular system in the 9 cm pig foetus, left dorsolateral view on the lumbar region after removal of the left mesonephros and metanephros. Colour codes: red: arterial system, blue: venous system, dark green: sympathetic trunk, pale green: mesonephros, brown: right kidney. Numbers followed by an accent (') indicate right-sided structures. 3: cranial part of the caudal vena cava, 7: common iliac vein, 10: cranial abdominal vein, 16a: right hemiazygos vein, 34: third lumbar vein, 38: sixth lumbar artery, 41: renal artery and vein, 42: anastomosis between 10 & 16a, 44: median sacral artery and vein, 45: mesonephric arteries.

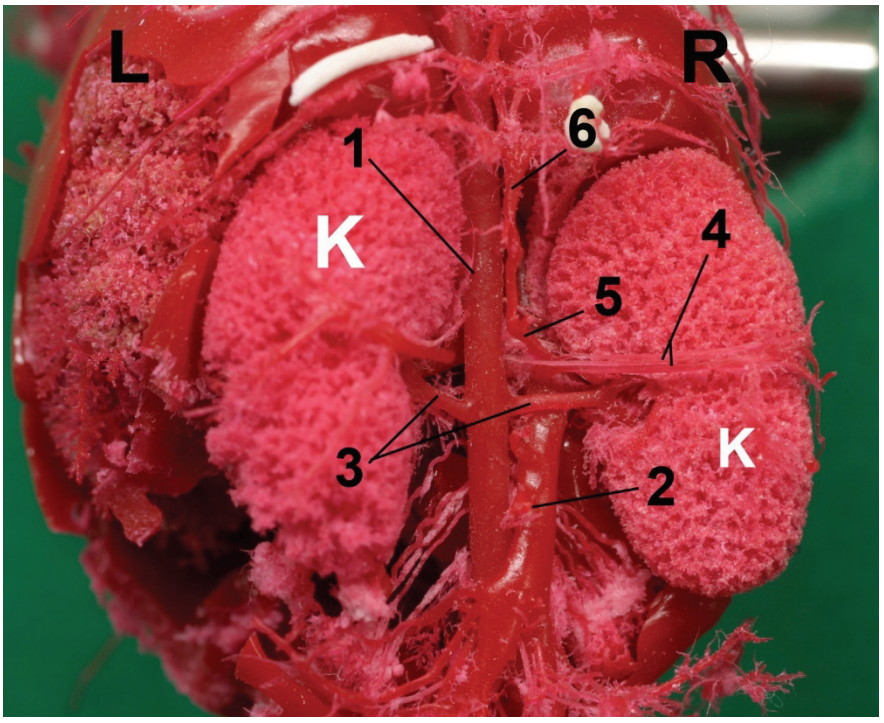

Fig. 38: Detailed view of the dorsal aspect of a vascular corrosion cast in the lumbar region of a 9 cm pig embryo. The vasculature of the vertebral column dorsal to the abdominal aorta has been clipped away. The connection of the caudal cardinal vein with the right hemiazygos vein through a branch of the right cranial abdomen vein is clearly visible (indicated by number 5). K: Kidneys, 1: aorta, 2: infrarenal part of the caudal vena cava, 3: renal arteries, 4: right cranial abdominal artery and vein, 5: connection of the caudal vena cava with the azygos system, 6: right hemiazygos vein.

4.2.7. Discussion

The main purpose of this part of the investigation was to find out whether the construction of the infrarenal part of the caudal vena cava in the pig is linked with the development of the azygos and hemiazygos veins that are built from the supracardinal veins that are present in the late embryonic stages. The purely descriptive term “sublumbar veins” was introduced to enable an unbiased description and evaluation of the embryonic veins ultimately evolving into the caudal vena cava in the lumbar region. Although a substantial rearrangement of the venous system was observed in the lumbar region of the studied embryos, the right sublumbar vein (8’) clearly acted as the direct precursor of the caudalmost segment of the caudal vena cava and exhibited no major conformational changes throughout all developmental stages. By combining these findings with the results in the previous section, it can be demonstrated that the infrarenal segment of the caudal vena cava in the pig is built from the right caudal cardinal vein, and that the supracardinal veins are not involved in the construction of the caudal vena cava.

In the previous section, we have shown that in the early embryonic stages of the pig, the caudal cardinal veins are displaced dorsally in the lumbar region by the migrating umbilical arteries and enlarging metanephroi. In the 18 mm pig embryo, these veins cover the dorsal surface of the developing kidneys and are identical to the veins identified as the sublumbar veins in the 20.0 mm embryo in the present study. As the right sublumbar vein eventually forms the lumbar segment of the caudal vena cava, it can be concluded that the dorsally displaced segment of the right caudal cardinal vein is in fact the precursor of the infrarenal part of the caudal vena cava in the pig.

Furthermore, and in contrast to general belief, no strong relationship has been found between the developing azygos system and the caudalmost segment of the caudal vena cava. This invalidates the proposition that the sublumbar veins should be considered as the abdominal extensions of the supracardinal veins, which are primarily responsible for the construction of the azygos and hemiazygos veins in the thorax. However, according to the original theories, the supracardinal veins are described as late embryonic veins that are present in both the thorax and abdomen, just dorsolateral to the aorta. They eventually separate into a cranial component building the azygos system and a caudal component responsible for the construction of the infrarenal segment of the caudal vena cava (Huntington and McClure, 1920). Each supracardinal vein initially arises from two

independent dorsomedial branches of the caudal cardinal veins, one developing in the thorax and extending caudally and the other one extending from the iliac anastomosis in cranial direction. At the summit of their development, both segments fuse with each other at the level of the kidneys to form a single, temporarily continuous channel before splitting up again (McClure and Butler, 1925). Only occasionally, this transitory fusion does not occur in the pig embryo (Butler, 1927).

Major descriptive, temporal and spatial inconsistencies between the development of the sublumbar veins in the present study and the original description of the supracardinal veins as summarized above strongly suggest that the sublumbar veins are not related to the supracardinal system, and that the supracardinal veins are consequently not involved in the construction of the caudal vena cava. The connection observed between the sublumbar veins and the developing azygos system through a branch of the cranial abdominal veins at the level of the third lumbar veins (Fig. 36 n° 42 & 37 n° 42') is one of the key elements in this discussion. First of all, the connection found in the present study is a developmental end-stage rather than a transient embryonic feature, as in the adult pig an anastomosis between the caudal vena cava and the left azygos vein through the second or third lumbar vein is commonly described (Barone, 1996) (Fig. 36). As the left azygos vein in the adult pig often terminates already in the caudal half of the thorax, the right hemiazygos vein frequently has to substitute for its function in the caudal thoracic and cranial lumbar region (Schummer et al., 1981), which can explain the configuration observed in the 9 cm foetuses (Fig. 37).

Another reason why the sublumbar vein cannot be seen as the extension of the supracardinal vein is the fact that both developing vessels are not located in line with each other. The sympathetic trunk hampers the proper construction of a single straight connection between both veins, as the supracardinal vein is located dorsomedial to the ipsilateral trunk whilst the sublumbar vein was clearly observed to course ventrolateral to the sympathetic chain.

The fourth and fifth lumbar veins are also located medial to the sympathetic trunk and they experience similar difficulties to drain into the right sublumbar vein. They have to curve along the medial and ventral side of the right sympathetic trunk to reach the developing caudal vena cava (Fig. 35). In different other species, the successive lumbar veins join each other ventral to the lumbar vertebral bodies to form a bilateral longitudinal channel, which connects cranially with the azygos system in the thorax. Such longitudinal

channels are very prominent in the human and are called the ascending lumbar veins (Walls, 1981). Based on the present observations and data from literature, it appears that the supracardinal veins are involved in the formation of the azygos veins, and that they are topographically and functionally more related to the lumbar veins than to the veins constructing the infrarenal part of the caudal vena cava. Therefore, it can be concluded that the supracardinal veins in the pig embryo do not contribute in the construction of the caudal vena cava.

The sublumbar veins observed in this study are located ventrolateral to the sympathetic trunks, and therefore they have sometimes been called the lateral sympathetic line veins to differentiate them from the azygos system that arises from the medial sympathetic line veins (Williams et al., 1993; Rahalkar, 2002). However, the lateral sympathetic line veins were believed to run in the thorax as well, which is dissimilar to the observations in the present study. Therefore, based on the current observations, the term lateral sympathetic line vein, although topographically correct, should not be used to indicate the venous segment responsible for the construction of the lumbar segment of the caudal vena cava in the pig.

In species such as the rabbit and the rat, the role of the right caudal cardinal vein in the construction of the infrarenal part of the caudal vena cava has been recognized long ago (Butler, 1927). Despite the many contradictive studies on this matter in the human embryo, Gladstone (1929) has also described that the infrarenal caudal vena cava in human embryos arises from the caudal segment of the right caudal cardinal vein, which is subsequently pushed upwards by the developing right kidney to a position ventrolateral of the sympathetic trunk. The present finding of a similar developmental pattern in the pig embryo is of particular interest, as it was previously assumed that this pattern was only applicable to animal species characterized by small and barely functional mesonephroi during embryonic development (Butler, 1927).

By excluding the supracardinal veins as normal contributors in the construction of the caudal vena cava, several hypotheses that were put forward for explaining anatomical variations of the caudal vena cava should be reconsidered. In particular, the origin of the retrocaval ureter should be re-evaluated based on the current findings. This congenital malformation is characterized by the abnormal course of the right ureter, which passes the caudal vena cava dorsally and emerges between the aorta and caudal vena cava.

Compression of the ureter between both these vessels eventually results in upper urinary tract obstruction. This condition is well-documented in man (Perimenis et al., 2002), has been experimentally inducted in laboratory rabbits (Scortichini et al., 1986), and has recently also been reported in the dog (Doust et al., 2006) and the cat (Cornillie et al., 2006). It was generally believed that this condition occurred when the infrarenal segment of the caudal vena cava was formed by a persisting right caudal cardinal vein, which was supposed to be located lateral to the ureter, instead of by the right supracardinal vein which is located dorsomedial to the ureter (Bass et al., 2000; Gundeti et al., 2006). However, it has been shown in the current investigation that the right caudal cardinal vein is the normal contributor to the infrarenal part of the caudal vena cava and that it is always located medial to the ipsilateral ureter. The only longitudinal embryonic vessel coursing lateral to the ureter is the anastomosis between the caudal end of the subcardinal vein and the ipsilateral common iliac vein, as occasionally seen in the 27.6 mm embryo. These observations suggest the possible involvement of persistent subcardinal veins in the occurrence of retrocaval ureters as proposed by some other authors (Perimenis et al., 2002; Soundappan and Barker, 2004). However, in embryos belonging to the species in which the occurrence of a retrocaval ureter has been reported, the identity and exact topography of the embryonic veins surrounding and encircling the ureters have been described equivocally, requiring a more species-specific approach to unravel the true pathogenesis of a circumcaval or retrocaval ureter.

4.3. Literature

Barone, R. (1996). Anatomie comparé des mammifères domestiques, tome cinquième: Angiologie. Editions Vigot, Paris, p. 589-591 & 662-663.

Bass, J.E., M.D. Redwine, L.A. Kramer, P.T. Huynh and J.H. Harris (2000). Spectrum of congenital anomalies of the inferior vena cava: cross-sectional imaging findings. *Radiographics* 20, 639-652.

Butler, E.G. (1927). The relative role played by the embryonic veins in the development of the mammalian vena cava posterior. *American Journal of Anatomy* 39, 267-353.

Carlson, B.M. (1994). Human Embryology and Developmental Biology. Mosby - Year Book Inc., Saint-Louis, p. 340-345.

Cornillie, P. and P. Simoens (2005). Prenatal development of the caudal vena cava in mammals: review of the different theories with special reference to the dog. *Anatomia, Histologia, Embryologia* 34, 364-372.

Cornillie, P., T. Baten and P. Simoens (2006). Retrocaval ureter in a cat. *The Veterinary Record* 159, 24-25.

Doust, R.T., S.P. Clarke, G. Hammond, C. Paterson and A. King (2006). Circumcaval ureter associated with and intrahepatic portosystemic shunt in a dog. *Journal of the American Veterinary Medical Association* 228, 389-391.

Gladstone, R. (1929). Development of the inferior vena cava in the light of recent research, with especial reference to certain abnormalities, and current descriptions of the ascending lumbar and azygos veins. *Journal of Anatomy* 64, 70-93.

Grünwald, P. (1938). Die Entwickelung der Vena cava caudalis beim Menschen. *Zeitschrift für Mikroskopisch-Anatomische Forschung* 43, 275-331.

Gundeti, M.S., P.G. Duffy and I. Mushtaq (2006). Robotic-assisted laparoscopic correction of pediatric retrocaval ureter. *Journal of Laparoendoscopic and Advanced Surgical Techniques part A* 16, 422-424.

Huntington, G.S. and C.F.W. McClure (1920). The development of the veins in the domestic cat (*Felis domestica*) with especial reference, 1) to the share taken by the

supracardinal veins in the development of the postcava and azygos veins and 2) to the interpretation of the variant conditions of the postcava and its tributaries, as found in the adult. *Anatomical Record* 20, 1-30.

McClure, C.F.W and E.G. Butler (1925). The development of the vena cava inferior in man. *American Journal of Anatomy* 35, 331-383.

Nomina Embryologica Veterinaria (2006), 2nd edition. Prepared by the International Committee on Veterinary Embryological Nomenclature, Ghent, p. 16. http://www.wava-amav.org/Downloads/nev_2006.pdf

Perimenis, P., K. Gyftopoulos, A. Athanasopoulos, V. Pastromas and G. Barbalias (2002). Retrocaval ureter and associated abnormalities. *International Urology and Nephrology* 33, 19-22.

Rahalkar, M.D. (2002). Dr. N. G. Gadekar Memorial Oration. 55th conference of IRIA, Kolkata. *Indian Journal of Radiology and Imaging* 12, 109-114.

Rüsse, I. (1991). Harn- und Geslechtsorgane. In: Rüsse, I. and F. Sinowatz (editors) Lehrbuch der Embryologie der Haustiere. Verlag Paul Parey, Hamburg, p. 304-337.

Sabin, F.R. (1909). The lymphatic system in human embryos, with a consideration of the morphology of the system as a whole. *American Journal of Anatomy* IX, 43-91.

Sadler, T.W. (1985). Langman's Medical Embryology, fifth edition. Williams & Wilkins, Baltimore, p. 250.

Schummer, A., H. Wilkens, B. Vollmerhaus and K.-H. Habermehl (1981). The circulatory system, the skin and the cutaneous organs of the domestic animals. In: Nickel, R., A. Schummer and E. Seiferle (Editors), The Anatomy of Domestic Animals. Verlag Paul Parey, Hamburg, p. 184-187.

Scortichini, B.H., J.A. John-Greene, J.F. Quast and K.S. Rao (1986). Teratologic evaluation of dermally applied diethylene glycol monomethyl ether in rabbits. *Fundamental and Applied Toxicology* 7, 68-75.

Soundappan, S.V. and A.P. Barker (2004). Retrocaval ureter in children: a report of two cases. *Pediatric Surgery International* 20, 158-160.

Walls, E.W. (1981). The blood vascular and lymphatic systems. In: Romanes, G. J. (Editor), Cunningham's Textbook of Anatomy, twelfth edition. Oxford University Press, Oxford, p. 871-1008.

Williams P.L., R. Warwick, M. Dyson and L. M. Bannister (1993). Gray's Anatomy, 37th edition, reprint. Churchill Livingstone, Edinburgh, p. 219-226.

GENERAL DISCUSSION

GENERAL DISCUSSION

Two particular findings in the present research are of major interest as they actually shed a new light on our current understanding regarding several morphological and topographical aspects of the embryonic development of the caudal vena cava in the pig.

First, it has been demonstrated that the caudal cardinal veins persist much longer than commonly described and that the right caudal cardinal vein is actually involved in the final construction of the infrarenal part of the caudal vena cava. However, this statement is not a revolutionary idea, as it has been indicated in section 2.1.2.2. that in certain animal species such as rodents and rabbits, a seemingly similar developmental pattern has been described (Butler, 1927). Furthermore, in the very first studies on the development of the caudal vena cava in mammals, it was also concluded that caudal to the mesonephroi, the caudal cardinal veins contribute to the formation of the caudal vena cava (Hochstetter, 1893). On the other hand, in this caudal cardinal model (Butler, 1927), it was indicated that on the course of the caudal cardinal veins, a peri-ureteric venous ring is formed of which only the dorsal limb persists as a part of the supracardinal vein during further development, whilst its ventral limb, as a part of the caudal cardinal vein, disappeared. In the present study, a peri-ureteric venous ring has also been found in a certain number of embryos of about 27.5 mm. However, rather than being part of the caudal cardinal vein, the ventral limb of this ring was built of the caudal end of the subcardinal vein whilst its dorsal and cranial segment was in fact a part of the caudal cardinal vein that had adopted a more dorsal position compared to its initial location.

The second particular feature of the development pattern of the caudal vena cava observed in this study is the displacement of the caudal ends of the caudal cardinal veins following the migration of the umbilical arteries and expansion of the metanephroi. This particular event is, based on the present observations, the direct cause of the typical right-angled configuration of the caudalmost segment of the caudal cardinal veins, consisting of a longitudinal part abruptly followed by a short vertical segment. Only when during further development the kidneys migrate to a more cranial and lateral position, this structure is flattened out and a smooth continuation of the caudal vena cava is formed out of the right-sided components. Although similar right-angled configurations have been observed in early

human embryos (see section 2.1.2.6.), the configuration described by McClure and Butler (1925) (supracardinal model) and Grünwald (1938) (sacrocardinal model) is not comparable with the present findings as in both authors described this configuration to be located dorsal and lateral to the developing metanephroi, whilst in the present work, it was initially seen dorsal and cranial to the metanephroi and in a later stage dorsal to the ureters and medial to the kidneys (Fig. 41).

As the present findings are clearly not entirely comparable with any of the currently available models describing the embryonic development of the caudal vena cava, a stepwise description of the main features of this developmental pattern based on the insights gathered during this research is therefore at its place. However, rather than hereby once again creating a new theory on this matter, a more harmonizing model, with respect to the pre-existing hypotheses, will be put forward below.

Little discussion exists on the venous basic pattern in the primitive embryo (Fig. 39A). In the 3.7mm pig embryo, the only somatic veins caudal to the heart are the caudal cardinal veins, bilaterally present in the mesoderm just dorsal to the anlage of the mesonephroi. They merge cranially with the cranial cardinal veins into the ipsilateral common cardinal veins draining into the sinus venosus of the heart.

From the 4.6 mm embryo onwards, the caudal cardinal veins and underlying mesonephroi can be observed crossing the umbilical arteries dorsally near their branching from the aorta (Fig. 39B). In this region, the caudal cardinal veins are still straight continuous vessels, without any further large tributaries. Different mesonephric veins drain individually along the medial and dorsal surface of the mesonephros in the caudal cardinal veins. In the midregion of the mesonephros, some of these segmental veins already join each other form a short longitudinal channel, which can be indicated as the primitive subcardinal vein, along the medial surface of each mesonephros. At the same level, the ipsilateral caudal cardinal vein can locally be interrupted. However, the caudal cardinal veins remain the main drainage route towards the heart as the cranial end of each subcardinal vein still exclusively connects along a mesonephric branch with the ipsilateral caudal cardinal vein.

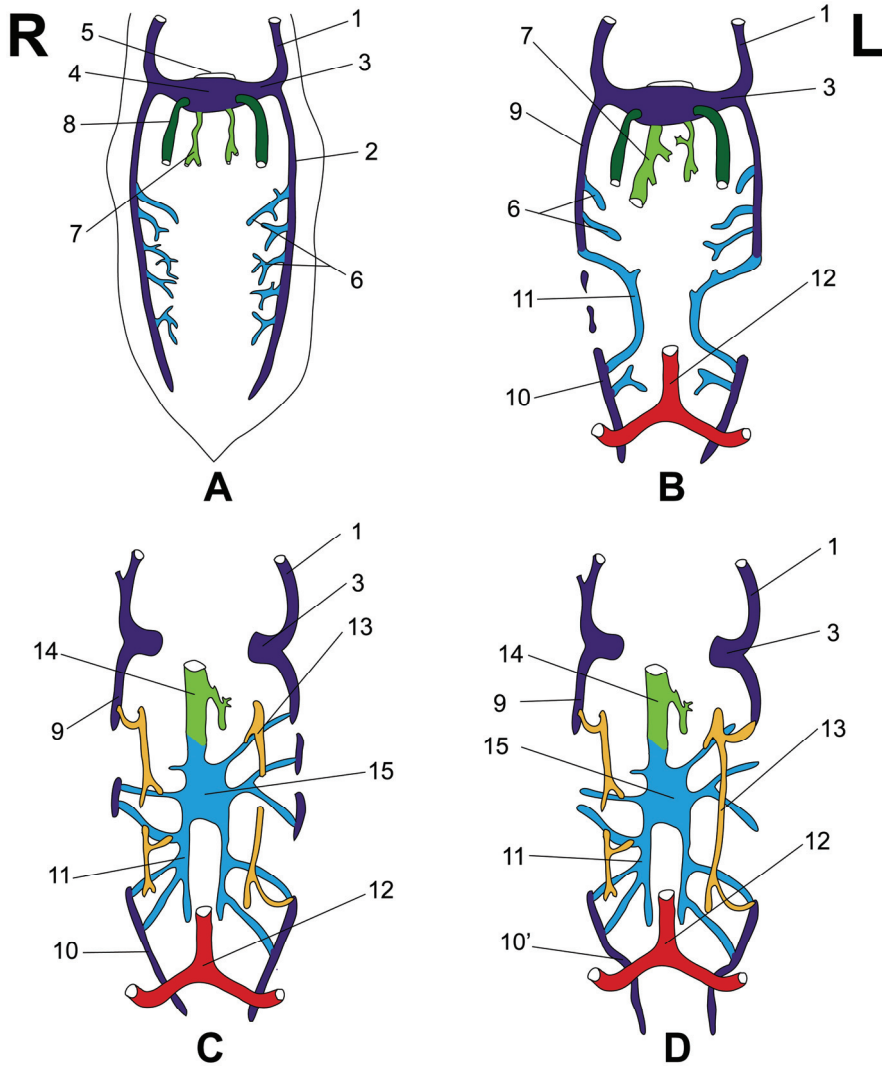

Fig. 39: Schematic representation of the development of the caudal vena cava according to the comprehensive model proposed in this study on pig embryos from 3.7 till 12.0 mm, ventral views. Stage descriptions: A: venous basic pattern as seen in the 3.7 mm embryo. B: creation of the subcardinal veins in the 4.6 mm embryo. C: subcardinal sinus connected to the vitelline system in the 10 mm embryo. D: initial dorsal deflection of the caudal cardinal veins by the umbilical arteries in the 12.0 mm embryo. Continued in figure 40. 1: left cranial cardinal vein, 2: left caudal cardinal vein, 3: left common cardinal vein, 4: sinus venosus, 5: entrance to the heart, 6: mesonephric branches forming the left subcardinal plexus, 7: right vitelline vein, 8: right umbilical vein, 9: cranial segment of the right caudal cardinal vein, 10: caudal segment of the right caudal cardinal vein, 10': dorsally deflected part of 10, 11: right subcardinal vein, 12: terminal branching of the aorta in the left and right umbilical artery, 13: left ventral mesonephric vein, 14: hepatic segment of the caudal vena cava built from the right vitelline vein, 15: subcardinal sinus.

This situation is drastically changed in the 10 mm pig embryo (Fig. 39C). From this stage onwards, the subcardinal veins become the most important somatic vessels draining the blood towards the heart. Blood entering the subcardinal veins is collected in the subcardinal sinus that is formed following the fusion of the left and right subcardinal veins ventral to the aorta in the midregion of mesonephroi. Subsequently, this blood is passed through a newly formed anastomosis between the cranial segment of the right subcardinal vein and the underlying vitelline vein emerging from the craniodorsal aspect of the developing liver. The caudal cardinal veins are now totally interrupted in the middle two quarters of the mesonephroi. Their cranial segments still drain the blood coming from the cranial aspects of these organs towards the heart, whilst their caudal components, now fully extending beyond the caudal surface of the mesonephroi, are connected through several mesonephric branches with the subcardinal veins and subcardinal sinus.

So far, these findings parallel to a considerable extent with the descriptions that can be found in the human and porcine supracardinal model exemplified by McClure and Butler (1925) and Butler (1927), and in the human sacrocardinal model as proposed by Grünwald (1938). However, in all models worked out on human embryos, it is described that the veins draining the lumbar and pelvic regions are already arranged in the typical dorsally deflected, right-angled configuration as described earlier[*]. This is dissimilar to our own observation and to the descriptions by Butler (1927), as the caudal cardinal veins in this region of the 10 mm pig embryo still can be found as single, straight continuous vessels.

Only in the 12 mm pig embryo (Fig. 39D), this dorsal deviation of the caudal cardinal veins in the lumbar and pelvic region is initiated due to the cranial migration of the umbilical arteries along the dorsal surface of the mesonephroi, thereby locally stripping off the caudal cardinal veins from these organs. However, the typical right-angled configuration of the veins in the lumbar region can in the pig only be found from the 18 mm-stage onwards. At that specific moment, the caudal cardinal veins, which were until then only gently and locally pushed upwards by the umbilical arteries, now truly are deviated in dorsal direction by the developing metanephroi in this region.

[*] According to Grünwald (1938), these more dorsally located vein segments must be regarded as newly developed veins which he called the sacrocardinal veins, whilst McClure and Butler (1925) still regarded these venous channels as a part of the caudal cardinal veins. For more details: see the discussion in section 2.1.2.6.

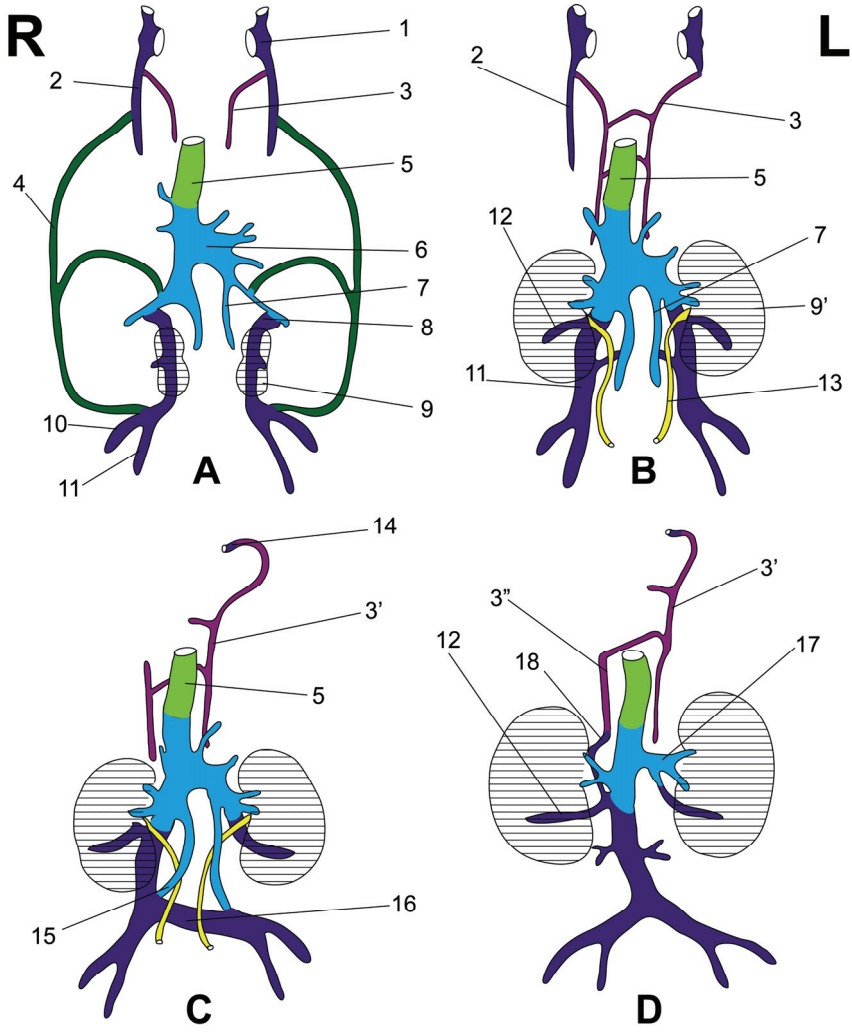

Fig. 40: Schematic representation of the development of the caudal vena cava according to the comprehensive model proposed in this study on pig embryos from 18 mm till 9 cm, ventral views. Stage descriptions: A: phase of the right-angled venous architecture in the lumbar region as observed in the 18-20 mm embryo. B: developmental stage after migration of the kidneys in the 22.5 mm embryo. C: disappearance of the left caudal cardinal vein in the 27.6 mm embryo. D: caudal vena cava near completion in the 3.5-9 cm foetus. 1: Entrance of the left common cardinal vein in the sinus venosus, 2: cranial segment of the right caudal cardinal vein, 3: left supracardinal vein, 3': left azygos vein, 3": right hemiazygos vein, 4: right lateral mesonephric vein, 5: hepatic segment of the caudal vena cava built from the right vitelline vein, 6: subcardinal sinus, 7: caudal segment of the left subcardinal vein, 8: vertical segment of the left caudal cardinal vein in the lumbar region, 9: developing left metanephros, 9' left kidney after migrating to its adult position, 10: right external iliac vein, 11: internal iliac vein, 12: right cranial abdominal vein, 13: left ureter, 14: azygos vein entering in the sinus coronarius, 15: subcardinal-iliac anastomosis, 16: iliac anastomosis, 17: left renal vein, 18: venous branch connecting the caudal vena cava with the azygos system.

The transition of the venous configurations observed in the lumbar region of the 18 & 20 mm pig embryos to the situation in the 22.5 mm embryo are the most difficult stages to compare with the data from literature. However, as a common feature for all available theories including the present observations, it can be stated that during this developmental stage, a rearrangement of the venous vasculature in the lumbar region must be performed to allow the developing kidneys migrating to a more lateral and cranial position.

According to the observations In the present study, the caudal cardinal veins in the 18 and 20 mm course dorsal to the metanephroi and subsequently bend in ventral direction at the cranial pole of these developing kidneys to merge with a mesonephric tributary of the ipsilateral subcardinal vein (Fig. 40A). Due to this configuration, the kidneys are barely hampered in their transition in lateral and cranial direction, which is in great contrast with descriptions in the currently available models (Fig. 41). When evolving to the developmental stage observed in the 22.5 mm embryo, the longitudinal segments just slip of the metanephroi along the dorsomedial surface of these organs, and the short vertical segment adopts a position medial to the cranial pole and hilus of the ipsilateral metanephros.

Fig. 41: Schematic representation of the different opinions on the development of the embryonic venous system in the lumbar region, changing from the typical right-angled configuration (column 1 on the left) into the next developmental stage in which the metanephroi (kidneys) have migrated to a more lateral and cranial location in the embryo (column 2 on the right), right lateral views. Situation in the **A**: human embryo according to the supracardinal model by McClure and Butler (1925), **B**: human embryo according to the sacrocardinal model by Grünwald (1938), **C**: pig embryo according to the supracardinal model by Butler (1927), and **D**: pig embryo according to the observations in this study.

The red solid arrows on the left indicate the migratory path of the developing kidney. Notice the difference between the original position of the metanephros in the human embryo compared to that in the porcine embryo. Dashed lines in the left-sided images indicate the future location of veins and venous branches that will develop in the next embryonic stage. Dashed lines in the right-sided images indicate the former positions of the venous segments that had to regress to allow the kidneys migrating towards their final position.

Equally coloured structures have a common origin. Unlabeled structures in images B-D are comparable with the corresponding structures in image A. **1**: aorta, **2**: right umbilical artery, **3**: right subcardinal vein / subcardinal sinus, **4**: right metanephros, **4'**: right kidney after migration to its adult position, **5**: right caudal cardinal vein, **6**: vertical segment of the right caudal cardinal vein, **7**: caudalmost, elevated segment of the right caudal cardinal vein, **8**: right common iliac vein, **9**: lumbar segment of the right supracardinal vein (precursor of the infrarenal segment of the caudal vena cava), **10**: cranial segment of the right supracardinal vein constructing the right (hemi)azygos vein, **11**: right sacrocardinal vein (precursor of the infrarenal segment of the caudal vena cava), **12**: right lateral mesonephric vein.

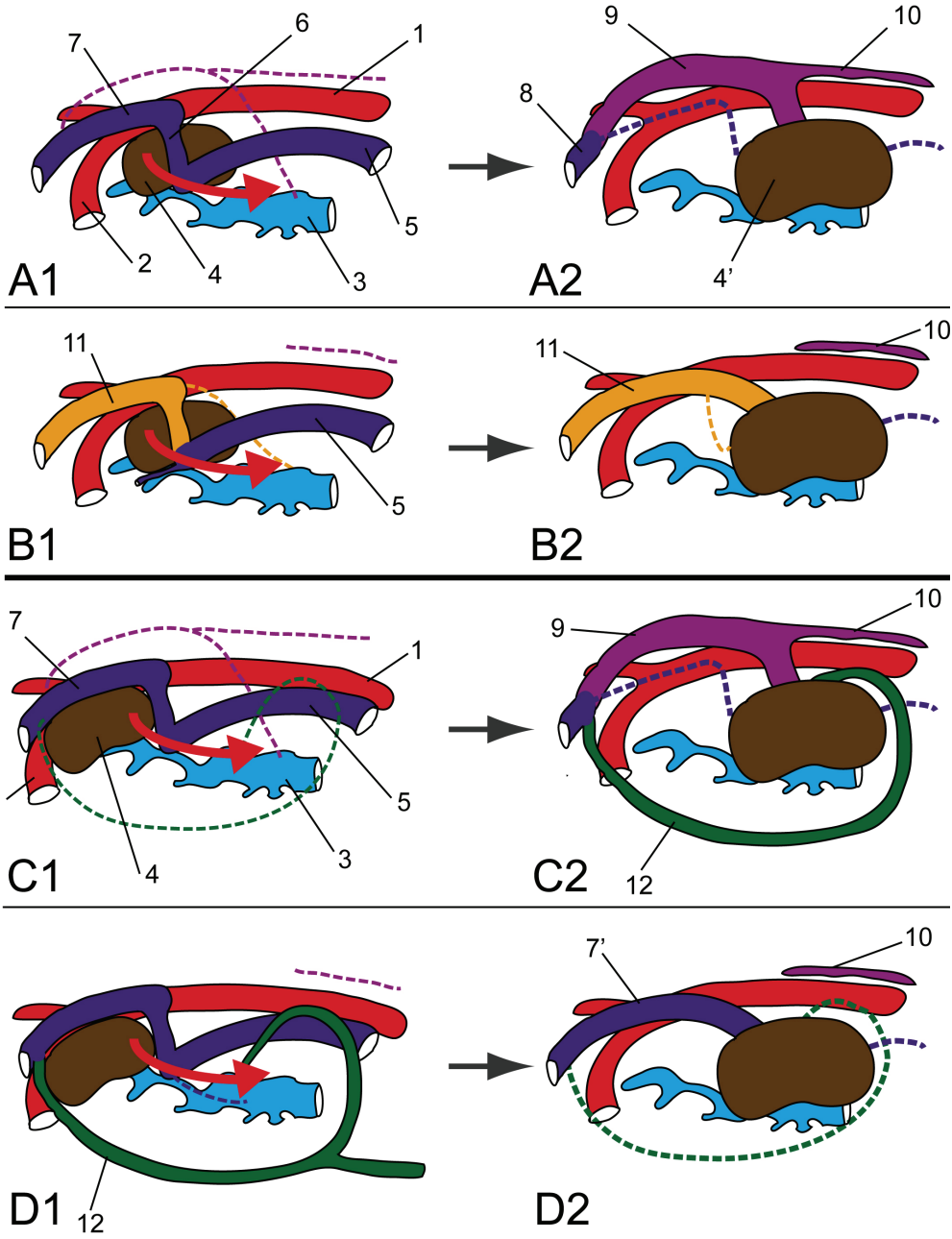
7
6
1
5
2
4
3
A1
9
10
8
4'
A2
11
5
B1
11
10
B2
7
1
2
5
4
3
C1
9
10
12
C2
12
D1
7'
10
D2

Remarkably, despite the major conflicts in literature regarding the venous architecture in the 18-20 mm pig embryo and analogous stages of human embryos, this next developmental stage in the 22.5 mm embryo (Fig. 40B) is again highly comparable with the descriptions in the different other models, regardless of the animal species studied by the original authors. In fact, the dissimilarities between the different models and the present study can for this specific development stage be reduced to a nomenclatural discussion only. On the other hand, an in-depth comparative study that might have revealed some more inconsistencies on the topographical relationships of these vessels to the different surrounding structures between displayed in the different models was difficult to perform, as not every original author included essential structures such as the sympathetic trunks, lymphatic system or ureters in their original descriptions.

However, based on the continuity of the findings in the 22.5 mm embryo with the situation in earlier embryos, the lumbar venous channels draining the iliac veins are in the present study still regarded as the segments of the caudal cardinal veins. During this research, there was no need to change the name of these vessels into “sacrocardinal veins” in order to differentiate them from segments of the caudal cardinal veins coursing ventral of the umbilical arteries as suggested by Grünwald (1938). Furthermore, it also seemed inappropriate to called these vessels “supracardinal veins” as, in contrast with the descriptions of the group of Huntington and McClure (1920), McClure and Butler (1925) and Butler (1927), only little similarities were found between these segments and the supracardinal veins constructing the azygos system in the thorax. In fact and as already put forward by Gladstone (1929), these lumbar segments were observed to course ventrolateral of the sympathetic trunks, whilst the supracardinal veins in the thorax were located medial to these sympathetic side chains. The use of the term “lateral sympathetic veins” to indicate these longitudinal veins in the lumbar region was also rejected as these veins were not found to course along the entire length of the sympathetic trunks as suggested by some other authors (Williams et al., 1993; Rahalkar, 2002).

A very interesting developmental stage in the present study was found in embryos of about 27.5 till 30.0 mm crown-rump length (Fig. 40C). In this stage, the left caudal cardinal vein disappears, and its former location is gradually taken in by the expanding lymphatic system in this region. To ensure a proper drainage of the blood coming from the left hindlimb and pelvic region, an anastomosis between the left and right common iliac veins is formed

dorsal to the aorta at the level of the sixth lumbar artery. Furthermore, these common iliac veins are also sometimes partially drained by the caudal ends of the subcardinal veins, which course, contrary to any other major vessel at this stage, lateral to the ureters.

Unfortunately, this particular developmental stage is not specifically described in the only other available theory on the development of the caudal vena cava in pig embryos as described by Butler (1927), so further comparison with these observations was impossible. However, Butler (1927) already described the iliac anastomosis in the 22-24 mm embryo, whilst nor in this embryo, nor in the 30-35 mm embryo, he mentioned the observation of a connection of the subcardinal veins with the common iliac veins. Only in the cat studied by Huntington and McClure (1920), such a connection is also described.

Finally, in the 36.7 mm foetus, the construction of the caudal vena cava is nearly complete (Fig. 40D). The entire system is somewhat stretched out, and the course of the caudal vena cava is somewhat straightened and smoothened. Both in the 36.7 mm and 9 cm foetus, the lumbar segment of the caudal vena cava is connected with the azygos veins through a lumbar branch of one or both the cranial abdominal veins. The topography of this bendy connection curving along the ventral and medial surface of the ipsilateral sympathetic trunk highly resembles the spatial arrangement of the individual lumbar veins. Based on this fact, it is suggested in the present work that the supracardinal veins constructing the azygos system in the thorax are functionally and topographically more related to the lumbar veins in the abdomen than to the infrarenal part of the caudal vena cava.

According to the model proposed above, the caudal vena cava in the pig is finally built from the following major segments (from caudal to cranial):

- The right caudal cardinal vein forming the infrarenal segment of the caudal vena cava collecting the common iliac veins
- The right part of the subcardinal sinus collecting the renal and cranial abdominal veins
- The right vitelline vein which contributed to the formation of the hepatic and intrathoracic part of the caudal vena cava.

Taking in account the mesonephric anastomosis between the right caudal cardinal vein and subcardinal sinus and the mesenteric anastomosis between the right subcardinal

vein and right vitelline vein, the caudal vena cava in the pig is constructed out of 5 different embryonic venous segments.

The formulation of this more harmonizing theory on the developmental pattern of the caudal vena cava meets with the first scientific aim of this thesis to provide more insights on the controversial aspects of the different available models. One of the frustrations in chapter 2 regarding the existing models on the development of the caudal vena cava was that none of them could be used as a solid base to explain some venous variations, in particular the cases #2 & 3 in section 2.1.3.. By re-evaluating the three hypotheses on the pathogenesis of this venous anomaly formulated in section 2.1.3.2., the first suggestion by May (1960) and Wallace (1960) that the azygos continuation of the caudal vena cava is caused by the persistence of the right supracardinal vein along its entire length can now be rejected, as it has clearly been shown that the supracardinal veins do not contribute in the construction of the caudal vena cava at all. Involvement of a persisting right caudal cardinal vein as put forward by Lohse et al. (1976) and Barthez et al. (1996) is back a possibility, as the basis for its rejection as a possible option, namely the assumption that the caudal cardinal veins course lateral to the urinary system, has now been refuted by the present findings which clearly indicate that the caudal cardinal veins first course dorsal to the kidneys and later on are shifted towards their medial aspects.

However, some involvement of the subcardinal veins in the formation of the present anomaly cannot be neglected as a part of the anomalous vein coursed along the ventral side of the cranial pole of the right kidney, a location which is in the embryo only occupied by the subcardinal sinus. Therefore, based on the outcome of the current research, and with some reservations as the normal development of the caudal vena cava in the pig is used below to explain a variation encountered in another species, *i.c.* the dog, following hypothesis for the exact ontogeny of the azygos continuation of the caudal vena cava is put forward:

- In the lumbar region, both the longitudinal as vertical segments of the right caudal cardinal vein evolve normally into the infrarenal segment of the caudal vena cava. This corresponds to the finding in the anomalous dogs that caudal to the kidneys, the caudal vena cava displayed no topographical variations.

- The vertical segment of the right caudal cardinal vein enters along with the renal veins into the subcardinal sinus. However, rather than draining into the right vitelline vein, the subcardinal sinus passes the collected blood through the anastomosis with the right supracardinal vein just dorsal to the cranial pole of the right kidney and constructing the azygos system in the thorax.

This hypothesis is highly similar with the third assumption presented in section 2.1.3.2. and formulated by Ingham (1969), Vitums (1972), Martin and Gerrity (1980) and McClure and Constantinescu (1987). As a novel finding, the present study identifies the connecting vessel between the infrarenal segment of the caudal vena cava and the azygos veins.

Whilst in the paragraph above the currently presented model describing the embryonic development of the caudal vena cava is used to explain some variations of the venous system encountered in the adult, other congenital malformations can conversely be used to further substantiate some particular aspects of this developmental model proposed in this study. A major dissonant in the harmonizing theory on the development of the caudal vena cava described above is the stage indicated as the moment on which the veins in the lumbar region have to be rearranged to allow the kidneys migrating in cranial and lateral direction, which corresponds to the situation in the 18-20 mm pig embryo. Furthermore, the present investigations also could not provide sufficient evidence to support the hypothesis that a retrocaval ureter is caused by the persistence of the caudal segments of the right subcardinal vein as infrarenal part of the caudal vena cava.

Morphological appearances of some congenital malformations however can be applied to further validate some of the formulated hypotheses on this matter. A congenital malformation of major interest in this respect is the horseshoe kidney. A horseshoe kidney is a large U-shaped kidney that is formed due to the fusion of the caudal poles of the left and right metanephroi in the axial midline of the developing embryo. Because of this arrangement, the developing kidneys cannot migrate towards their more cranial and lateral location as the tissue bridge between both kidneys gets trapped early during migration caudal to the root of the caudal mesenteric artery, impeding further transition of the kidneys

towards their position in the adult (Yoshinaga et al., 2002). Furthermore, due to the link between both kidneys, migration of longitudinal blood vessels along the dorsoventral axis medial to the kidneys is impossible.

In the rare event that a horseshoe kidney is associated with a retrocaval ureter, it is found that the caudal vena cava is coursing ventral to the isthmus linking both kidneys instead of dorsal to it as observed in the uncomplicated cases of a horseshoe kidney (Knutson and Hawas, 2004). This does not only support the hypothesis that a anomalous development of the caudal vena cava is involved in the ontogeny of the retrocaval ureter, it also highly indicative for the fact that a retrocaval ureter is caused by the persistence of the right subcardinal vein forming the infrarenal segment of the caudal vena cava. In fact, in all currently available models on the development of the caudal vena cava, only the subcardinal veins are described to course ventral to the caudal poles of the developing metanephroi.

On the other hand, the congenital malformation of a horseshoe kidney combined with a duplication of the caudal vena cava might be reflecting an arrest in embryonic development at a stage very similar to the situation found in the 18-20 mm embryo. In fact, in both situations, the migration of the kidneys as well as the further evolution of a bilateral symmetric venous system into a single right-sided caudal vena cava in the lumbar region has not been executed (yet). Reports of a duplicated caudal vena cava in combination with a horseshoe kidney have so far always included the finding that the caudal venae cavae are located dorsomedial to the kidney moieties (Wu et al., 2005). This is comparable to the topographical relationship of the caudal cardinal veins to the metanephroi in the 18-20 mm pig embryo of the present study, whereas most other theories on the development of the caudal vena cava indicated that the caudal cardinal veins course dorsal to the caudal poles and lateral to the cranial poles of these developing kidneys (Fig. 41). However, it cannot be excluded that in cases of horseshoe kidney, despite the absence of the specific need to rearrange the venous system to allow the kidneys migrating in cranial and lateral direction, this remodelling of the venous system as depicted in figure 41 still takes place, and the vascular system progresses to a stage similar to the currently investigated 22.5 mm pig embryo. Also in this stage, the caudal cardinal veins are still bilaterally present and a subsequent developmental arrest will also result in duplication of the caudal vena cava medial to the kidneys.

As it has specifically for the human embryo been described that the caudal cardinal veins are located lateral to the cranial poles of the developing kidneys (McClure and Butler, 1925; Grünwald, 1938), re-evaluation of the species-specific topographical arrangement of the venous system at this specific developmental stage in the human embryo as well as a more profound interspecies comparative study on this matter need to be executed to further elucidate this major discordance in the comprehensive model on the development of the caudal vena cava as presented in this work.

The last scientific aim of the present study was to provide a suitable model study the molecular mechanisms involved in angiogenesis in a more physiological environment. The changes observed in the venous architecture in the lumbar region of 27.5 – 30.0 mm embryo display a high number of morphological features that are allegedly be influenced by the angiopoietins and their receptors.

First of all, the left-sided caudal cardinal vein was found to regress and disappear into an undifferentiated capillary network. Rather than being disintegrated and falling apart, the left caudal cardinal vein undergoes morphological changes typically ascribed to reverse angiogenesis and more specifically to the effects of Angiopoietin 2 (Ang2) in absence of Vascular Endothelial Growth Factor (VEGF) (Fam et al., 2003).

Secondly, a new major blood vessel is formed, connecting the left and right common iliac vein with each other. The formation of this iliac anastomosis is an example of bridging between to existing vessels, a typical angiogenic feature that is supposed to be controlled by the combined action of Ang2 together with VEGF (Yancopoulos et al., 2000).

A third important feature present in the same embryo is the fact that the right caudal cardinal vein is stabilised as it is provided with a muscular wall (see figure 33: although the wall of the right cardinal vein is thinner than the solid muscular wall of the aorta, it is clearly thicker than the simple endothelial lining of the lymphatic system in the area). Vessel stabilisation and muscular wall formation is said to occur under a dominating influence of Angiopoietin 1 secreted by the pericytes and activating the Tie2 receptor of the endothelial cells (Papetti and Herman, 2002).

A last intriguing aspect is the apparent involvement of the lymphatic system in this vascular remodelling. Further research is necessary to point out whether the lymphatic

system only profits from the disappearance of the left caudal cardinal vein to expand in this region or whether it actively induces this vein to regress. However, a strong morphological relationship between venous development and lymphangiogenesis has not only since long been proven (Sabin, 1909), it has recently also been indicated through molecular studies that during development, lymphatic capillaries are formed out of endothelial cells recruited from embryologic veins and that both developing systems work in a tightly regulated matter (Scavelli et al., 2004; Adams and Alitalo, 2007).

In conclusion, the present study has provided new perspectives for angiogenesis research with the presentation of a model combining several different aspects of blood vessel formation in a, both in time and space, confined physiological environment. It has furthermore been demonstrated that, despite the existing controversies on the exact development of the caudal vena cava in the different mammalian species, the anatomical configuration of the venous system in the 27.5 mm pig embryo as an angiogenic model, is at least morphologically representative for the venous architecture that can be found in similar stages of the human embryo. These elements allow the further research on the mechanisms involved in this vascular rearrangement. In fact, initial experiments on this matter are currently already conducted at our department as follow-up of the present study. Expression patterns and colocalisation of the different angiogenic mediators of interest in this specific model studied by using different approaches including state-of-the-art technology such as optical projection tomography, will in all probability lead to better insights in this particular field of angiogenesis.

Literature

Adams, R.H. and K. Alitalo (2007). Molecular regulation of angiogenesis and lymphangiogenesis. *Nature Reviews Molecular Cell Biology* 8, 464-478.

Barthez, P.Y., L.M. Siemens and P.D. Koblik (1996). Azygos continuation of the caudal vena cava in a dog : radiographic and ultrasonic diagnosis. *Veterinary Radiology and Ultrasound* 37, 354-356.

Butler, E.G. (1927). The relative role played by the embryonic veins in the development of the mammalian vena cava posterior. *American Journal of Anatomy* 39, 267-353.

Fam, N.P., S. Verma, M. Kutryk and D.J. Stewart (2003). Clinician guide to angiogenesis. *Circulation* 108, 2613-2618.

Gladstone, R. (1929). Development of the inferior vena cava in the light of recent research, with especial reference to certain abnormalities, and current descriptions of the ascending lumbar and azygos veins. *Journal of Anatomy* 64, 70-93.

Grünwald, P. (1938). Die Entwickelung der Vena cava caudalis beim Menschen. *Zeitschrift für Mikroskopisch-Anatomische Forschung* 43, 275-331.

Hochstetter, F. (1893). Beiträge zur Entwickelung des Venensystems der Amnioten, (3) Säuger. *Morphologisches Jahrbuch* 20, Bd. 4, Heft S, 543-648. (Cited by Butler, 1927).

Huntington, G.S. and C.F.W. McClure (1920). The development of the veins in the domestic cat (*Felis domestica*) with especial reference, 1) to the share taken by the supracardinal veins in the development of the postcava and azygos veins and 2) to the interpretation of the variant conditions of the postcava and its tributaries, as found in the adult. *Anatomical Record* 20, 1-30.

Ingham, B. (1969). An unusual configuration of the posterior vena cava in a Beagle. *Zeitschrift für Versuchstierkunde* 11, 276-278.

Knutson, T. and B. Hawas (2004). Horseshoe kidney with a circumcaval ureter. *Scandinavian Journal of Urology and Nephrology* 38, 348-350.

Lohse, C.L., R.R. Selcer and P.F. Suter (1976). Hepatoencephalopathy associated with situs inversus of abdominal organs and vascular anomalies in a dog. *Journal of the American Veterinary Medical Association* 168, 681-688.

Martin, J.E. and L.W. Gerrity (1980). Azygos continuation of the caudal vena cava in the dog. *Southwestern Veterinarian* 33, 155-157.

May, N.D.S. (1960). Absence of the prerenal segment of the posterior vena cava of the dog. *Australian Veterinary Journal* 36, 67-68.

McClure, C.F.W and E.G. Butler (1925). The development of the vena cava inferior in man. *American Journal of Anatomy* 35, 331-383.

McClure, R.C. and G.M. Constantinescu (1987). An uncommon right azygos vein and caudal vena cava in the dog. *Anatomia, Histologia, Embryologia* 16, 84.

Papetti, M. and I.M. Herman (2002). Mechanisms of normal and tumor-derived angiogenesis. *American Journal of Physiology. Cell Physiology* 282, C947-C970.

Rahalkar, M.D. (2002). Dr. N. G. Gadekar Memorial Oration. 55th conference of IRIA, Kolkata. *Indian Journal of Radiology and Imaging* 12, 109-114.

Sabin, F.R. (1909). The lymphatic system in human embryos, with a consideration of the morphology of the system as a whole. *American Journal of Anatomy* IX, 43-91.

Scavelli, C., E. Weber, M. Aglianò, T. Cirulli, B. Nico, A. Vacca and D. Ribatti (2004). Lymphatics at the crossroads of angiogenesis and lymphangiogenesis. *Journal of Anatomy* 204, 433-449.

Vitums, A. (1972). Anomaly of the vena cava caudalis in a dog. *Zentralblatt für Veterinärmedizin Reihe* C 1, 149-152.

Wallace, C.R. (1960). Absence of posterior vena cava in a dog. *Journal of the American Veterinary Medical Association* 136, 27-28.

Williams P.L., R. Warwick, M. Dyson and L. M. Bannister (1993). Gray's Anatomy, 37th edition, reprint. Churchill Livingstone, Edinburgh, p. 219-226.

Wu, H.-H., C.-T. Chang, T.-H. Yen and C.-C. Hung (2005). A case of adrenal aldosteronoma with horseshoe kidney and duplicated inferior vena cava. *Nephrology Dialysis Transplantation* 20, 2858-2860.

Yancopoulos, G.D., S. Davis, N.W. Gale, J.S. Rudge, S.J. Wiegand and J. Holash (2000). Vascular-specific growth factors and blood vessel formation. *Nature* 407, 242-248.

Yoshinaga, K., K. Kodama, I. Tanii and K. Toshimori (2002). Morphological study of a horseshoe kidney with special reference to the vascular system. *Anatomical Science International* 77, 134-139.

SUMMARY

SUMMARY

Recent advances in angiogenesis research have led to the discovery and characterisation of a high number of molecules and mechanisms involved in blood vessel formation and regression. Based on these insights, several therapeutic strategies to interfere with tumour vascularisation or to enhance neovascularisation in ischemic tissues have been worked out. However, as the clinical outcomes of the currently developed drugs targeting this vascular remodelling do not yet meet the preset expectations, it is now realized that further research on the possible interactions and delicate balance between the numerous molecules controlling blood vessel formation and regression under more physiological but still easily accessible and assessable circumstances is needed.

In this thesis, the development of the caudal vena cava in pig embryos is proposed as such an equilibrated model. In fact, this natural developmental pattern is characterised by a well-orchestrated remodelling process involving both the formation of new blood vessels and vascular regression. However, although this process is well-documented in literature, certain unravelled aspects on the true identity, topography and time of appearance and disappearance of some important embryonic veins involved in the construction of the caudal vena cava impede the practical application of this model in angiogenesis research. The specific aims of this study were therefore first of all to demystify these particular aspects by performing an in-depth three-dimensional morphological study of the developing vascular system in the pig embryo and secondly to identify certain specific developmental stages that can be of particular interest in angiogenesis research.

When focusing on the molecular and morphological aspects of vasculogenesis and angiogenesis, the combined functions of Vascular Endothelial Growth Factors (VEGF) and the more recently discovered Angiopoietins (Ang) are of particular interest in the present perspective. VEGF acts as inducer of capillary growth, but can on itself only promote the formation of unstable, immature and leaky vessels which are just lined by a simple endothelium. It is suggested that Ang1, secreted by the surrounding tissue and activating the Tie2 receptor on the endothelial cells, is needed to stabilize these vessels, hereby ensuring their survival and allowing their expansion, and to provide them with a proper wall. This process is allegedly reversed by the action of Ang2, the natural inhibitor of Ang1, which binds

the Tie2 receptor without activating it. After Ang2-mediated regression of the vascular wall and loosening of the endothelial cells, in the presence of VEGF, new capillaries can sprout from these pre-existing vessels. However, in absence of VEGF, the Ang2 mediated vascular destabilisation eventually leads to the complete regression of the vessel. Interestingly, angiopoietins and related receptors have already been proven to be of vital importance in the creation of a left-right asymmetry during embryonic venous development, which is essential for the proper construction of the caudal vena cava.

The controversies in literature regarding the exact developmental pattern of the caudal vena cava in mammals impeding its practical application in angiogenesis research are mostly confined to discussions on the exact origin of the infrarenal part of the caudal vena cava. In fact, the caudal vena cava is during development gradually built out of different segments of the right-sided components of various embryonic vein pairs. Its caudalmost segment, located between the common iliac and renal veins, is the last segment to be constructed during development after a relatively long period of vascular remodelling in this area. Five different models can be found on the exact ontogeny of this infrarenal segment. In this work, these models have been named according to the embryonic veins that are indicated as direct precursors of this caudalmost segment of the caudal vena cava: viz. the supracardinal model, the caudal cardinal model, the sacrocardinal model, the lateral sympathetic model and the subcardinal model. Species-specific diversity, erratic observations due to technical artefacts and biased interpretation of the original data are three major reasons for the dissimilarity between the five theories, but they cannot explain all differences.

During a 2-year study on 120 dog cadavers, eight anatomical variations of the venous system were discovered at anatomical dissection. In the same period and during similar dissections on cats, a unique case of a retrocaval ureter, which is considered to be caused by an anomalous development of the caudal vena cava, was found. These congenital malformations were matched with the different available models on the development of the caudal vena cava to determine which of these models could pre-eminently be used to properly explain the discovered anomalies from developmental point of view. Whereas persistence of left-sided venous segments could easily be explained by using any of the different models, none of them could univocally clarify the ontogeny of the azygos continuation of the caudal vena cava as well as the retrocaval ureter.

Therefore, it was decided to reinvestigate the development of the caudal vena cava in the pig embryo as a model, with special attention to certain topographical aspects that are currently a matter of debate. Sixty-eight pig embryos collected in local abattoirs were histologically processed, serially sectioned and stained with haematoxylin and eosin. The sections of nine reference embryos distributed in the range of 3.7 and 36.7 mm crown-rump length, each representing a different embryonic stage, were photographed with a microscopical camera and subsequently loaded into the Amira ResolveRT reconstruction software. After slice alignment, each pixel of the individual slices was semi-automatically assigned to a certain material corresponding with a particular tissue, organ or vessel type. Based on this segmentation, a three-dimensional reconstruction of the individual embryos was made. Sections of all remaining embryos served as control samples for the findings in the corresponding reference embryo. To complete the series of developmental stages of the caudal vena cava, also some microvascular corrosion casts of 9 cm pig foetuses were made.

The venous architecture of the 3.7 mm embryo corresponded to the general basic pattern displayed in all available models: the caudal cardinal veins could be observed dorsal to the left and right mesonephroi, cranially connecting with the cranial cardinal veins to merge into the ipsilateral common cardinal veins which drained into the sinus venosus of the heart. In the mesonephric mid-region of the 4.6 mm, the caudal cardinal veins were obliterated and the drainage of this specific region of the developing mesonephroi was taken over by the subcardinal veins, two newly formed collaterals of the caudal cardinal veins medial to the mesonephroi. On the other hand, the caudal ends caudal cardinal veins were still proliferating and could be followed until the level of the umbilical arteries, which they clearly crossed dorsally. In the 10 mm embryo, the middle segments of both left and right subcardinal vein fused in the axial midline to form a subcardinal sinus. The cranial connections of the subcardinal veins with the caudal cardinal veins were lost and all blood from the subcardinal sinus was shifted through a newly formed anastomosis between the right subcardinal vein and underlying vitelline vein draining into the heart. In the lumbar region, the caudal cardinal veins were still present as straight longitudinal channels draining along the dorsomedial surface of the mesonephroi into the ipsilateral subcardinal veins. From the 12 mm embryo onwards, these lumbar segments of the caudal cardinal veins were gradually displaced in dorsal direction, first by the cranially migrating umbilical arteries, and later, in the 18-20 mm embryo due to the growth and expansion of the metanephroi, leading

to a typical right-angled configuration of these longitudinal veins now draining through an abrupt vertical connection cranial to the developing kidneys into the subcardinal venous system. In the 22.5 mm embryo, the developing metanephroi have migrated to a more cranial and lateral position. As a consequence, the path of the lumbar segments of the caudal cardinal veins was somewhat smoothened and these vessels could now be found dorsomedial to the developing kidneys, but still lateral to the sympathetic trunks and aorta. Conversely, the supracardinal veins constructing the azygos system in the thorax were found dorsomedial to the sympathetic side chains and dorsolateral to the aorta. In the 27.6 mm embryo, the left caudal cardinal vein in the lumbar region was found to regress, and an anastomosis between the left and right common iliac vein was formed dorsal to the terminal bifurcation of the aorta into the umbilical arteries. In the 36.7 mm and 9 cm foetuses, the adult venous configuration could more or less be observed.

It was generally concluded that, based on the present observations as well as by taking in account the different other theories on the development of the caudal vena cava, the infrarenal part of the caudal vena cava in the pig is built out of a dorsally displaced segment of the right caudal cardinal vein. This segment is cranially continued by the renal part of the caudal vena cava derived from the right-sided part of the subcardinal sinus, whilst the hepatic and intrathoracic parts of the caudal vena cava originate from the right vitelline vein. Conversely, the azygos veins are built from the supracardinal veins which are, despite their connection with caudal vena cava at the level of the cranial abdominal veins, ontogenetically unrelated to the vessels constructing the caudal vena cava. Discrepancies between the current observations and the pre-existing theory were mostly confined to the stage of the right-angled venous configuration in the lumbar region, and could largely be attributed to species-specific variability and interpretational differences.

Finally, the specific vascular rearrangement in the 27.5 till 30.0 mm embryo is put forward as a potential model for angiogenesis research as in the lumbar region of these embryos three particular angiogenic events attributed to the combined action of angiopoietins and VEGF can be found in the same confined space: vascular regression of the left caudal cardinal vein into an undefined capillary network, vessel stabilisation and formation of a muscular wall in the right caudal cardinal vein, and the creation of a new blood vessel, i.c. the iliac anastomosis, as a connection between the two pre-existing common iliac veins.

SAMENVATTING

SAMENVATTING

Recente ontwikkelingen in het onderzoeksdomein van de angiogenese hebben geleid tot de identificatie en karakterisering van een groot aantal moleculaire mechanismen betrokken in bloedvatontwikkeling en vasculaire regressie. In navolging van dit fundamenteel onderzoek werden een aantal therapeutische mogelijkheden gesuggereerd waarin de interferentie met bloedvatontwikkeling noodzakelijk voor tumorale ontwikkeling alsook de stimulatie van nieuwbloedvatvorming in ischemisch weefsel centraal staan. De eerste klinische resultaten van de ontwikkelde geneesmiddelen binnen deze categorieën losten de hooggespannen verwachtingen hieromtrent echter niet volledig in. Hierdoor is het duidelijk geworden dat nog verder fundamenteel onderzoek nodig is, dat zich voornamelijk dient te richten op het delicate evenwicht tussen de verschillende angiogenetische mediatoren in een controleerbare en verifieerbare fysiologische omgeving.

In deze thesis wordt de embryonale ontwikkeling van de vena cava caudalis bij het varken voorgesteld als een dergelijk studiemodel. Immers, het natuurlijk ontwikkelingspatroon van dit grootste bloedvat in het lichaam is gekenmerkt door een sterk gereguleerde omvorming van de primitieve embryonale veneuze architectuur naar de volwassen configuratie waarbij zowel processen van nieuwbloedvatvorming als vasculaire regressie voorkomen. Hoewel dit proces meermaals geïllustreerd werd in de literatuur, blijkt er echter nog onduidelijkheid te bestaan rond de origine, topografie en tijdstip van ontwikkeling en verdwijnen van een aantal relevante embryonale bloedvaten betrokken in de ontwikkeling van de vena cava caudalis, waardoor dit ontwikkelingspatroon niet eenvoudigweg kan gebruikt worden als angiogenetisch model. De doelstellingen van dit onderzoek waren daarom enerzijds het ontrafelen van deze onduidelijke aspecten en anderzijds het aanduiden van een welbepaalde embryonale ontwikkelingsfase als ideaal model in het onderzoek naar de mechanismen betrokken in vasculaire ontwikkeling en regressie.

Op moleculair gebied zijn in deze optiek voornamelijk de interacties tussen enerzijds Vascular Endothelial Growth Factor (VEGF) en de recentelijk ontdekte angiopoietines (Ang) zeer interessant. VEGFs stimuleren immers de groei van nieuwe capillairen, maar kunnen op zichzelf enkel instaan voor de ontwikkeling van labiele, ongematureerde en lekkende

bloedvaten. Ang1 is nodig om deze capillairen te verstevigen, hun uitbouw tot grotere bloedvaten te promoten en hen te voorzien van een musculaire wand. De actie van Ang1 op de Tie2 receptoren van de vasculaire endotheliale cellen wordt echter tegengewerkt door Ang2 die binding van Ang1 met deze receptor blokkeert. Onder invloed van Ang2 verliezen de bloedvaten hun omgevende wand en worden de stevige bindingen tussen de endotheliale cellen gelost. In aanwezigheid van VEGF kunnen hierna nieuwe capillairen vanuit deze gedestabiliseerde bloedvaten ontspruiten. Anderzijds, in afwezigheid van VEGF, gaat de destabilisatie van het bloedvat onder invloed van Ang2 gewoon verder wat finaal resulteert in vasculaire regressie. Daarnaast is eveneens aangetoond dat angiopoietines en hun gerelateerde receptoren betrokken zijn bij het ontstaan van een links-rechts asymmetrie van het embryonale venensysteem, wat noodzakelijk is voor de correcte uitbouw van de vena cava.

De huidige controverse rond het exacte ontwikkelingspatroon van de vena cava caudalis die de applicatie van dit model in angiogenetisch onderzoek in de weg staat, situeert zich voornamelijk rond de specifieke origine van het infrarenale segment van dit bloedvat. De vena cava wordt immers tijdens de embryonale ontwikkeling segmentaal aangelegd uit verschillende rechter fragmenten van meerdere embryonale venenparen. Het meest caudale stuk van de vena cava caudalis, namelijk dit tussen de venae iliacae communes en de venae renales wordt als laatste aangelegd na een relatief lange periode van vasculaire reorganisatie in deze regio. Vijf verschillende theorieën rond de exacte ontogenie van dit veneuze segment kunnen in de literatuur teruggevonden worden en werden in dit werk genoemd naar het oorspronkelijke embryonale bloedvat dat in de respectievelijke modellen aangeduid wordt als precursor van dit infrarenale segment van de vena cava caudalis, namelijk het supracardinaal model, het caudaal cardinaal model, het sacrocardinaal model, het lateraal sympathische model en tenslotte het subcardinaal model. Species-specifieke diversiteit, erratische observaties als gevolg van technische beperkingen tijdens het gevoerde onderzoek en alternatieve interpretaties van gelijkaardige bevindingen zijn de drie grootste redenen voor de discrepanties tussen de verschillende modellen, maar konden niet elke tegenstelling verklaren.

In een periode van 2 jaar werd tijdens anatomische dissecties op een totaal van 120 hondenlijken bij een 8-tal honden een anatomische variatie van de vena cava teruggevonden. In dezelfde periode werd ook bij een dissectie van een kat een uniek geval van een

retrocavale ureter vastgesteld, een aandoening die zijn oorsprong zou vinden in een abnormale ontwikkeling van de vena cava caudalis. Al deze afwijkingen werden vergeleken met de vijf beschikbare theorieën rond de ontwikkeling van de vena cava caudalis om te achterhalen welk van deze modellen de beste basis vormde om de waargenomen afwijkingen vanuit embryonaal standpunt te verklaren. Terwijl alle modellen aangewend konden worden om het persisteren van een normaal afwezige linker veneuze component te verklaren, bleek dit onmogelijk voor de beschreven gevallen van een voortzetting van de abdominale vena cava in de vena azygos alsook voor de retrocavale ureter.

Daarom werd er besloten om de ontwikkeling van de vena cava caudalis opnieuw te onderzoeken, met het varken als diermodel, en hierbij bijzondere aandacht te verlenen aan de verschillende topografische aspecten die momenteel aan de basis liggen van de huidige controverse. Achtenzestig varkensembryo's werden verzameld in lokale slachthuizen. Na fixatie en paraffine inbedding werden van deze embryo's haematoxyline-eosine gekleurde seriecoupes gemaakt. Van alle coupes van negen referentie-embryo's, variërend van 3,7 tot 36,7 mm kruin-stuitlengte, waarbij elk embryo representatief was voor een bepaald ontwikkelingsstadium, werden microscopische opnames gemaakt die vervolgens in de Amira ResolveRT reconstructiesoftware werden geladen. Na het aligneren van de verschillende coupes werden op iedere foto de belangrijkste anatomische structuren op een semi-automatische wijze gelabeld. Op basis van deze segmentatie werd van ieder embryo een driedimensionale reconstructie gemaakt. De bevindingen na studie van deze reconstructies werden vergeleken met de coupes van de resterende embryo's. Aanvullend bij dit onderzoek werden van 6 varkensfoeti met een kruin-stuitlengte van 9 cm vaatafgietsels gemaakt.

Het veneuze bouwplan van het 3,7 mm embryo was vergelijkbaar met het algemene veneuze bouwplan beschreven in elk van de vijf verschillende modellen rond de ontwikkeling van de vena cava caudalis. Dorsaal van de mesonephroi konden de caudale cardinaalvenen waargenomen worden. Ze versmolten craniaal samen met de ipsilaterale cardinaalvenen tot een gemeenschappelijke cardinaalvene die uitmondde in de sinus venosus van het hart. In het middenstuk van de mesonephroi van het 4,6 mm embryo waren deze caudale cardinaalvenen onderbroken en werd de drainage van de mesonephroi overgenomen door de linker en rechter subcardinaalvenen als collaterale bloedvaten van de caudale cardinaalvenen, mediaal van deze organen. Anderzijds waren de caudale delen van caudale cardinaalvenen nog in volle ontwikkeling en konden ze waargenomen worden dorsaal van de

terminale bifurcatie van de aorta in de beide arteriae umbilicales. In het 10 mm embryo, waren de middelste delen van de beide subcardinaalvenen ventraal van de aorta samengesmolten tot een grote subcardinale sinus. Craniaal waren de subcardinaalvenen niet meer verbonden met de caudale cardinaalvenen. Het bloed uit de subcardinale sinus werd door een nieuwe anastomose tussen het craniale deel van de rechter subcardinaalvene en de onderliggende vitelliene vene rechtstreeks in de richting van het hart afgevoerd. In de lendenstreek waren de caudale segmenten van de caudale cardinaalvenen nog steeds aanwezig als beiderzijds aangelegde, rechtlijnige kanalen. Deze venensegmenten werden vanaf het 12 mm embryo initieel door de migratie van de arteriae umbilicales en later, in het 18-20 mm embryo, door de ontwikkeling van de metanephroi dorsaalwaarts verplaatst. Hierdoor werd het verloop van deze venen gekenmerkt door het voorkomen van een typische rechte hoek: de longitudinale venen in de lendenstreek bogen craniaal van de zich ontwikkelende nieren abrupt af in ventrale richting om uit te monden in de subcardinale venen. Door de migratie van de nieren in craniale en laterale richting werd het traject van deze lumbale segmenten van de caudale cardinaalvenen wat afgevlakt in het 22,5 mm embryo, waardoor deze venen mediaal tot dorsomediaal van de nieren, maar nog steeds lateraal van de sympathische zijstreng en aorta, waargenomen konden worden. Anderzijds kon in de thorax de ontwikkeling van het azygossysteem uit de supracardinaalvenen gevolgd worden, waarbij duidelijk bleek dat deze venen dorsomediaal van de sympathische zijstreng gelegen waren. In het 27,6 mm embryo was het lumbale deel van de linker caudale cardinaalvene in volle regressie, terwijl tussen beide venae iliacae communes een anastomose dorsaal van de terminale bifurcatie van de aorta werd uitgebouwd. Het veneuze patroon van de 36,7 mm en 9 cm foeti kwam grotendeels overeen met de veneuze configuratie van het volwassen dier.

Als algemeen besluit, niet alleen gebaseerd op de huidige observaties maar ook rekening houdend met de voorgaande theorieën inzake de ontwikkeling van de vena cava caudalis, kan gesteld worden dat het infrarenale segment van de vena cava caudalis ontstaat uit het dorsaal verplaatste deel van de rechter caudale cardinaalvene. Het hierop craniaal aansluitende renale deel van de vena cava caudalis is afgeleid van het rechter deel van de subcardinale sinus, terwijl de hepatische en intrathoracale delen origineel afstammen van de rechter vitelliene vene. Anderzijds werd aangetoond dat de vena azygos en hemiazygos afstammen van de supracardinaalvenen die, ondanks hun connectie met de vena cava

caudalis ter hoogte van de craniale abdominale venen, niet betrokken zijn in de totstandkoming van de vena cava caudalis. De voornaamste verschilpunten tussen de reeds beschikbare modellen rond deze veneuze ontwikkeling en de huidige observaties situeren zich voornamelijk rond het embryonale stadium gekenmerkt door het abrupt hoekige verloop van de belangrijkste venen in de lendenstreek en konden grotendeels gerelateerd worden aan interspecies diversiteit en interpretatieverschillen van dezelfde kenmerken.

Finaal werd de vasculaire reorganisatie in het 27,6 mm embryo naar voor geschoven als mogelijk studiemodel binnen de angiogenese aangezien in de lendenstreek van dit embryo drie specifieke angiogenetische gebeurtenissen plaatsvinden in een nauw omschreven gebied: enerzijds de regressie van de linker caudale cardinaalvene tot een ondefinieerbare capillaire plexus, ten tweede de stabilisatie en uitbouw van de rechter caudale cardinaalvene die daarbij voorzien wordt van een musculaire wand en tenslotte het ontstaan van een nieuwe vasculaire anastomose tussen de reeds bestaande, linker en rechter vena iliaca communis.

DANKWOORD

In de eerste plaats zou ik zeker mijn promotoren, Prof. dr. dr.h.c. Paul Simoens en Prof. dr. Wim Van den Broeck hartelijk willen danken voor alles wat zij voor mij betekend hebben in de lange aanloop naar dit doctoraat. Hierbij denk ik niet alleen aan de wetenschappelijke omkadering waarbinnen ik de vrijheid en het vertrouwen kreeg om een eigen onderzoeksonderwerp uit te bouwen, hun opbouwende kritieken en de inspirerende en motiverende discussies die we samen hadden; ook hun professionele gedrevenheid inzake onderwijs en onderzoek in het algemeen heeft bij mij diepe impressies nagelaten. De passie voor het lesgeven en de liefde voor het vak uitgestraald door Prof. Simoens is reeds sinds mijn studententijd een voorbeeld voor mij geweest. Zijn bezorgdheid om zijn personeel, de losse babbels die we samen voerden en de warme, bijna familiale sfeer waarbinnen ik onder zijn leiding mocht werken gaven kleur aan het dagelijkse leven op een campus van beton en staal. Van Prof. Van den Broeck draag ik mijn verdere leven steeds dat net ietsje meer mee, het telkens durven hoger leggen van de lat en het verruimen van de eigen horizonten buiten de anatomische cocon. Ik ben hem zeer dankbaar voor het helpen zoeken naar nieuwe technologieën die uiteindelijk in deze studie werden toegepast alsook voor het aantrekken van noodzakelijke fondsen om het uitgebreid arsenaal aan basismateriaal, noodzakelijk om dit onderzoek te kunnen voeren, te vernieuwen en verbeteren.

Mijn dankbaarheid gaat eveneens uit naar de leden van mijn begeleidingscommissie, Prof. dr. A. Weyns, Prof. dr. A. Van Soom, Prof. dr. S. Sys en Prof. dr. G. Van Loon voor hun opbouwende kritiek, hun verruimende reflecties vanuit een ander standpunt en hun suggesties naar de opbouw van dit werk toe.

Een bijzondere plaats in dit dankwoord moet zeker en vast weggelegd worden voor de collega's aan de vakgroep Morfologie. Liliane en Lobke, ik ben de tel al lang kwijtgeraakt, maar een ruwe schatting leert me toch dat jullie samen in het kader van dit onderzoek meer dan 30.000 coupes hebben gemaakt. Voor jullie was dit steeds een evidentie, voor mij echter ondenkbaar zonder jullie hulp. Ook de bijstand die ik van Lobke kreeg bij het fotograferen van ongeveer evenveel preparaten weet ik zeker te waarderen.

Patrick, de giraf en olifant liegen er niet om, de samenwerking met jou was altijd bijzonder. Door je inspanningen beschikten we ook steeds over een voldoende aantal honden

en je hulp bij het verzamelen van drachtige varkensbaarmoeders was tevens meer dan welkom. Voor dit laatste mag ik echter ook de bijdrage van Ward en Jurgen niet vergeten, aan wie ik alle succes toewens in het verdere moleculaire onderzoek dat ontstaan is in het kielzog van deze thesis.

Bart, Eric en Raf, jullie bijdrage aan dit werk is niet in enkele zinnen samen te vatten. Wat ik jullie ook vroeg, ik wist dat ik er altijd op kon rekenen dat het resultaat er zou zijn net zoals ik het voor ogen had. Onbetaalbaar, onmisbaar en onvervangbaar,… bedankt!

Sofie, Monique, Martine, Winny en Els, door jullie inspanningen kon ik echt ten volle voor mijn onderzoek gaan. Gelukkig waren er anderzijds nog die momenten waar ik even van achter mijn computer en microscoop kon komen om wat in de snijzaal te komen 'ventileren', waarbij het telkens even aangenaam was om samen met jullie tussen de studenten te staan.

Griet, mijn sympathieke bureaugenote; Steven, Mylène en Christel, aan wiens voorbeeld ik me kon optrekken, en alle huidige assistenten aan de vakgroep Morfologie wil ik bedanken voor de aangename werksfeer en samenwerking. In het bijzonder wil ik hierbij mijn 'buurman' Christophe vermelden, in wie ik toch een academische zielsverwant gevonden heb.

Andere goede buren waar ik eveneens veel dank aan verschuldigd ben, zijn de professoren en het personeel van de dienst Pathologie die me steeds op de hoogte brachten wanneer ze op autopsie interessante congenitale afwijkingen tegenkwamen die nuttig waren voor mijn onderzoek.

De directie, dierenartsen en personeelsleden van de slachthuizen van Lokeren, Zele, Zedelgem en Eeklo ben ik zeer dankbaar voor hun medewerking bij het verzamelen van de drachtige baarmoeders, alsook dhr. Luc De Keyser die het voor ons mogelijk maakte ook de jongste embryonale stadia te pakken te krijgen. De reconstructie van het allerjongste embryo uit deze reeks heb ik volledig te danken aan collega Sofie Lesperoy als deel van haar toenmalige eindejaarsscriptie. De firma Skyscan ben ik erkentelijk voor het ter beschikking stellen van hun µCT-technologie tijdens de voorbereidende testfases van dit onderzoek.

Het Fonds voor Wetenschappelijk Onderzoek Vlaanderen en het facultaire onderzoeksfonds wil ik bedanken voor de financiële steun die ik mocht genieten om een aantal aspecten van mijn onderzoek te kunnen presenteren op het voorbije EAVA congres te Messina, er mijn kennisgebied uit te breiden en tevens vele wetenschappelijke connecties uit te bouwen.

De boog kan echter niet altijd gespannen staan. Gelukkig kon ik op de steun van vele mensen rekenen om even wat stoom af te laten en mijn zinnen te verzetten. Ik denk hier onder meer aan de vrijwilligers van Rode Kruis Ieper tijdens de vele diensten, activiteiten, opleidingen en bijscholingen, het hele Pl-Oef-team: Ulrike en Stefaan, Frans, Joanique en Geert, alsook alle kernleden en “gastjes” van het Jeugd Rode Kruis: bedankt voor al die toffe momenten! Ook de verschillende gezellige avonden gevuld met gezelschapsspelen samen met mijn broer Bart en Valerie waren steeds een verademing.

Marraine, net zoals iedereen van de familie toonde je je ook steeds geïnteresseerd in mijn werk en vorderingen, wat steeds een extra duw in de rug was.

Mijn schoonouders José en Bavonne ben ik zeer dankbaar voor hun onmetelijke bekommernis en inzet, waardoor het voor mij mogelijk was om zowel eens goed door te werken aan dit doctoraat, als om de nodige ontspanning tussendoor te vinden. Van de thuiswacht en zorg voor de kindjes over een keertje goed gaan eten tot het werk met Sep en de schapen: stuk voor stuk hebben deze elementen in belangrijke mate bijgedragen tot dit eindresultaat!

Pa en Ma, heb ik jullie ooit al bedankt voor alles wat jullie tot nu toe voor mij betekend hebben? Vast wel meerdere keren, maar dit kan onmogelijk in verhouding staan tot de eindeloze steun, zorg, begeleiding, interesse, hulp en opportuniteiten die ik van jullie mocht ontvangen. Ongelooflijk bedankt voor alles, al blijf ik bij jullie in het krijt staan!

Hiermee ben ik gekomen tot de meest uitzonderlijke persoon die ik in mijn leven mocht ontmoeten. Leen, liefste schat, al noemde je je soms een ‘doctoraatsweduwe’, je was voor mij mijn ware promotor achter de schermen. Grootgebracht mede door jouw inspanning en geduld verbleekt dit werk echter tot het niets in vergelijking met je eindeloze liefde en toewijding voor ons ondertussen vierpersoonsgezinnetje, zeker omdat ik me ten volle realiseer dat het vaak ten koste ging van die vele dingen die we anders samen konden doen. Ik beloof je dat daar gauw verandering in komt. Jasper en Robin, nu nog altijd even blij hun papa te zien zelfs al was hij de avond ervoor met bedtijd nog niet thuis, moeten maar tijdig van hun oren maken: beloofd is beloofd!

CURRICULUM VITAE

Pieter Karel Lea Noël Cornillie werd op 25 december 1978 geboren te Roeselare. Hij groeide op in Ieper waar hij in 1996 zijn humaniora in de richting Latijn-Wetenschappen aan het Sint-Vincentiuscollege met vrucht afsloot. Na het verwerven van het diploma van kandidaat-dierenarts in 1999 behaalde hij in 2002 zijn einddiploma van dierenarts met grote onderscheiding aan de Universiteit Gent. In dit afstudeerjaar werd zijn scriptie onder het promotorschap van Prof. Verschooten eveneens bekroond met de Pharmacia & Upjohn prijs.

Op 1 oktober 2002 trad hij als assistent in dienst aan de vakgroep Morfologie van de Faculteit Diergeneeskunde, UGent. Naast het uitbouwen van een eigen onderzoek binnen het deeldomein van de embryologie, wat geleid heeft tot onderhavige thesis, stond hij mee in voor het verzorgen van het praktisch onderwijs in de anatomie, histologie en embryologie aan studenten Bachelor in de Diergeneeskunde. Daarnaast ontwikkelde hij binnen het vakgebied Embryologie een aantal lessen rond ontwikkelingsbiologie en geschiedenis van de embryologie, alsook een didactische CD-ROM embryologie en teratologie als illustratiemateriaal bij de syllabus. Voor de basiscursus Laboratory Animal Science en de vervolmakingcursussen tot vakdierenarts aan de Faculteit Diergeneeskunde verzorgde hij ook het theoretisch opleidingsonderdeel Embryologie. Verder stond hij in voor een aantal lessen anatomie in de externe opleiding Fysiotherapie bij Huisdieren. Hij is tevens de promotor en commissaris van talrijke scripties en masterproeven.

Op wetenschappelijk gebied werkte hij nauw samen met verschillende diensten aan de faculteit alsook met de afdeling abdominale transplantatiechirurgie van het U.Z. Gasthuisberg aan de K.U.Leuven. Daarnaast is hij eveneens coördinator van de Eerste Interventieploeg Diergeneeskunde die optreedt tijdens noodsituaties op de eigen campus.

Sinds 2006 is hij lid van European Association of Veterinary Anatomists en lid van de editorial board of the International Committee on Veterinary Embryological Nomenclature. Hij is op regelmatige basis reviewer voor drie internationale wetenschappelijke tijdschriften.

Hij behaalde in 2006 het certificaat van proefleider en verwierf in 2008 zijn getuigschrift van de postgraduaat-doctoraatsopleiding in de Diergeneeskunde. Hij is auteur van meerdere publicaties in nationale en internationale tijdschriften en nam actief deel aan verschillende internationale en nationale wetenschappelijke congressen.

BIBLIOGRAPHY

PUBLICATIONS

- Cornillie, P., J. Laureyns and P. Simoens (2004). Een geval van prosencephale hypoplasie bij een doodgeboren kalf. *Vlaams Diergeneeskundig Tijdschrift* 73, 29-43.
- Cornillie, P., S. Van Lancker and P. Simoens (2004). Two cases of brachymelia in cats. *Anatomia, Histologia, Embryologia* 33, 115-118.
- Gabriel, S., P. Geldhof, I.K. Phiri, P. Cornillie, B.M. Goddeeris and J. Vercruysse (2005). Placental transfer of immunoglobulins in cattle infected with *Schistosoma mattheei*. *Veterinary Immunology and Immunopathology* 104, 265-272.
- Cornillie, P. and P. Simoens (2005). Prenatal development of the caudal vena cava in mammals: review of the different theories with special reference to the dog. *Anatomia, Histologia, Embryologia* 34, 364-372.
- Cornillie, P., T. Baten and P. Simoens (2006). Retrocaval ureter in a cat. *The Veterinary Record* 159, 24-25.
- D'Haeseleer, M., P. Cornillie, P. Simoens and W. Van den Broeck (2006). Localisation of estrogen receptors within various bovine ovarian cell types at different stages of the oestrous cycle. *Anatomia, Histologia, Embryologia* 35, 334-342.
- Cornillie, P., W. Van den Broeck and P. Simoens (2007). Prolonged gestation in two Belgian Blue cows due to inherited adenohypophyseal hypoplasia in the foeti. *The Veterinary Record* 161, 388-391.
- Cornillie, P., S. Cools, L. Vandaele, A. de Kruif and P. Simoens (2007). Ichthyosis in the Belgian White and Red cattle breed. *Vlaams Diergeneeskundig Tijdschrift* 76, 345-351.
- Breugelmans, S., S. Muylle, P. Cornillie, J. Saunders and P. Simoens (2007). Age determination of poultry: a challenge for customs. *Vlaams Diergeneeskundig Tijdschrift* 76, 423-430.
- Cornillie, P., W. Van den Broeck and P. Simoens (2008). Three-dimensional reconstruction of the systemic vasculature in early pig embryos. *Microscopy Research and Technique* 71, 105-111.

- Barrand, K.R. and P.K.L.N. Cornillie (2008). Bilateral hindlimb adactyly in an adult cat. *Journal of Small Animal Practice* 49, 252-253
- Govaere, J., M. Hoogewijs, C. De Schauwer, A. Van Zeveren, K. Smits, P. Cornillie and A. De Kruif (2008). A monozygotic twin abortion in a warm blood mare. *Reproduction in Domestic Animals*, *accepted*
- Cornillie, P., W. Van den Broeck and P. Simoens (2008). Origin of the infrarenal part of the caudal vena cava in the pig. *Anatomia, Histologia, Embryologia*, *in press*
- Casteleyn C., P. Cornillie, P. Simoens and W. Van den Broeck (2008). Stereological assessment of the epithelial surface area of the ovine palatine and pharyngeal tonsils. *Anatomia, Histologia, Embryologia, accepted*

ORAL PRESENTATIONS AT SCIENTIFIC CONGRESSES

As invited speaker:

- Cornillie, P., S. Cools, L. Vandaele, A. De Kruif and P. Simoens (2008). Ichthyosis fetalis: an emerging lethal condition endangering the Belgian Red and White cattle breed. XXV World Buiatrics Congress, Budapest, July 8-11, 2008.

During open sessions:

- Cornillie, P., W. Van den Broeck and P. Simoens (2005). Computer assisted three-dimensional reconstruction of the developing caudal vena cava in the pig embryo. 3rd meeting of the Young Generation of Veterinary Anatomists, Ghent-Antwerp, July 13-15, 2005.
- Cornillie, P. and P. Simoens (2006). Role of the supracardinal veins in the construction of the caudal vena cava: a three-dimensional study in the pig embryo. XXVIth congress of the European Association of Veterinary Anatomists, Messina, July 19-22, 2006. *Published in: Italian Journal of Anatomy and Embryology* 111 suppl. 1, 60.
- Cornillie, P., W. Van den Broeck and P. Simoens (2007). Application of computer assisted three-dimensional visualization techniques in histology, medical computer tomography and nuclear magnetic resonance imaging. 4rd meeting of the Young

Generation of Veterinary Anatomists, Ljubljana, July 8-10, 2007. *Published in: Slovenian Veterinary Research* 44, 46.

- Cornillie, P., W. Van den Broeck and P. Simoens (2008). New insights in the development of the caudal vena cava gained by three-dimensional reconstruction techniques. XXVIIth congress of the European Association of Veterinary Anatomists, Budapest, July 23-27, 2008.
- Simoens, P.J.M., P.K.L.N. Cornillie and W.L.M. Van Den Broeck (2005). Digital didactic resources for veterinary anatomical and embryologic instruction developed at Ghent University. Joint meeting of WAVA and AAVA, The University of Tennessee, Knoxville, Tennessee, USA, July 20-August 1, 2003. *Published in: Anatomia, Histologia, Embryologia* 34, 205.

POSTER PRESENTATIONS

- Cornillie, P., S. Van Cruchten and P. Simoens (2003). Anatomical variations of the venous system in the dog. Expovet, 13th edition, Ghent, December 12-14, 2003.
- P. Cornillie, C. Jacobs, S. Breugelmans and P. Simoens (2006). Abnormal connections between the digestive tract and respiratory system is a frequent finding in dicephalic calves. XXVIth congress of the European Association of Veterinary Anatomists, Messina, July 19-22, 2006. *Published in: Italian Journal of Anatomy and Embryology* 111 suppl. 1, 99.
- Verberckmoes, S., P. Cornillie, A. Van Soom and A. de Kruif (2004). Effect of the Utero-tubal Junction Insemination on the Integrity of the Bovine Endometrium. VIIIth annual conference of ESDAR, Warsaw, September 23-25, 2004. *Published in: Reproduction in Domestic Animals* 39*,* 278*.*
- Casteleyn, C., P. Cornillie, W. Van den Broeck and P. Simoens (2008). Epithelial surface area of the ovine palatine and pharyngeal tonsils. First Belgian Week of Pathology, March 12-15, 2008.

CONTRIBUTIONS TO BOOKS / COURSE SYLLABI

- Simoens, P., I.A. Constantinescu, P. Cornillie, G. Fehér, C. Knospe, G. Michel, C. Pfarrer, N. Pospieszny, A. Vodenicharov (2006). Nomina Embryologica Veterinaria, second edition. Prepared by the International Committee on Veterinary Embryological Nomenclature (I.C.V.E.N.) and authorized by the General Assembly of the World Association of Veterinary Anatomists (W.A.V.A.) Knoxville, TN (U.S.A.) 2003. Paul Simoens (Editor), Ghent, Belgium, 65 pp.
- Cornillie, P. (2005-). Anatomie van het varken, deel 4: voortplantingsstelsel / Embryologie: normale ontwikkeling & afwijkingen. Postgraduaatsopleiding vakdierenarts varken. Faculteit Diergeneeskunde, Universiteit Gent.
- Cornillie, P. (2006-). Embryology of Laboratory Animals. Basic Course in Laboratory Animal Science partim 1: general topics. Master in Laboratory Animal Science, Faculty of Veterinary Medicine, Ghent University.